Year : 2019

Role of Notch signaling in fibroblasts of secondary lymphoid organs

Cannelle Hélène

Cannelle Hélène, 2019, Role of Notch signaling in fibroblasts of secondary lymphoid organs

Originally published at : Thesis, University of Lausanne

Posted at the University of Lausanne Open Archive http://serval.unil.ch
Document URN : urn:nbn:ch:serval-BIB_0672DDFDEA026

UNIL | Université de Lausanne
Faculté de biologie et de médecine

Département de Biochimie

Role of Notch signaling in fibroblasts of secondary lymphoid organs

Thèse de doctorat ès sciences de la vie (PhD)

présentée à la

Faculté de biologie et de médecine
de l'Université de Lausanne

par

Hélène CANNELLE

Ingénieure en génie biologique diplômée de l'Université de Technologie de Compiègne (UTC), France

Jury

Prof./Dr François Spertini, Président
Prof./Dr Sanjiv Luther, Directeur de thèse
Prof./Dr Werner Held, Expert
Prof./Dre Greta Guarda, Experte
Prof./Dr Mark Coles, Expert externe

Lausanne 2019

UNIL | Université de Lausanne
Faculté de biologie et de médecine

Ecole Doctorale
Doctorat ès sciences de la vie

Imprimatur

Vu le rapport présenté par le jury d'examen, composé de

Président·e	Monsieur	Prof.	François	**Spertini**
Directeur·trice de thèse	Monsieur	Prof.	Sanjiv	**Luther**
Expert·e·s	Monsieur	Prof.	Werner	**Held**
	Madame	Prof.	Greta	**Guarda**
	Monsieur	Prof.	Mark	**Coles**

le Conseil de Faculté autorise l'impression de la thèse de

Madame Hélène Cannelle

Ingénieure en génie biologique, Université de Technologie de Compiègne, France

intitulée

Role of Notch signaling in fibroblasts of secondary lymphoid organs

Lausanne, le 22 août 2019

pour le Doyen
de la Faculté de biologie et de médecine

F. Spertini

Prof. François Spertini

TABLE OF CONTENTS

Acknowledgements

First of all, thank you Sanjiv for giving me the opportunity to work in this lab and to let me work on this Notch project.

I would like to thank all the members of my thesis committee, Prof. Greta Guarda, Prof. Mark Coles and Prof. Werner Held for accepting to be part of my thesis committee, for helping me and giving me input for this project.

Une petite pensée pour l'équipe d'Iteos Therapeutics, ainsi que pour Sandra Cauwenberghs sans qui cette aventure n'aurait probablement pas commencé.

Thanks to everybody in the group for providing a friendly atmosphere, without it, I am not sure to have been able to finish this thesis.
Un grand merci à Stéphanie ! Merci pour toutes nos discussions, nos « coffee break », pour ta gentillesse et tes coups de pouce ! Mais aussi merci pour ton expertise et ta conscience professionnelle. Merci à François, mon doctorant « jumeau » ou mon copain de galères, pour tous nos moments de rigolade, nos expériences ratées et nos sorties en dehors du labo. Merci Stéphanie et François, la « dream-team », de m'avoir soutenue dans les bons comme les mauvais moments, vous avez été mon pilier dans cette aventure.
Thank Patricia for your smile, your positive attitude, all your advice and your support. Thank you to have shared with me, from the early beginning, this magic life experience called Nico!
Merci à toi Karin pour ta sagesse, tes conseils et pour m'avoir donné l'opportunité d'être le deuxième auteur de ton article malgré toutes nos malchances expérimentales ! Merci Léo pour ton expertise et ton travail. Thank-you Hsin-Ying to have shared with me your scientific rigour, your protocols and your expertise of lymph-node digestion.
*Merci à Seyran, mon étudiante en master, pour son travail, son implication et sa motivation à l'égard de mon projet qui m'ont beaucoup touchée. Merci aussi M**e**gane pour ton travail ! Un grand merci à Léonor pour son travail avec les souris et sa conscience professionnelle, tu nous as changé la vie !*

Merci Pierre pour ton soutien dès mes débuts à Lausanne ! Merci pour tes conseils, nos soirées, nos discussions autour d'un thé, tes cartes postales … Je te souhaite tellement de bonheur dans ta nouvelle vie aux Etats-Unis.

Merci à Benoît, mon voisin de bâtiment mais surtout mon ami. Merci d'avoir pris du temps pour m'apprendre les injections, pour les « coffee break » thérapeutiques et merci pour tes encouragements (j'en avais bien besoin !).
Merci à tous ceux qui m'ont soutenu de près ou de loin, Zinnia, Léna, Thomas, Matthias, Quentin, Manoah, Nathalie … J'en oublie certainement, un doctorat ça ne se fait jamais seule !

Le doctorat c'est aussi une histoire de famille !

Merci à mon frère Bastien pour sa complicité, et aussi pour son incroyable capacité à me faire voyager (et ce n'est pas fini) ! La plus belle chose que j'ai apprise avec toi : la passion qu'on peut avoir pour son métier.

Cette thèse c'est aussi et surtout le résultat de l'investissement de mes parents. Merci maman pour ton soutien sans faille, la logistique de toutes mes études, et tes leçons de savoir-vivre (j'ai encore de belles images dans ma tête !). Merci papa pour ton aide, de mes devoirs de CP à mes cours de mathématiques en prépa, tu as toujours été là. Merci pour tes analyses, pour tes coups de pouce, tes citations philosophiques et pour ta façon de me remettre sur les rails quand ça ne va pas !
Et bien sûr, merci pour tous ces déménagements ☺ ! Ce doctorat c'est surtout grâce à vous.

Merci au soutien de toute ma famille ainsi que de ma belle-famille.

Et puis merci à la personne qui partage ma vie : Erwan; pour ta confiance de tous les instants et toute la fierté que tu as lorsqu'on parle de mon travail. Tu as toujours su être là dans les bons comme les mauvais moments ! Encore merci de me pousser vers le haut !

Encore MERCI, je n'arrive pas forcément à trouver les bons mots pour chacun mais je suis très reconnaissante pour le soutien que j'ai reçu pendant cette dure mais belle aventure qu'a été ce doctorat !

To be or Notch to be …

Abstract

Spleen and lymph nodes (LN) are compartmentalized into functionally distinct microenvironments, which are thought to optimize antigen presentation to naïve recirculating lymphocytes. These microenvironments are formed to a large extent by fibroblasts: Follicular Dendritic Cells (FDC) in the B cell follicles with the remaining fibroblasts being collectively termed Fibroblastic Reticular Cells (FRC). FRC have an important role in the architecture of these organs by their network organisation as well as their matrix production. But FRC are also the main cell type responsible for the compartmentalization of these organs into B and T cell rich-zones through production of chemokines. By these different aspects, FRC have a central role in the development of adaptive immune responses.

Gene array analysis of lymph node FRC showed expression of Notch receptors (Notch1, 2 and 3), RBP-Jκ the main transcription factor of Notch signaling as well as Hes1 and Hey1 genes, well known target genes of this signaling pathway. Using flow cytometry, cell surface expression of Notch1 and Notch2 on naive LN FRC was confirmed. These findings suggested the presence of an active Notch signaling in LN FRC.

In this thesis work, I aimed to investigate the role of Notch signaling in FRC development and function. The Notch pathway is an evolutionary conserved signaling pathway important for cell fate decision and differentiation, as well as cell metabolism and survival. By genetic loss-of-function experiments, we have investigated the function of Notch1 and Notch2 genes selectively in CCL19Cre recombinase expressing fibroblasts, both during homeostasis and immune response.

Combined deletion of Notch1 and 2 affects the T zone FRCs in multiple ways, by altering the usually regular 3D network organisation, and by decreasing the extra-cellular matrix (ECM) and CCL19 production. Combined Notch1/2 deletion in FRC also affects neighbouring cells: While the general compartmentalization of lymph nodes is preserved, we observed a marked loss of T cells particularly in naïve mice, an altered B-cell follicle shape and an aberrant presence of lymphatic and blood vessels within the T-cell zone of pLN. Nevertheless, T cell responses developed relatively normally.

Single floxed mice analyses showed that Notch2 is the key receptor in the observed phenotypes found in combined knockout mice. Through the study of the specific deletion of RBP-Jκ in CCL19cre+ FRC, we were able to conclude that the phenotypes observed upon Notch2 deletion were mainly RBP-dependent. Most of these phenotypes are already present in the early postnatal mouse life.

Based on these results, we postulate that active Notch signaling in FRC or their precursors does not seem to alter their differentiation into distinct FRC subset but is an important developmental regulator of FRC organisation and function, thereby impacting also on neighbouring hematopoietic and stromal cells. We hypothesized that modification of chemokine production but also possible modification of VEGF and podoplanin signalings in FRC with Notch1/2 deletion could be potential causes of neighbouring cell modifications.

Together, these findings will improve our understanding of fibroblast development, function and interaction with neighbouring hematopoietic and stromal cells which generate microenvironments that ultimate impact on adaptive immunity and thereby immune control of pathogens and tumours.

Résumé

La rate et les ganglions lymphatiques sont des organes lymphoïdes secondaires compartimentés en divers micro-environnements fonctionnels. L'architecture de ces organes est faite pour optimiser la présentation des antigènes ainsi que la circulation des lymphocytes naïfs. Ces microenvironnements sont en grande partie formés par des fibroblastes : les cellules dendritiques folliculaires (FDC) présentes dans les follicules et les autres fibroblastes nommés cellules fibroblastiques réticulaires (FRC). Ces FRC jouent un rôle primordial dans l'architecture de ces organes lymphoïdes secondaires par leur organisation en réseau 3D ainsi que par la production de matrice extra-cellulaire. Mais grâce à leur production de chimiokines, ces FRC sont aussi les acteurs principaux du cloisonnement de ces organes en deux types de régions, les régions riches en lymphocytes B et les régions riches en lymphocytes T (zone T). Grâce à ces différentes fonctions, les FRC occupent une place centrale dans le développement de la réponse immunitaire adaptative.

L'analyse par microarrays du transcriptome des FRC, provenant de ganglions lymphatiques naïfs de souris, a révélé l'expression des récepteurs Notch (Notch1,2 et 3), du facteur de transcription principal RBP-Jκ de la voie de signalisation Notch ainsi que Hes1 et Hey1, deux principaux gènes cibles de cette voie de signalisation. L'analyse par cytométrie en flux des FRC, provenant de ganglions lymphatiques, a confirmé l'expression en surface de Notch1 et Notch2. Ces diverses données suggèrent une activation de la voie de signalisation Notch dans ces FRC. L'objectif de ce travail de thèse était d'examiner le rôle de la voie Notch dans le développement et les fonctions des FRC.

La voie de signalisation Notch est une cascade de signalisation conservée chez les métazoaires. Elle est fréquemment impliquée dans des choix de différenciations cellulaires, de métabolisme ainsi que dans la survie des cellules. Grâce à l'utilisation du système de recombinaison Cre-lox qui empêche la transcription des gènes Notch1 et Notch2 (récepteurs de la voie Notch), par excision sélective, dans les FRC exprimant CCL19, nous allons examiner quelles sont les fonctions de cette voie Notch dans les FRC dans l'homéostasie ou lors d'une réponse immunitaire.

La suppression de Notch1 et Notch2 affecte l'organisation 3D du réseau de FRC dans la zone T ainsi que la production de la matrice extra-cellulaire et de la chimiokine CCL19. En supprimant Notch1 et Notch2 dans les FRC, les autres cellules hématopoïétiques ou stromales, partageant leurs environnements sont aussi affectées.

Bien que l'organisation générale du ganglion soit préservée, la suppression de Notch1 et Notch2 entraine une remarquable diminution du nombre de cellules T, une structure modifiée des follicules et une présence aberrante de vaisseaux au sein de la zone T. Malgré ces altérations, la réponse immunitaire des lymphocytes T semble se dérouler normalement.

L'analyse des modèles génétiques de suppression de Notch1 ou Notch2 dans les FRC a démontré que Notch2 est le récepteur jouant le plus grand rôle dans les phénotypes précédemment observés. L'utilisation d'un autre modèle de suppression du gènes RBP-Jκ dans les FRC nous permet de conclure que la plupart des phénotypes dus à la suppression de Notch2 sont aussi dépendant du facteur de transcription RBP-Jκ. La plupart de ces phénotypes sont aussi présents chez de jeunes souris, âgées de trois semaines.

En s'appuyant sur ces divers résultats, nous pouvons conclure que la voie de signalisation Notch dans les FRC ou leurs précurseurs, est un important système de régulation de l'organisation des FRC ainsi que de leurs fonctions, qui régule indirectement les cellules avoisinantes. Plusieurs hypothèses ont été envisagées, comme la modification de la production de chimiokines ou la possible modification des facteurs vasculaire de croissance (système VEGFR/VEGF) et de la podoplanine dans les FRC, pour comprendre comment la suppression de Notch1/2 dans les FRC pourrait modifier les cellules avoisinantes.

Ces données vont permettre d'approfondir nos connaissances sur les fonctions des fibroblastes ainsi que leur interaction avec les cellules hématopoïétiques et stromales avoisinantes afin de générer un micro-environnement impactant la réponse immunitaire adaptative et ainsi le contrôle des pathogènes et des tumeurs.

Abbreviations

APC	Antigen presenting cells
BEC	Blood endothelial cells
CA	Central arteriole
ChIP	Chromatin immunoprecipitation
DC	Dendritic cells
DLL	Delta-like ligand
ECM	Extra-cellular matrix
EGF	Epidermal growth factor
FDC	Follicular dendritic cells
FRC	Fibroblastic reticular cells
GC	Germinal center
HEV	High endothelial venules
ICAM-1	Intercellular adhesion molecule 1
ILC	Innate lymphoid cells
LEC	Lymphatic endothelial cells
LN or pLN	Lymph-nodes or peripheral lymph-nodes
LTo	Lymphoid tissue organizer
LTβR	Lymphotoxin β receptor
Lyve-1	Lymphatic vessel endothelial hyaluronan receptor-1
MAdCAM	Mucosal addressin-cell adhesion molecule
MedRC	Medullary reticular cells
MFI	Mean fluorescence intensity
MRC	Marginal reticular cells
MZ	Marginal zone
MZB	Marginal zone B cells
NICD	Notch intra-cellular domain
OVA	Ovalbumin
pdpn	Podoplanin
RBP-Jκ	Recombination signal binding protein for immunology kappa J region
RP	Red pulp
SCS	Subcapsular sinus
SLO	Secondary lymphoid organ
SMA	Smooth muscle actin

TCR	T-cell antigen receptors
TRC	T-zone reticular cells
VEGF	Vascular endothelial growth factor
WP	White pulp
WT	Wildtype

Introduction

I. Secondary lymphoid organs (SLO)

1. Function and compartmentalization of the immune system

The immune system has evolved to protect and help the host to eliminate environmental pathogens and also toxic or allergenic substances that enter through mucosal surfaces. Due to the huge range of pathogenic microbes, toxins and allergens, the immune system uses a complex array of protective mechanisms to control and eliminate these organisms and toxins through recognition of self and response to non-self. The immune system acts through two mechanisms: the rapidly induced innate immune response, acting in a rather non-specific manner, and the adaptive immune response taking days to develop but showing a very high pathogen specificity along with immunological memory.

The innate immune response is responsible for the second line of defense against invading pathogens, with the first one including physical, chemical and microbiological barriers. The innate immunity is composed of cellular components such as neutrophils, macrophages and dendritic cells (DC) that are constantly monitoring peripheral tissues and bloodstream for pathogens. These innate immune cells are capable of recognizing microbial non-self from self through the recognition of evolutionarily conserved structures present in large groups of microorganisms and referred to as pathogen-associated molecular patterns (PAMP). If pathogens manage to enter the body, innate immune cells rapidly arrive at the site of infection to defend the host. Then, pro-inflammatory molecules are secreted to recruit more immune cells and to activate the adaptive immune response.

Adaptive immune responses are based on the antigen-specific receptors expressed on the surface of T and B lymphocytes.

The challenge of the immune system is to bring antigen-presenting cells (APC) including DC and follicular dendritic cells (FDC) together with rare antigen-specific T cells, and soluble antigen together with rare-antigen specific B cells. The interaction between those cells is the primary function of secondary lymphoid organs (SLO) such as lymph-nodes (LN), spleen and mucosal-associated lymphoid tissue, the latter including Peyer’s patches, tonsils and nasal and bronchial-associated lymphoid tissues. In addition to SLO, primary lymphoid organs such as thymus and bone-marrow are dedicated to the development and “education” of immune cells. In the adult, the bone-marrow is the production site of innate and adaptive immune cells and it is where B cells are educated.

The thymus is the place where T cell progenitors, derived from the bone-marrow, undergo important maturation steps. Repertoire of T-cell antigen receptors (TCR) expressed by T cell progenitors is generated by DNA rearrangements, then T cells are positively selected for their capacity of their TCR to recognize peptide and major histocompatibility complexes presented on cortical thymic epithelial cells (Takaba and Takayanagi 2017). But TCR rearrangement process also generates autoreactive T cells that recognize self-antigens; such auto-reactive T cells which are negatively selected and eliminated in the thymic medulla (Takaba and Takayanagi 2017)

2. SLO display highly compartmentalized structures that are adapted to their function

The trafficking of immune cells through SLO, including the spleen and the approximately 450 LN strategically dispersed within the human body, has a crucial role in immunity. SLO are the sites where primary adaptive immune responses are initiated as they bring together rare antigen-specific B with FDC and T cells with professional antigen-presenting cells such as DC. This interaction leads to priming, activation and differentiation of antigen-specific T and B cells. Division and clonal expansion of each T cell produces effector cells which will leave the lymphoid tissue and are guided to the site of inflammation. Two major types of effector T cells have been described, CD4+ helper T cells which orchestrate the immune response by providing signals to induce B and CD8+ T cells proliferation, and CD8+ cytotoxic T cells that trigger their response through lytic attack on target cells and the production of cytokines to attract inflammatory cells.

Therefore, SLO play a crucial role in adaptive immunity. Both spleen and LN behave similarly, but while LN filter the lymphatic fluid, the spleen filters the blood fluid.

In mice, the process of SLO organogenesis is initiated during embryogenesis and extends into the early postnatal period (Mebius 2003). LN development starts around embryonic day 10 to 17 (depending of the LN) with further steps of development such as recruitment of lymphocytes, T/ B segregation and formation of mature B cell follicles starting around birth or after birth (Randall, Carragher et al. 2008). The spleen is first detectable at embryonic day 13 when it consists essentially of the red pulp (RP), with the second compartment, the lymphoid tissue structure called white pulp (WP) developing postnatally in mice, with most processes occurring between day 0.5 to day 8.5 (Schaeuble, Britschgi et al. 2017).

LN and spleen are compartmentalized into functionally distinct microenvironments, B-cell follicles (cortex or B zones) and T cell rich zones (T zones or paracortex) (**Fig.1A**).

A complete segregation of T/B cell compartments is achieved only after birth in mice, both in LN and spleen, with the SLO structure being fully developed and functional only around 3 weeks after birth. In adult mice, naive lymphocytes continuously recirculate and upon entry into the spleen and LN rapidly home into their compartment.

Naïve T and B-lymphocytes that circulate in the blood, enter LN through specialized blood vessels called high endothelial venules (HEV) (**Fig.1A**). This lymphocyte homing to LN is mediated by a cascade of molecular adhesive interactions and chemoattractant signals by CCL19 and CCL21 chemokines (von Andrian and Mempel 2003). In contrast, DC, a major cell population of APC, migrate to the LN via afferent lymphatics to initiate the immune response (von Andrian and Mempel 2003)(**Fig.1A**).

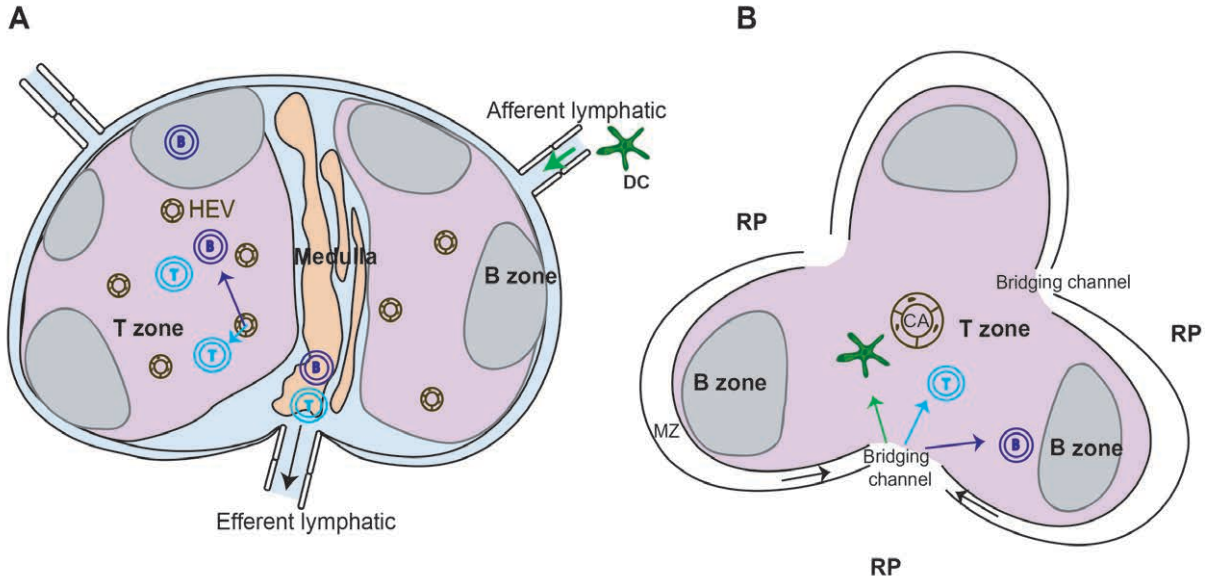

Figure 1: Schematic representation of murine SLO: a peripheral lymph-node (A) and a splenic white pulp (WP) (B). SLO are divided into different microenvironments such as B-cell follicles (B-zone), T-zone and medulla for the lymph node. **(A)** Naïve lymphocytes enter LN through HEV via interaction of adhesion molecules before migrating to their specific regions through chemoattractant molecules, while DC immigrate into LN via the afferent lymphatic vessels. All lymphocytes leave LN by efferent lymphatics of the marginal zone called medulla. **(B)** Naïve lymphocytes and DC enter the splenic WP from the marginal zone (MZ) via bridging channels with the help of chemoattractant molecules. Lymphocytes and DC leave the spleen through veins in the red pulp (RP). HEV, high endothelial venules; CA, central arteriole, RP, red pulp.

Segregation of T/B zones is done by expression of chemoattractant molecules in the different regions such as T cell and DC attractant CCL19/CCL21 molecules expressed within the T-zone and B cell attractant CXCL13 expressed in B-cell follicles (Link, Vogt et al. 2007). Lymphocytes actively migrate inside the LN to survey the organ for antigen. They leave LN by the medulla through efferent lymph vessels and return to the bloodstream through the thoracic duct.

For the spleen, branches of the lymphoid compartment called WP are embedded in the RP. These regions are separated by an interface called the marginal zone (MZ).

Blood circulation in the spleen is open, afferent arterial blood from the RP ends in sinusoids in the MZ and blood flows through the MZ to the red pulp into venous sinuses which collect into efferent splenic veins. Due to the open-connection of the RP with the bloodstream, the main function of this compartment is to filter the blood and to efficiently remove pathogens, cellular debris and old erythrocytes (Mebius and Kraal 2005). The WP, which is compartmentalized as LN with T-and B-cell zones, is arranged around the arterial vessels called central arterioles (CA)(**Fig.1B**). This region, surrounded by the MZ, contains specific cell populations including macrophages and marginal zone B cells (MZB) (Kraal 1992). The MZ is a transit area for lymphocytes and APC that are leaving the bloodstream and are entering the WP by the help of chemoattractant molecules such as CCL19/CCl21, express in the T-zone, to guide their migration (**Fig.1B)** (Bajenoff, Glaichenhaus et al. 2008). As LN, lymphocytes segregate in the different T/B zone though chemoattactant molecules such as CCL19/CCL21 for T-cells (within the T-zone) and CXCL13 for B cells (within the B-zone). Lymphocytes and DC exit from the spleen mostly through the splenic veins in the red pulp.

Naïve T and B-lymphocytes that circulate in the blood continuously enter the SLO and actively migrate inside for antigen survey. If these lymphocytes fail to recognize specific antigen, they return to the blood circulation. On a daily basis, millions of lymphocytes enter and exit each peripheral LN (pLN) and spleen every hour. A key aspect of SLO function is the strong dependence on cell migration, which is itself highly dependent on the SLO structure. The organization of SLO is designed to optimize antigen concentration and presentation to naïve recirculating lymphocytes.

It is known that this compartmentalization is achieved by a network of specialized resident stromal cells. In the following, the focus will be on pLN which were the principal SLO analysed in this thesis work.

II. Resident stromal cells of lymph-nodes

The different SLO microenvironments, such as T-cell zone, B-cell follicles and medulla for the LN are formed to a large extent by stromal cells. Stromal cells not only have an important architectural role for the compartmentalization of SLO, they also have a central function for immune cell trafficking as well as LN and spleen homeostasis. Stromal cells comprise fibroblastic cells that form immune cell niches providing physical support and chemical signals.

Fibroblasts of the B-cell zone are called follicular dendritic cells (FDC) and the other remaining fibroblasts are collectively called fibroblastic reticular cells (FRC).

As LN are at the interface of blood and lymph circulations, stromal cells comprise also two vessel types composed of blood endothelial cells (BEC) or lymphatic endothelial cells (LEC).

1. Blood endothelial cells (BEC)

The use of cutting-edge imaging and computational techniques has allowed to perform a 3D analysis of vascular networks of murine pLN in order to get a complete picture of the vasculature with a high resolution going from capillaries with diameters of only 4µm to an exiting vein with a diameter of up to 90µm (Kelch, Bogle et al. 2015). BEC are commonly defined by the expression of the endothelial marker CD31 while not expressing the marker podoplanin (pdpn). A well-known subset of BEC line specialized blood vessels named HEV, which support the migration of naïve lymphocytes from the bloodstream into SLO. HEV differentiate during neonatal life when the endothelial cells lining them adopted a distinct morphology and expressed the peripheral node addressin (PNAd) (Ager and May 2015). HEV endothelial cells are defined by their cuboidal morphology due to the presence of lymphocyte pockets within the abluminal side of the cells (Chang and Turley 2015). By the formation of pockets where lymphocytes are temporarily retained, HEV behave as traffic control checkpoint that control lymphocyte entry in order to adapt to the needs of LN (Mionnet, Sanos et al. 2011). A sequence of interactions with adhesion molecules allows the adherence of lymphocytes to the inner surface of HEV to enter within LN. This multistep process of lymphocyte extravasation also requires chemoattractant molecules. One of these chemokines is CCL21, the first molecule to be described for its role in naive T lymphocyte migration, was shown to be expressed by HEV endothelial cells (Gunn, Tangemann et al. 1998). CCL19, a T cell chemoattractant as CCL21, CXCL12, a naive T and B cell attractant of secondary importance, and CXCL13, a B-cell chemoattractant, all of which have been shown to be produced by perivascular fibroblasts and then get transported to the luminal surface of HEV where they get presented on proteoglycans at the HEV surface to attract lymphocytes (Miyasaka and Tanaka 2004).

2. Lymphatic endothelial cells (LEC)

LN are organs where soluble and cell-associated antigens that are drained from peripheral tissues via lymphatic vessels are filtered. These lymphatic vessels are lined by a monolayer of LEC. The main function of LN LEC is to guide the flow of incoming lymph across specific areas filled with phagocytes that can filter out pathogens.

Lymphatic vessels drain the lymph all over LN, from the subcapsular (SCS) zone, with the draining of the afferent lymph below the LN capsule, to the B and T-cell zones before joining the medulla, where the efferent lymph is drained.

SCS LEC line the outside of the LN, drain the afferent lymph and contain CD169+ macrophages that phagocytose incoming pathogens and particulate antigens (Junt, Moseman et al. 2007). Medullary LEC found in the medulla, form invaginated sinuses full of phagocytic macrophages and drain the efferent lymph along with emigrating lymphocytes (Kedl and Tamburini 2015). The last subset is the cortical LEC that forms vessels across the T-cell zone and connects the SCS LEC via the cortex and paracortex with medullary LEC (Kedl and Tamburini 2015). The latter vessels are much more prevalent in humans than mice. LEC are defined by their expression of the lymphatic vessel endothelial hyaluronan receptor-1 (Lyve-1) as well as the transcription factor Prox-1 responsible of their cell fate specification (Mishima, Watabe et al. 2007). They can also be distinguished by their expression of the endothelial marker CD31 as well as podoplanin (pdpn). However, peripheral LEC also express CCL21 (Gunn, Tangemann et al. 1998) in order to attract antigen-presenting DC that express CCR7 and enter into the LN via afferent lymphatic vessels. It has also been shown that S1P that interacts with the G-protein-coupled receptor S1PR1 expressed by naïve lymphocytes is produced locally by medullary LEC which is essential for lymphocyte egress via efferent lymph (Pham, Baluk et al. 2010).

Besides LEC and BEC, the other stromal cells that directly interact with lymphocytes within pLN are fibroblasts, more precisely FDC and FRC.

3. Follicular Dendritic Cells (FDC)

B-cell follicles are predominantly composed of recirculating B cells and contour specialized stromal cell subset called FDC localizing to the follicular center. They have a central role in T cell dependent B-cell responses by fulfilling several functions. They secrete CXCL13 to recruit into follicles CXCR5-expressing B cells as well as T follicular helper cells or to retain germinal center (GC) B cells within the follicle (Aguzzi, Kranich et al. 2014).

The 3D network organisation of FDC within follicles has been shown to actively support B cell migration (Bajenoff, Egen et al. 2006). FDC are essential for the regulation of humoral immune response as they are able to trap native antigen coated with Immunoglobulin or complement via Fc or complement receptors (CR1 and CR2), respectively, over weeks to months to present it to GC B cells (El Shikh and Pitzalis 2012) (Heesters, Myers et al. 2014). FDC also produce the cytokine B-cell activating factor (BAFF) that promotes follicular and GC B cell survival (Aguzzi, Kranich et al. 2014). Recognition of bacterial lipopolysaccharide

(LPS) by Toll Like Receptors (TLR) on FDC upregulates CXCL13 for the recruitment, BAFF for the survival and TGFβ for the class switch of GC B cells (Aguzzi, Kranich et al. 2014). FDC also contribute to the prevention of autoimmunity by the removal of apoptotic germinal center B cells by secretion of the “eat-me” molecule milk fat globule-EGF factor 8 (Mfge8) (Kranich, Krautler et al. 2008). Recently FDC has been reported to produce the extra-cellular matrix (ECM) protein cochlin, present in the conduit network of B-cell follicles of SLO, that regulates recruitment of immune effector cells and bacterial clearance during innate immune response against bacteria (Py, Gonzalez et al. 2013).

FDC are identified by their expression of intercellular adhesion molecule 1(ICAM-1), vascular cell adhesion molecule (VCAM-1), CD35/21, MAdCAM, CD157 (BP3) and LTβR (Balogh, Aydar et al. 2002) (Aguzzi, Kranich et al. 2014). FDC and some FRC subsets such as Marginal reticular cells (MRC) share the expression of similar markers, due to the fact that they arise from a common precursor (Castagnaro, Lenti et al. 2013), but have different localization and function, as discussed further below.

III. Fibroblastic reticular cells (FRC)

FRC represent a heterogeneous population based on localization, morphology, surface markers and function. They are found in all three compartments of pLN and they can be distinguished from the other stromal cell types by their surface expression of pdpn and platelet-derived growth factor receptor-α (PDGFR-α) and the lack of CD45 (hematopoietic marker), CD31 (endothelial marker) and CD35 (FDC marker) expression (Chang and Turley 2015).

1. FRC development

In LN, FRC was described to develop from a specialized stromal progenitor named lymphoid-tissue organizer (LTo) cells (Fletcher, Acton et al. 2015). The complete molecular mechanism that drives LN FRC development is not completely defined.

During embryonic development, pre-adipocytes migrate to LN and upregulate CXCL13, to become early LTo-committed stromal precursors, characterized by the expression of lymphotoxin β receptor (LTβR). Then, development of these LTo requires a cross talk with type3 innate lymphoid cells (ILC), via RANK and lymphotoxin signals, that activates LTβR in LTo.

LTβR signal induces differentiation of early LTo in mature LTo that triggers the expression of CXCL13, CCL19 and CCL21 in addition of adhesion molecules such as MAdCAM. This new expression profile leads to clustering and accumulation of more ILC3. FRC precursors are suggested to derive from mature LTo with a crucial intervention of CLEC-2/pdpn axis. LTβR signaling is also required at later stages for the final maturation of FRC precursors into mature FRC (Roozendaal, Mebius et al. 2008, Chai, Onder et al. 2013) (Fletcher, Acton et al. 2015).

The FRC population itself can be divided into three subsets, according to their MAdCAM and CD157 expression, which also separates them into FRC of different localisation and function: T-zone FRC (TRC), Marginal Reticular Cells (MRC) and Medullary FRC (MedRC) (**Fig.2**) (Mueller and Germain 2009, Fletcher, Acton et al. 2015).

2. T-zone FRC (TRC)

TRC are the most prominent subset of FRC as they represent 60-70% of all pLN FRC. TRC express CD157 but are negative for MAdCAM expression. They form a 3D sponge-like network throughout the pLN T-zone which physically guides lymphocyte migration (Luther, Vogt et al. 2011). Due to the proximity between HEV (entry site of naïve lymphocyte) and TRC, lymphocytes immediately associate with TRC once they have left the blood circulation and crawl along the TRC network that define migration roads within LN (Bajenoff, Egen et al. 2006).

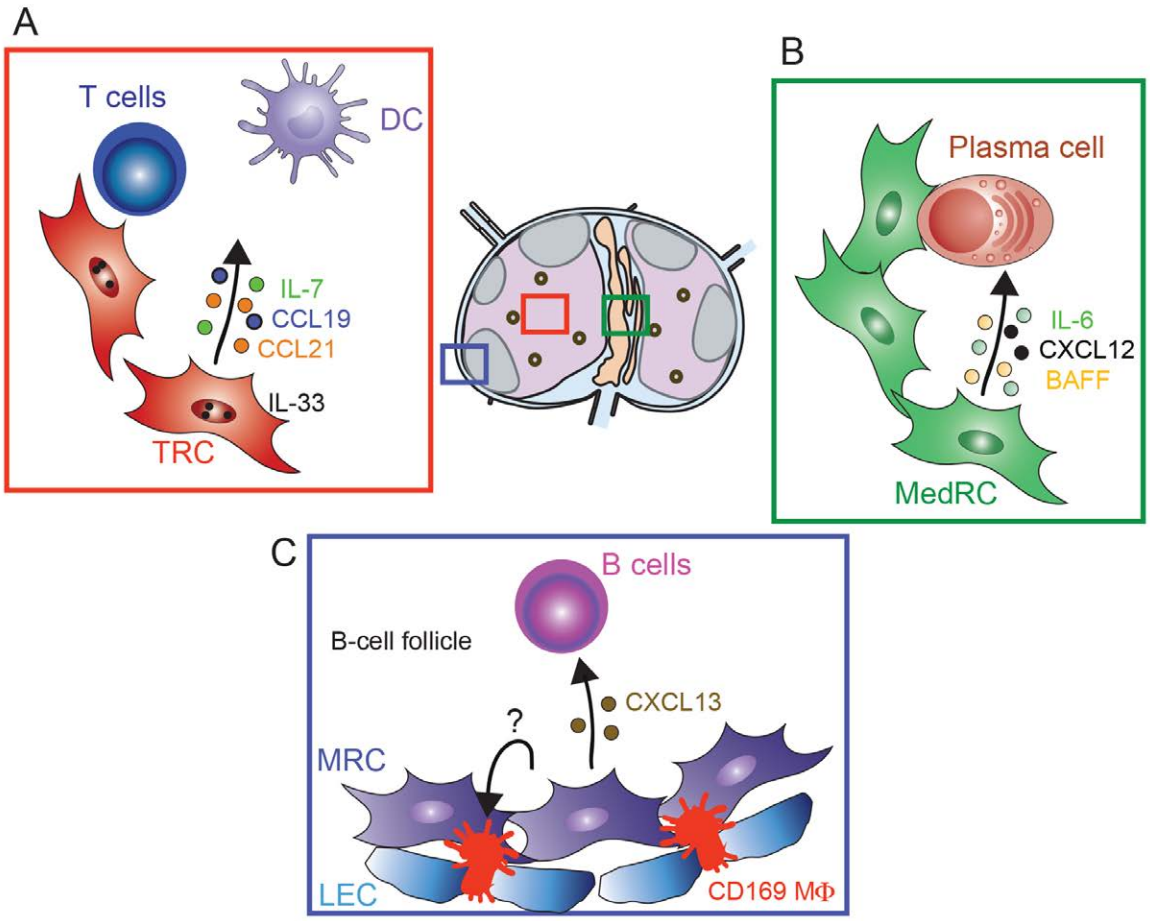

Figure 2: FRC subsets and their interactions with immune cells. (A) FRC of the T-cell zone (TRC) are the main source of CCL19 and CCL21 to attract CCR7+ cells such as T cells and DC within the T-zone. They also produce IL-7 a survival factor for naive and memory T cells, and a nuclear larmin IL-33 capable of boosting T cell responses. **(B)** Within the medulla, MedRC form a niche for plasma cells through the production of plasma cell survival factors such as IL-6, CXCl12 and BAFF. **(C)** MRC present in the SCS region of the B-cell follicle produce CXCL13 to attract CXCR5+ B cells. Recent data suggest a possible role for MRC in the localization and function of CD169+ macrophages.

TRC also secrete ECM, which is arranged in 3D network known as the conduit system. TRC not only produce this conduit network but also enwrapped it, to form this dense 3D cellular network within the T-cell zone (Katakai, Hara et al. 2004). As previously described for lymphocytes, APC such as DC also adhere to this network. This conduit network, surrounded by TRC, facilitates the interaction of T-cells with antigen-presenting DC that share the same environment and are therefore thought to enhance the efficiency by which rare antigen-specific lymphocytes can be identified (Bajenoff, Egen et al. 2006).

This conduit network not only formed a complex roadway, it also provides mechanical strength to the tissue as well as making spaces for motility of immune cells within SLO (Katakai, Hara et al. 2004).

Conduit network system forms a shortcut from the SCS to HEV of the T-zone that allows the fast delivery of the lymph that contains lymph-born chemokines (Sixt, Kanazawa et al. 2005). SCS acts as a physical barrier for high molecular weight molecules and therefore only small molecules (< 70kDa) have been described to enter to this conduit network (Gretz, Norbury et al. 2000). Larger substances cannot use the conduit system but use the lymphatic sinuses. A recent study has highlighted the role of the diaphragms formed by plasmalemma vesicle-associated proteins (PLVAP) fibrils to create a physical sieve that controlled, in a size-dependant manner, the entrance of lymph-born molecules into the conduit network system (Rantakari, Auvinen et al. 2015).

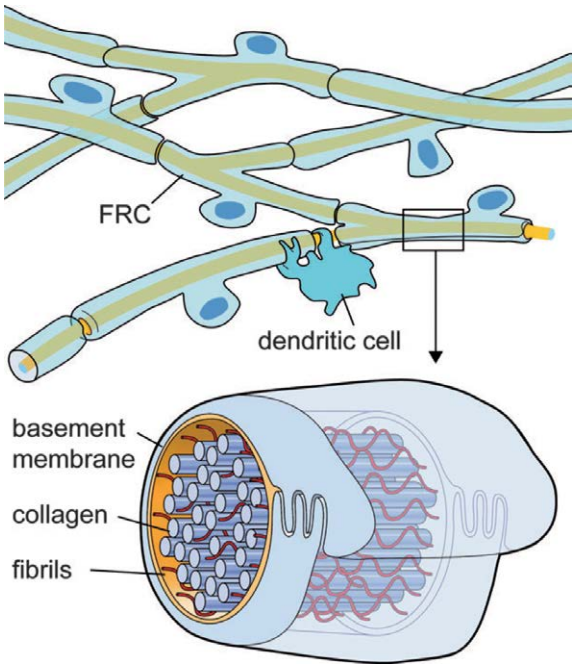

Figure 3: The conduit network system within the LN. FRC are wrapped around an organized tube formed out of basement membrane (containing laminin, collagen type IV and fibronectin) with the inner core consisting of collagen fibers (containing type I and III collagen) that are associated with fibrils (fibrillin-1 and -2, ERTR7). This tubular conduit transports lymph fluid along with small molecules such as antigens and chemokines, going from the subcapsular sinus via the conduits to the HEV. Some DC also adhere to the basement membrane and catch antigens from the conduit content (From (Roozendaal, Mebius et al. 2008))

This conduit system is composed of network of collagen fibers (20-200 type I and III collagen fibers in a bundle) associated with a meshwork of fibrils, which constitute the microfibrillar component stabilizing the collagen network by forming links between collagen fibres (Sixt, Kanazawa et al. 2005, Roozendaal, Mebius et al. 2008) (**Fig.3**). The monoclonal antibody ER-TR7, that recognizes an undefined antigen (Van Vliet, Melis et al. 1986), is often used to identify the microfibrillar zone between the collagen I core. This microfibrillar zone is also constituted of fibrillin-1 and fibrillin-2 (Sixt, Kanazawa et al. 2005)(**Fig.3**).

The collagen core containing fibrils is surrounded by a basement membrane, composed of laminin, collagen IV and fibronectin and it forms a tube (Sixt, Kanazawa et al. 2005)(**Fig.3**). This conduit network system is created by TRC and surrounded by them with no involvement of endothelial cells, and to prevent spread of lymph-borne antigens to the LN cortex (Thierry, Kuka et al. 2018) (**Fig.3**).

Subcutaneous injection of fluorescent tracer revealed that within one minute, the tracer already accumulates in the SCS, T-zone and medullary sinuses of the draining LN with the dextran entering the conduit network gradually from the SCS to the HEV within the T-cell zone (Sixt, Kanazawa et al. 2005). The tracer was also observed in the wall and in the lumen of HEV (Sixt, Kanazawa et al. 2005). This finding highlights the main function of the conduit network: the fast delivery of low molecular weight substances (< 70kDa) such as cytokines from the peripheral site of inflammation to the lumen of HEVs in order to recruit additional leukocytes. Several cytokines have been reported to use this conduit network such as MCP-1 to recruit monocytes, and CXCL13 to recruit B-cells within B-cell follicles (Palframan, Jung et al. 2001, Roozendaal, Mempel et al. 2009). Approximately 90% of the fiber surface of the conduit network is covered by FRC. Nevertheless some DC adhere directly to the basement membrane of conduits, which are not covered by FRC, in order to sample the conduit content such as antigens, internalize and process them (Sixt, Kanazawa et al. 2005). Semi 3D culture suggests that to produce conduit network, FRC receive a TNF/LT signal from lymphocytes (Katakai, Hara et al. 2004).

Therefore LN conduit network has multiple functions, it provides tissue stability, a scaffold for immune cell migration and fast delivery of small molecules through the whole LN in order to recruit immune cells.

For the splenic white pulp a similar conduit network was described consisting also of a basement membrane tube with a fibrillar core wrapped on the outside by reticular fibroblasts (Nolte, Belien et al. 2003). Contrary to LN, splenic conduits are not connected to the lymphatic system but to the bloodstream through connection of the conduit network from the MZ to the CA (Nolte, Belien et al. 2003). Large molecules will not be able to enter the conduit network, as previously described for the LN, but for the small molecules the 3D configuration or electrostatic charge, rather than the molecular weight, is decisive to enter within the conduit system (Nolte, Belien et al. 2003). This previous observation suggests that molecules transported by LN or splenic conduit system have different natures as well as functions.

However, the splenic conduit network allows the transport of smaller molecules and of locally produced chemokines such as CCL21 and CXCL13 through the white pulp (Nolte, Belien et al. 2003). Splenic conduit system has a role in the distribution of blood borne and locally produced chemokines to splenic white pulp in order to help lymphocyte migration.

TRC not only constitute a structural support for SLOs via their 3D network and production of conduits, but they also directly interact with and regulate neighboring immune cells such as DC and lymphocytes, by producing many cytokines and factors (Malhotra, Fletcher et al. 2012, Fletcher, Acton et al. 2015). TRC have been described to be the main source of CCL19, CCL21 and IL-7 (Link, Vogt et al. 2007, Luther, Vogt et al. 2011) (**Fig.2A**). CCL19 and CCL21 were described to be critical for the recruitment of DC and naïve T cells into the T-cell zone (Luther, Tang et al. 2000) (Nakano and Gunn 2001) but also to promote random T cell motility (Kaiser, Donnadieu et al. 2005) (Asperti-Boursin, Real et al. 2007) (Nandagopal, Wu et al. 2011).

IL-7 expressed by TRC, and LEC (Onder, Narang et al. 2012), was described to promote T-cell survival within the LN (Link, Vogt et al. 2007), but it is also constitutively required for normal migration of lymphocytes into LN through homeostatic maintenance of type 3 ILC (Yang, Cornelissen et al. 2018). An unpublished study performed in our lab (Aparicio-Domingo et al. *in preparation*) shows that TRC also express the nuclear alarmin IL-33 that has a crucial role to boost CD8+ anti-viral response against LCMV infection (**Fig.2A**).

3. Medullary FRC (MedRC)

Medullary FRC have been described only very recently (Huang, Rivas-Caicedo et al. 2018) (Rodda, Lu et al. 2018). They can be distinguished from TRC by their lack of expression of CD157 and from MRC by their lack of MAdCAM expression. They are anatomically, morphologically and functionally different from TRC. MedRC constitute a dense network throughout the medullary cords and they also produce ECM which forms a functional conduit network (Huang, Rivas-Caicedo et al. 2018). This conduit network is also composed of collagen fibers that are less regularly organized than within the T-zone, and MedRC are less enwrapping these ECM structures compared to TRC (Huang, Rivas-Caicedo et al. 2018).

MedRC, by their network formation and presumably by their expression of adhesion molecules, physically guide plasma cell migration and residence within the medulla (Fooksman, Schwickert et al. 2010) (Huang, Rivas-Caicedo et al. 2018). MedRC form niche-like structures in which plasma cells and innate immune cells like macrophages reside.

They not only form a physical niche, but also provide survival factors to plasma cells including IL-6, CXCL12 and BAFF (Huang, Rivas-Caicedo et al. 2018) (**Fig.2B**). MedRC represent the major local source of CXCL12 along with blood vessels (Huang, Rivas-Caicedo et al. 2018) (Bannard, Horton et al. 2013).

4. Marginal reticular cells (MRC)

MRC are another subset of FRC which localize between B-cell follicles and the SCS lined by lyve1+ LEC (Katakai 2012). In the spleen, MRC localize between the B cell follicle and the marginal zone (Katakai, Suto et al. 2008). In both cases they form mostly a single layer of cells rather than a 3D network like TRC.
MRC can be identified by their expression of the integrin ligand MAdCAM as well as of RANKL/TRANCE, a TNF family cytokine that is essential for LN development (Kong, Yoshida et al. 1999).
In pLN, MRC have also been identified as FDC progenitors, and during inflammation they also actively proliferate before differentiating into FDC (Jarjour, Jorquera et al. 2014). MRC were proposed to be directly derived from LTo cells (Cupedo, Vondenhoff et al. 2004), responsible for lymph node organogenesis (Coles, Kioussis et al. 2010), as they share many characteristics such as similar localisation as well as expression of various markers such as CXCL13, RANKL and MAdCAM (Katakai 2012) (Katakai, Suto et al. 2008).

The functional significance of MRC in adult SLO is still unclear. Due to their localisation in the outer part of the follicle, close to the SCS, MRC have been suggested to be involved in antigen detection and transport (Katakai, Suto et al. 2008). In fact, MRC have been shown to construct a conduit network in the outer follicle, which is sparse and poorly branched compared to T-zone conduits (Bajenoff and Germain 2009). This conduit network connects the SCS to the FDC areas in order to deliver small soluble antigens to follicular B cells and FDC (Katakai 2012) (Das, Heesters et al. 2017). MRC similar to FDC also express CXCL13 that has a role in the attraction of CXCR5+ B cells. But loss-of-function experiments suggest that CXCL13+ MRC are not sufficient for maintaining B-cell follicles (Chang and Turley 2015)(**Fig.2C**). High magnification pictures in histology suggest that CXCL13, secreted by MRC, enters the conduits and provides an attractant molecule to CXCR5+ B cells (Ansel, Ngo et al. 2000), close to soluble antigens deposited on FDC within the center of follicles (Roozendaal, Mempel et al. 2009).

CD169+ macrophages, localized in the SCS in close proximity to MRC, were defined as a first line of defense due to their strategic position as first cell type to bind antigens as well as their cytokine production to activate innate immune cells (Grabowska, Lopez-Venegas et al. 2018) (Phan, Green et al. 2009). The proximity of MRC with CD169+ macrophages suggests a possible bidirectional role for MRC in the localisation and function of these macrophages (Katakai 2012)(**Fig.2C)** and macrophages in MRC functions.

In summary, FRC create a 3D open-network that provides strength and flexibility to the LN. They also produce and ensheath ECM components that create a conduit network that rapidly transports soluble antigens in the entire LN. But FRC not only support LN architecture, they are also essential for regulation of immune cells by providing a scaffold for immune cells but also recruit them into niches by secreting chemokines. The flexibility of FRC network also has an important role during LN activation.

5. FRC network plasticity during LN activation

Under various conditions that induce LN activation such as infections and cancers, LN undergo a drastic remodelling of their size and organization (Zhu and Fu 2011). This increased LN size optimizes the initiation of adaptive immune response through a massive trapping of naïve lymphocytes and the proliferation of antigen-specific lymphocytes. All stromal cells, that form the backbone of LN, modulate this remodelling. After activation, the entrance of APC and lymphocytes within LN is strongly facilitated by the expansion of afferent lymphatic vessels as well as by the increase size and number of HEV (Angeli, Ginhoux et al. 2006) (Webster, Ekland et al. 2006). FRC network also strongly expands through cell proliferation during activation (Yang, Vogt et al. 2014), as well as ECM production with still functional conduit network system (Gretz, Norbury et al. 2000). FRC also increased in size and granularity quickly after activation, and changed their surface phenotype by upregulating podoplanin expression that was suggested to serve as an activation marker for FRC (Yang, Vogt et al. 2014).

It has been suggested that during activation, resident DC induce HEV/LEC stimulation that leads to an increase of naïve lymphocyte trapping which mediates FRC expansion (Chyou, Benahmed et al. 2011) (Yang, Vogt et al. 2014). A complete plasticity of LN structure as well as LN stromal components such as FRC is therefore inducing an optimized activation of the adaptive immune system in case of infections.

6. FRC subsets: a new approach

To regulate LN homeostasis and activation during immune response, different aspects of FRC have been highlighted in many studies which reflect the complexity of FRC functions and the heterogeneity of the different subsets.

Previous description of the different FRC subsets has underlined the presence of at least 4-6 fibroblast populations (Huang, Rivas-Caicedo et al. 2018) (Fletcher, Acton et al. 2015). This heterogeneity is due to differences in term of morphology, localization and functions. The use of a new technology called single-cell RNA sequencing, has brought to light an even greater FRC heterogeneity. The study of Rodda et al. on CD45- CD31- cells isolated from naive pLN, revealed that FRC could be subdivided into nine clusters (Rodda, Lu et al. 2018). MRC and FRC, that were previously described, TRC that could be divided into three subsets according to their expression of Ccl19 and Cxcl9, and other subsets such as perivascular cells, CD34+, Nr4a1+ and Inmt+ stromal cells (Rodda, Lu et al. 2018).

Therefore, this study shows the complexity and heterogeneity of FRC that reinforced the idea that a complete understanding of stroma cell population is not yet totally achieved and is needed to understand the various microenvironments within pLN.

Development of high-resolution techniques to investigate gene expression level through use of microarrays and single-cell RNA sequencing have brought a new overview on the stromal cell field. These data have been accessible to improve our understanding of stromal cell functions and investigate new mechanisms regulating stromal cell development and functions.

For example, analysis of the data generated by the Immunological Genome project (Malhotra, Fletcher et al. 2012) on stromal cells (FRC, LEC, BEC and pdpl- CD31- cells), of pooled skin-draining and mesenteric LN from naïve wild-type (WT) mice, revealed the expression of Notch receptors and Notch target genes in FRC. So far, no study has explored the role of Notch signaling in FRC. In the following part the Notch signaling pathway will be described, both for its role in immune and stromal cells.

IV. Notch signaling pathway: Complexity behind an apparent simplicity

Notch receptors represent an evolutionarily conserved cell-to-cell communication system observed across many species from flies to humans. The first observation of altered Notch signaling was made already in 1917 by Thomas Hunt Morgan and John Dexter when they described mutant fruit flies with notches of their wing blades (Morgan 1917). This notched wing phenotype, that later provided the name for the receptors involved, was described as the result of a partial loss of function of the Drosophilia Notch gene (Kidd, Kelley et al. 1986). Despite a simple molecular architecture, decades of research on it have revealed that this pathway operates in many different contexts, with a broad spectrum of functions. Notch signaling was first described for its role in the development of the nervous system in flies, that was the first clue of the role of Notch in development (Poulson 1945). Subsequently, Notch signaling has been reported to be involved in many aspects of embryonic development, as well as differentiation process and tissue homeostasis. Due to its crucial involvement in so many processes, the mutation of players in this pathway leads to diseases in various organs and tissues. Although Notch signaling mediates a large number of biological processes though a canonical signaling, many functions of a non-canonical Notch signaling have also been reported.

1. The canonical Notch signaling pathway

General Notch signaling pathway required a physical contact between adjacent cells to allow the binding of a ligand to a receptor, expressed at the cell surface.

Mammals possess four receptors (Notch1-4) that can be bound by five different ligands which belong either to the Jagged (Jagged1, Jagged2) and Delta-like ligand families (DLL1, DLL3, DLL4) (Radtke, Fasnacht et al. 2010)(**Fig.4A**). Receptors and ligands are transmembrane proteins with large extra-cellular domains that consist in epidermal growth factor (EGF)-like repeats that interact during the binding of the ligand to the receptor (Kopan and Ilagan 2009).

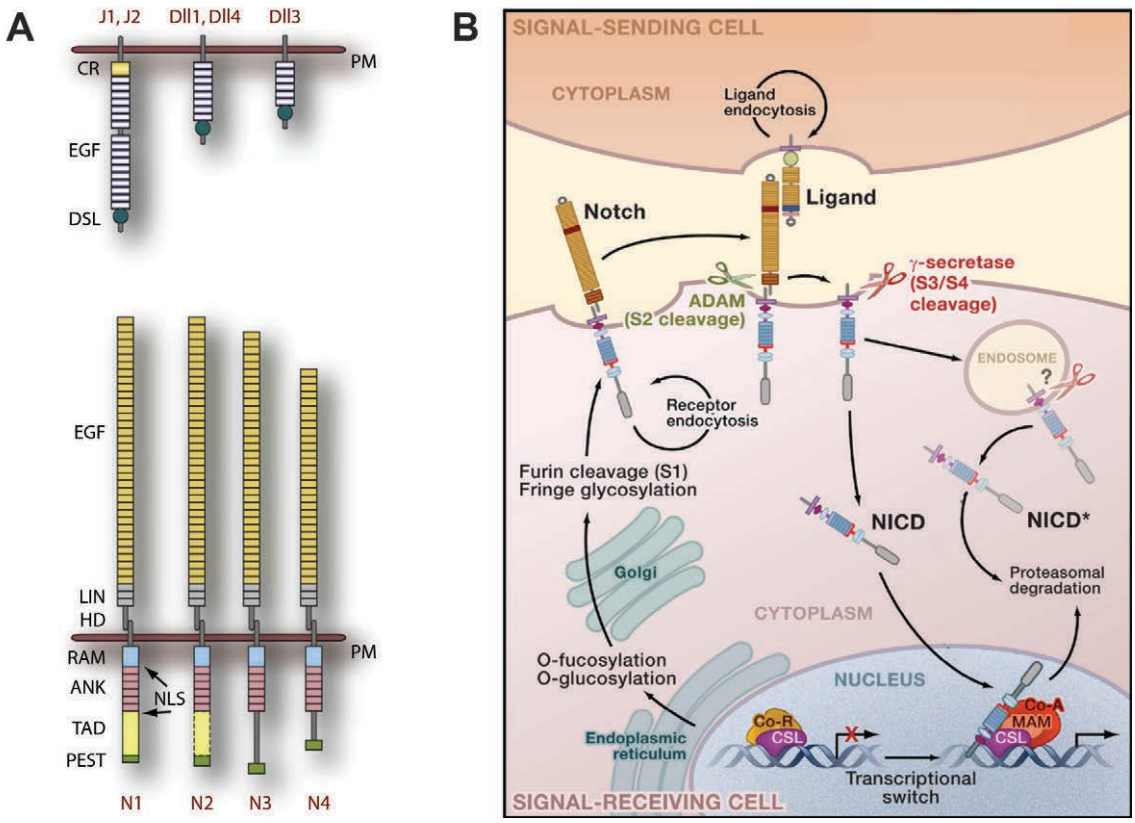

Figure 4: Key features of Notch signaling pathway. (A) Notch ligands and receptors. Five ligands are known Jagged 1 and 2 (J1, J2) and Delta-like ligand 1, 3 and 4 (DLL1, DLL3 and DLL4). They are composed of an amino-terminal domain called DSL (Delta, Serrate and Lag-2), followed by several EGF-like repeats. A cysteine-rich domain (CR) is present in J1 and J2 ligands. The four Notch receptors (Notch1-4) share a very similar structure. The extra-cellular domain is composed of many EGF-like repeats followed by cysteine-rich LIN domains and the heterodimerization domain (HD). The cytoplasmic domain is composed of a RAM domain followed by six ankyrin repeats (ANK) that bind to the CSL, a transactivation domain (TAD) and a PEST sequence. From Radtke, Fasnacht and MacDonald, 2010, Immunity. (**B**) Description of the canonical Notch signaling pathway. The newly synthetized notch receptor is cleaved, and its EGF-like repeats are glycosylated by Fringe proteins in the Golgi, before joining the cell surface. Notch receptors are modified by the addition of two O-linked glycans (O-linked glucose and O-linked fructose) within their EGF-like repeats. Activation of the signaling pathway starts with the binding of the receptor to a membrane-bound ligand on the neighboring cell. This binding is followed by two successive cleavages, first one mediated by ADAM-type metalloproteases and the second one by the γ-secretase complex, in order to release the Notch intracellular domain (NICD). NICD enters the nucleus where it associates with the DNA-binding protein CSL (also called RBP-Jκ in mice). Coactivators will be recruited in order to induce the transcription of different Notch target genes. Adapted from Kopan and Ilagan, 2009, Cell.

All receptors share a similar architecture: the extra-cellular domain is composed of 29-36 EGF-like repeats and three Lin-Notch repeats (LIN), the intracellular portion consists of ankyrin repeats (ANK), a recombination signal-binding protein Jκ (RBP-Jκ) associated molecule (RAM) domain, and a proline-glutamate-serine-threonine-rich (PEST) domain regulating protein stability (Lobry, Oh et al. 2014) (**Fig.4A**). Notch3 and Notch4 lack the transactivation domain (TAD) located in the C-terminal region of the ANK repeats (**Fig.4A**). This region was suggested to modulate Notch activity through posttranslational modifications that can affect molecular interactions (Ong, Cheng et al. 2006) (Bigas, Martin et al. 1998).

All ligands have a DSL (Delta-Serrate and Lag-2) motif involved in receptor binding associated with EGF-like repeats (Lobry, Oh et al. 2014) (**Fig.4A**).

Notch receptors are synthesized as a precursor protein that is cleaved into two parts by a furin-like protease within the Golgi, and their EGF-like repeats are also glycosylated by Fringe proteins, before being transported to the cell surface (Radtke, Fasnacht et al. 2010)(**Fig.4B**).

Notch signaling is initiated by ligand-receptor interactions, which leads first to a cleavage of the extracellular receptor portion at the S2 site with the cleavage being catalyzed by the two ADAM-family metalloproteases, ADAM10 and ADAM17 (Bray 2006) (**Fig.4B**). The cleaved extracellular part of the receptor is endocytosed by the ligand-expressing cell (**Fig.4B**). Then a second cleavage within the transmembrane domain (S3 site) is performed by a γ-secretase complex (Radtke, Fasnacht et al. 2010) (Bray 2006)(**Fig.4B**). This process releases the Notch intra-cellular domain (NICD) of the receptor from the membrane allowing its translocation to the nucleus (**Fig.4B**). NICD binds the DNA binding transcription factor RBP-Jκ (RBP-Jκ in vertebrates, Su(H) in *Drosophila*, Lag1 in *C.Elegans* but collectively referred as CSL) and then recruits other coactivators such as mastermind proteins (MAML1-3) to promote transcription of different Notch target genes (Radtke, Fasnacht et al. 2010) (**Fig.4B**).

In many tissues, transcription factors that are members of the Hairy enhancer of split (Hes) family such as Hes1, Hes5 and Hes7, or Hairy related (Hey) families such as Hey1, Hey2 and HeyL, have been identified as direct Notch target genes (Iso, Kedes et al. 2003). Several other direct target-genes have been identified, such as Deltex1 (Dtx1) (Izon, Aster et al. 2002), IL-2Ra, Gata-3 and c-Myc (Borggrefe and Oswald 2009) as well as p21 implicated in cancer progression (Rangarajan, Talora et al. 2001). Many direct Notch target genes are highly cell type and context (or tissue) dependent.

In the absence of NICD, RBP-Jκ forms a complex with a variety of co-repressors, such as SHARP, thereby suppressing the transcription of Notch target genes such as Hey1 (Hori, Sen et al. 2013) (Oswald, Winkler et al. 2005).

Nevertheless some Notch target genes might not be subject to repression by CSL repressor complexes, as it was described in *C.elegans* study where elimination of CSL did not cause derepression of the Notch target gene REF-1 (Neves, English et al. 2007).

Notch signaling has also been described to interact in a complex way with other well-known signaling pathways such as NFκB (Osipo, Golde et al. 2008), TGF-β (Andersson, Sandberg et al. 2011), AKT (Cornejo, Mabialah et al. 2011), Wnt (Collu, Hidalgo-Sastre et al. 2014) and the Hippo - YAP/TAZ (Totaro, Castellan et al. 2018).

The signaling previously described in commonly referred as the canonical Notch signaling. In mice, phenotypes produced by the depletion of RBP-Jκ are similar but not identical to loss-of-Notch function, which has led to the idea of a RBPj-independent Notch signaling pathway referred as the non-canonical Notch signaling (Bray 2006).

2. The non-canonical Notch signaling

Non-canonical Notch signaling can be grouped into three different pathways according to which step of the signaling differs from the canonical one, the use of other transcription factors, ligands or factors that bind to RBP-Jκ (Siebel and Lendahl 2017).

RBP-Jκ-independent Notch signaling has been described to be implicated in many phenotypes (Siebel and Lendahl 2017). For example, in the breast cancer context, RBP-Jκ was described as dispensable for Notch-mediated upregulation of IL-6, via involvement of the NFκB pathway (Jin, Mutvei et al. 2013). This link between Notch signaling and NFκB was studied in many publications. It has been shown that Notch1-ICD and NFκB form a complex on the IFN-γ promoter to positively regulate production of this cytokine in peripheral T cells in an RBP-Jκ independent way (Shin, Minter et al. 2006).

An uncleaved membrane-bound form of Notch has been shown to interact with β-catenin and modulate Wnt signaling in flies without involving Notch ligands and CSL (Andersen, Uosaki et al. 2012).Then, different ligands have been reported to activate Notch receptors that leads to activation of Notch signaling in RBP-Jκ independent way. Microfibrillar protein MAGP2, which is a structural component of lung, skin and vasculature, has been reported to induce Notch1 activation and leads to activation of Notch signaling pathway (Miyamoto, Lau et al. 2006). YB-1 a protein that was previously linked to inflammatory diseases such as asthma and mesangioproliferative nephritis, secreted by mesangial cells, was shown to activate Notch3 (Rauen, Raffetseder et al. 2009). It is not totally understood how these alternative ligands interact with Notch receptors.

The last group, which is the best understood regulation mode of non-canonical signaling at the molecular level, is defined as the regulation of RBP-Jκ by other factors than NICD (Siebel and Lendahl 2017). Viral proteins such as EBNA2 (derived from Epstein-Barr virus) and 13SE1A (from adenovirus) can bind RBP-Jκ and convert it from a repressor to an activator (Zimber-Strobl and Strobl 2001) (Henkel, Ling et al. 1994).

Consequently, these examples show that alternatives exist to the canonical Notch-signaling pathway, which renders it complex, in addition to the multiple ligand interactions and functions known.

3. Notch ligand-receptor interactions

As already described previously, the activation of Notch signaling starts with a binding of a ligand present on the cell surface to the receptor expressed on another cell surface, necessitating a cell-to-cell contact in the prototypical trans-activation mode. But receptors and ligands present on the same cell surface can also bind to each other (Chillakuri, Sheppard et al. 2012). Usually the presence of ligand and receptor on the same cell inhibits the Notch signaling by a downregulation of the Notch receptor from the cell surface, commonly referred to as cis-inhibition (Andersson, Sandberg et al. 2011).

The structure and affinity of the ligand binding is modulated by the binding of calcium ions on EGF-repeats of Notch receptors (Cordle, Redfieldz et al. 2008). Some studies reported that glycosylation of Notch receptors such as the addition of O-fucose glycans (**Fig. 4B**) could influence ligand-receptor binging by inducing conformational change of the Notch extracellular domain (Haines and Irvine 2003).

The four Notch receptors and the five ligands can lead to a large number of receptor-ligand combinations. No clear difference in signaling output was shown for the different ligand-receptor combinations.

However, Delta-like 3 (DLL3) was described to be rarely present at the cell surface and also incapable to activate Notch receptors in trans (Andersson, Sandberg et al. 2011). DLL3 is considered as an inhibitor of Notch signaling when expressed on the same cell as the Notch receptor, via cis-inhibition (Ladi, Nichols et al. 2005).

Despite a simple molecular architecture of the canonical Notch signaling, the presence of non-canonical alternatives, as well as modulation of the interaction between ligand-receptor highlight the complexity of this signaling. To have an overview of the main functions of Notch signaling, the implication of this signaling in major cell types will be described.

4. Notch signaling in immune cell regulation

One of the most established functions of Notch signaling is its role in the regulation of innate and adaptive immunity through its functions in immune cells. Several loss-of-functions experiments have highlighted the importance of Notch signaling during lymphocyte development.

First, the canonical Notch signaling is important for T cell lineage commitment. More precisely, the interaction between DLL4-expressing thymic epithelial cells and Notch1-expressing thymocyte progenitors will induce a transcriptional program in the cell to adopt a T cell instead of a B cell fate (Radtke, Fasnacht et al. 2010).

Another example is the Notch2 dependent development of MZ B cells. MZ B cells are a spleen-resident B cell subset that provides a first-line of defense against blood-borne pathogens by their ability to respond to antigens more rapidly than follicular B cells. B lineage progenitors leave the bone marrow to enter in the spleen where they will undergo the differentiation into either MZB or follicular B cells. Activation of canonical Notch 2 signaling in transitional type 2 (T2) B cells by DLL1-expressing splenic endothelial cells, induces specification of transitional B cells into MZ B cells instead of follicular B cells (Radtke, Fasnacht et al. 2010).

By loss-of-function experiments in mice with DC-specific deletion of Notch2, canonical Notch2 signaling has been described to play a role also for DC lineage development in spleen and intestinal lamina propria (Lewis, Caton et al. 2011).

Another example concerns ILC, that develop from common lymphoid progenitors with important roles in generation of SLO, tissue remodeling (after injury or infection) and innate immune responses to infectious pathogens. ILC development has been described to be regulated by Notch signaling (Radtke, MacDonald et al. 2013). More precisely, Notch signaling was described to be required for RORα and RORγt-dependent group2 and group3 ILC development and/ or expansion (Radtke, MacDonald et al. 2013).

Another role for Notch signaling in immune cells concerns immune responses through regulation of helper T cell functions as well as regulatory T cells. Non-canonical Notch signaling through Notch1 and subunits of NFκB, identified as potential partners of NICD, has been reported to regulate the transcription of T-bet, the master regulator of Th1 cell differentiation (Radtke, MacDonald et al. 2013). In contrast to Th1 cells, Notch function on Th2 cell differentiation was reported to be RBP-Jκ dependent with several mechanisms having been described. One mechanism is the direct effect of Notch on *IL-4* transcription (RBP-Jκ binding site) that is known to be a master regulator of Th2 differentiation (Radtke, MacDonald et al. 2013). Notch3 was reported to upregulate Foxp3 expression that promotes the development of regulatory T cells and improves their suppressive activity.

This Notch function observed for regulatory T cells gave rise to preclinical studies to selectively block notch signaling as potential tool to treat autoimmune diseases (Radtke, MacDonald et al. 2013).

In summary, Notch signaling is expressed in many immune cells and involved in key processes driving cell fate decisions during development and cell expansion at homeostasis or during immune response. However, Notch signaling functions are not restricted to immune cell regulation, other cell types such as endothelial cells and fibroblasts possess an active Notch signaling.

Lethality of Notch1-/-, Notch2-/- and RBP-Jκ-/- mice observed during embryonic development, between embryonic day 9.5 and day 11.5, revealed the importance of Notch signaling in embryonic developmental phases and the indispensable activity of this signaling in early cells present during development such as endothelial cells ((Hamada, Kadokawa et al. 1999, Huppert, Le et al. 2000) (Oka, Nakano et al. 1995).

5. Notch signaling in endothelial cell regulation

Despite its role for immune cells, Notch signaling has also been described to play an important role on LEC and BEC by the regulation of vascular endothelial growth factor (VEGF) receptors. Use of specific blocking antibodies against Notch1 and DLL4 in neonatal mice, results in defective postnatal lymphatic development in mice (Niessen, Zhang et al. 2011, blood). The Notch1-DLL4 axis regulates postnatal lymphatic development by modulating VEGFR3 signaling, that controls lymphangiogenic sprouting, via upregulation of EphrinB2 expression (Zheng, Tammela et al. 2011) (Niessen, Zhang et al. 2011). However, in adult mice, inhibition of Notch signaling, through injection of soluble form of DLL4 in ears, promotes lymphangiogenesis through VEGF/VEGFR2 pathway (Zheng, Tammela et al. 2011).

This discrepancy between postnatal development and adult mice may be explained by the dual function of Notch signaling in inducing cell differentiation and suppressing cell growth that may be differently regulate in embryonic development and in adults.

In Notch1-/- and Notch1-/-Notch4-/- mouse embryos, lethality was observed due to the fact that embryos failed to remodel the primary vascular plexus to form large and small blood vessels and then die, indicating that Notch signaling is essential for angiogenic vascular development (Huppert, Le et al. 2000) (Krebs, Xue et al. 2000). Loss-of-function experiments that focus on mouse retina suggest that Notch1 activation correlates with a reduction in vascular density, endothelial tip cells and vascular branch points (Kofler, Shawber et al. 2011). Several studies have shown that VEGF can modulate Notch1 and DLL4 gene expression in arterial endothelial cells that is responsible for the important role Notch signaling plays in arteriogenesis and angiogenesis (Liu, Shirakawa et al. 2003).

In summary, Notch signaling has been described as a complex but crucial regulator of signaling cascades triggering angiogenesis of blood and lymph vessels.

The function of Notch signaling is not only restricted to immune cells and endothelial cells, it is also key to fibroblasts.

6. Notch signaling in fibroblasts

Fibroblasts are mesenchymal cells that are part of the connective tissue that joins and supports all body tissues. Their best-known biological function is the production of ECM. During tissue injury or chronic inflammation, they get activated by inflammatory cytokines that promote their proliferation and differentiation into myofibroblasts, characterized by α-smooth muscle actin (SMA) expression, but also including the upregulation of ECM production in order to facilitate the repair process (Kendall and Feghali-Bostwick 2014). However, excessive matrix production during chronic inflammation can result in pathogenic scar formation and fibrosis.

In addition to its function in immune and endothelial cells, Notch signaling has also been described for its strong role in promoting myofibroblast differentiation during chronic fibrosis occurring in different tissues such as lung, kidney, liver, heart and skin, as indicated by α-SMA expression (Hu and Phan 2016). In patients with chronic lung diseases such as chronic obstructive pulmonary disease Notch2, Jagged-1 and Hes1 are upregulated indicating an active Notch signaling pathway (Tilley, Harvey et al. 2009). Similarly, in idiopathic pulmonary fibrosis an increase of Notch1 as well as α-SMA expression was observed in myofibroblasts during fibrosis process (Aoyagi-Ikeda, Maeno et al. 2011).

It has been reported than *in vitro* culture of airway fibroblasts from mouse and human, with stimulation of Notch signaling through addition of Jagged-1 or over-expression of NICD (using a lentiviral vector), induce collagen (col) I expression (Hu, Ou-Yang et al. 2014). Consistent with this finding, sequence analysis of human and mouse col1a1 and col1a2 promoters revealed the presence of several Hes binding site, that was confirmed by chromatin immunoprecipitation (ChIP) analysis (Hu, Ou-Yang et al. 2014). In bleomycin-induced pulmonary fibrosis in mice with selective deficiency of Notch1 in the mesenchymal compartment revealed a significant reduction of lung fibrosis (Hu, Wu et al. 2015), along with reduced collagen I and α-SMA expression (Hu, Wu et al. 2015). In summary, increased Notch1 signaling activity in airway fibroblasts leads to an aberrant secretion of collagen I, which is probably Hes-dependent.

Therefore, Notch signaling regulating collagen I expression could be a potential therapeutic target in patients with lung fibrosis.

In skin tissue, constitutive NICD expression was reported in keratinocytes, hair follicles, sebaceous gland endothelial cells and immune cells (Hu and Phan 2016).

In case of fibroproliferative skin diseases, such as keloids, hypertrophic scars, and dermatofibromas, an upregulation of NICD expression relative to normal skin was observed (Kim, Lee et al. 2014). In case of systemic sclerosis, skin sections of patients also show an increased presence of NICD as well as Hes1 in skin fibroblasts with Jagged-1 being expressed in infiltrating T cells, pointing to the potential Notch ligand source (Dees, Tomcik et al. 2011). Dermal fibroblasts derived from systemic sclerosis biopsies and cultured with Jagged-1-Fc release more collagen I protein and differentiate into α-SMA+ myofibroblasts (Dees, Tomcik et al. 2011). On the other side, inhibition of Notch signaling through blockade of the γ-secretase complex or siRNA against Notch1 induced an anti-fibrotic effect with a decrease in collagen I expression (Dees, Tomcik et al. 2011). In skin wound healing, keratinocytes and fibroblasts play an important role to close the wound and regenerate the skin tissue. *In vitro* culture of fibroblast monolayer subjected to scratch wounding in order to mimic skin wound healing, and treated with the γ-secretase inhibitor DAPT or Jagged peptide, revealed a significant inhibition of fibroblast migration upon Notch signaling inhibition using the γ-secretase inhibitor DAPT, while a Notch binding Jagged peptide significantly enhanced fibroblast migration (Chigurupati, Arumugam et al. 2007). The mechanism by which Notch signaling promotes fibroblast migration is not yet described.

In summary, in case of fibrotic diseases in lung, skin but also in kidney and liver an increase presence of Notch signaling is observed, that leads to an upregulation of the fibrotic aspect through the increase of ECM production (Hu and Phan 2016).

It has also been shown that Notch may be involved at sites of chronic inflammation. Synovial fibroblasts activated by TNF-α in *vitro* (mimicking the context of rheumatoid arthritis), show active Notch signaling, through a gradual time-dependant increase of Hes1. TNF-α stimulation also induces IL-6 production. *In vitro* inhibition of Notch signaling (with γ-secretase inhibitor), inhibited IL-6 secretion in response to TNF- α. Therefore, stimulation of Notch receptors in these synovial fibroblasts can mediate a TNF-α-induced IL-6 production (Jiao, Wang et al. 2012).

The main transcription factor of Notch signaling, RBPj, has been shown to act as negative regulator of p53 and also of multiple senescence genes in dermal fibroblasts with deletion of RBPj leading to senescence and induction of activation markers such as αSMA (Procopio, Laszlo et al. 2015).

Many evidences show the implication of Notch signaling in the process of pathogenesis of fibrosis or chronic inflammation in different cellular and tissular contexts.

The Notch signaling pathway seems to play multiple roles in tissue fibroblasts outside of SLO, by inducing fibroblast differentiation, extra-cellular matrix and inflammatory cytokine production as well as by impacting migration and cellular senescence (**Fig.5**).

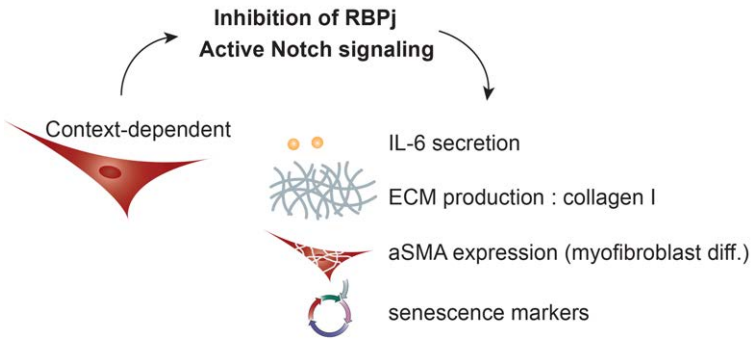

Figure 5: Summarized functions of Notch signaling in nonlymphoid tissue fibroblasts. Several studies performed in lung, skin, kidney and liver fibrotic diseases, and in chronic inflammatory disorders such as rheumatoid arthritis revealed an increased Notch signaling activity that has been linked to increased expression of IL-6, ECM (Collagen type I), α-SMA as well as senescence markers.

The previous study of Procopio et al. also bring evidence of various RBP-Jκ target genes by using ChIP assays on human dermal fibroblasts (Procopio, Laszlo et al. 2015). Identified RBP-Jκ binding sites was divided into different categories such as pro-inflammatory and growth cytokines, ECM and surface markers (Procopio, Laszlo et al. 2015) (**Fig.6**). Many of these identified binding sites are genes present in FRC of SLO as ECM genes but also IL-7, PDGFRα and VEGF (Chyou, Ekland et al. 2008), that could potentially reveal a function of Notch signaling in FRC (**Fig.6**).

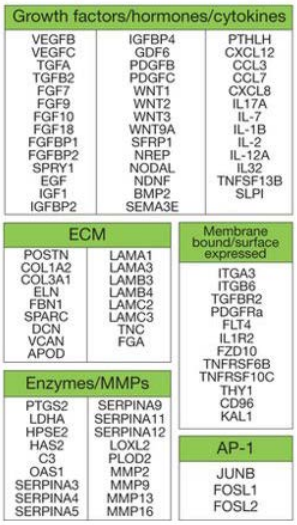

Figure 6: List of genes found to be targeted by RBP-Jκ by ChIP-Seq analysis in primary human dermal fibroblasts (From Procopio, Laszlo et al. 2015).

7. Notch signaling in SLO fibroblasts

Hardly anything is known on a role for Notch receptors on fibroblasts in SLO. In contrast, recent evidence points to a function for these fibroblasts as important Notch ligand source driving cell differentiation and several immune cell processes (Radtke, MacDonald et al. 2013). DLL1-mediated Notch2 signaling is known to be essential for splenic development of MZB cells and ESAM+ DC just outside of the WP (Hozumi, Negishi et al. 2004) (Saito, Chiba et al. 2003). Loss-of-function experiments using DLL1 fl/fl^{CCL19Cre} mice revealed that CCL19cre+ fibroblasts provide the critical DLL1 ligand, presumably within splenic B-cell follicles (Fasnacht, Huang et al. 2014).

T-cell specific ablation of Notch1 and Notch2 impaired differentiation of follicular helper T cells as well as deficient GC development and absence of high-affinity antibody in draining lymph-node of immunized mice (Auderset, Schuster et al. 2013). Similar loss-of-function experiments performed on DLL1 fl/fl^{CCL19Cre} and DLL4 fl/fl^{CCL19Cre} mice revealed the important role of DLL4-expressing LN stromal cells within the B-cell follicles and more precisely DLL4-expressing FDC, MRC and B zone reticular cells in Notch-mediated follicular helper T differentiation (Fasnacht, Huang et al. 2014). Implication of fibroblasts of SLO as Notch ligand source, that drives alloimmune response, was also described in graft versus host disease (Chung, Ebens et al. 2017). FRC and FDC DLL1/4-mediated Notch signals were delivered to donor T cells after bone-marrow transplantation, that lead to T cell autoreactivity and induce graft versus host disease (Chung, Ebens et al. 2017).

To conclude, fibroblasts of B-cell follicles as well as FRC form niches providing Notch ligands and thereby regulate immune cell differentiation in the spleen and activated LN but also drive alloimmune response after allogeneic bone-marrow transplantation.

8. Notch signaling: a clinical target

Given that Notch receptors play fundamental roles in many tissues, it is not surprising that mutations of this signaling pathway are involved in several different diseases. Above in chapter 6, I have summarized the evidence from the field of fibrosis showing that an overstimulated Notch signaling pathway in fibroblasts can give rise to disease in various tissues. Many studies indicate that Notch signaling also plays key roles in carcinogenesis and tumour progression. Weng et al. identified activating Notch1 mutations within the HD and PEST domains as the main oncogenic drivers of T-cell acute lymphoblastic leukemia (T-ALL) in children (Weng, Ferrando et al. 2004). The use of γ-secretase inhibitors in the clinics has been already initiated for patients suffering from T-ALL (Lobry, Oh et al. 2014).

Activating Notch1 mutations were also identified in patients suffering from chronic lymphocytic leukemia (CLL) which is the most frequent leukemia in adults. In splenic marginal zone lymphoma patients Notch2 has been identified as the most mutated gene consistent with an overactivated Notch2 pathway as driver of this disease (Lobry, Oh et al. 2014). Then, lymphangiogenesis in tumor cells, mediated by Notch signaling, promote tumor cell spread all over the body. Therefore, Notch signaling may be targeted in therapy to inhibit metastasis development by inhibition of tumor lymphangiogenesis (Niessen, Zhang et al. 2011). In summary, the implication of Notch signaling was described in many features of the tumor microenvironment such as vascular architecture, interaction and activation of the mesenchyme as well as functions in infiltrated immune cells (Meurette and Mehlen 2018). Therefore, various therapies that target Notch signaling at different levels have been developed (Ran, Hossain et al. 2017). Interference with Notch receptors or ligands was described by using either monoclonal antibodies, receptor decoys, siRNA or protease inhibitors that inhibit Notch signaling by inactivation of cleavages implicated in the release of the NICD into the cytoplasm. γ-secretase inhibitors that trigger apoptosis of tumor cells though inhibition of proteasome activity are currently the most extensively explored therapeutic approach (Yuan, Wu et al. 2015). However, clinical trials of γ-secretase inhibitors have been associated with considerable gastrointestinal issues in patients (Grosveld 2009). In fact, blocking of γ-secretase induces intestine toxicity due to an increase of goblet cell differentiation and arrested cell proliferation in the intestinal crypts (Milano, McKay et al. 2004).

The link between the Notch pathway and pathologies has been also extended to several other diseases including graft versus host disease after bone-marrow transplantation (Chung, Ebens et al. 2017) but also CADASIL syndrome (cerebral autosomal arteriopathy with subcortical infarcts and leukoencephalopathy) affecting the brain, Alagille syndrome affecting heart, eye and vertebrae and spondylocostal sysostosis affecting vertebrae and ribs (Andersson and Lendahl 2014).

The ability of the Notch signaling pathway to carry out many functions despite a simple molecular architecture relies on the broad spectrum of control levels which are context-dependent.

Achieving a more complete understanding of the signaling complexity will be a major challenge for future research, due to the implication of Notch signaling in many pathologies.

V. Aim of this thesis

Despite recent evidence showing FRC of SLO as important Notch ligand source driving cell differentiation and several immune cell processes, no study has shown the role of Notch receptor expression on FRC themselves (Fasnacht, Huang et al. 2014) (Chung, Ebens et al. 2017). Gene array data on murine LN stroma published by the Immunological Genome Project (Malhotra, Fletcher et al. 2012), as well as similar gene array data from our lab (unpublished), revealed the expression of Notch receptors, the downstream transcription factor RBP-Jκ and some of the Notch target genes (Hey-1, Hes-1) in FRC. I also observed the surface expression of Notch1 and Notch 2 protein in LN FRC. These data are consistent with the presence of an active Notch signalling pathway in FRC. Extensive literature describing an array of Notch functions in fibroblasts of non-lymphoid tissues such as ECM and cytokine production as well as differentiation suggests a possible role for Notch signalling in LN FRC. Therefore, this thesis aimed to understand the role of Notch signalling in LN FRC in development, homeostasis and immunity.

To address this aim, I made use of modern mouse genetics, by crossing mice with a CCL19Cre recombinase active specifically in FRC (Onder, Scandella et al. 2011, Chai, Onder et al. 2013) with mouse strains having conditional alleles of key Notch signaling molecules, namely Notch1 (Radtke, Wilson et al. 1999), Notch2 (Besseyrias, Fiorini et al. 2007), and RBP/J (Han, Tanigaki et al. 2002).

To understand the role of Notch signalling in LN FRC, the following points were investigated:

1. According to the implication of Notch signaling in differentiation, cell proliferation and/or survival in various cell types (Radtke, Fasnacht et al. 2010) (Niessen, Zhang et al. 2011), we hypothesized that Notch signaling in FRC may have such a role for FRC. Therefore, FRC numbers, subsets and organization were studied in pLN and spleens of Notch1/2 ^{CCL19Cre} mice, using flow cytometry and histology.
2. Notch signaling in fibroblasts has been mainly described to stimulate ECM production (Procopio, Laszlo et al. 2015, Hu and Phan 2016). In synovial fibroblasts, Notch signaling was also described to mediate TNF-α-dependent IL-6 production (Jiao, Wang et al. 2012). We therefore hypothesized that Notch signaling in FRC can regulate FRC functions such as ECM and cytokine production and investigated it by immunohistology and qRT-PCR in pLN and spleens of Notch1/2 ^{CCL19Cre} mice.

3. FRC are known to regulate neighbouring cell behaviour due to their network organization and capacity to secrete cytokines and chemokines which regulate the positioning and function of immune cells (Fletcher, Acton et al. 2015). By expressing VEGF, FRC also directly stimulate endothelial cells of the LN vasculature (Chyou, Ekland et al. 2008). We hypothesized that if Notch signaling regulates FRC functions, it may also impact neighbouring cells. Therefore, immune cells, LEC and BEC were investigated by flow cytometry and histology in Notch1/2 ^{CCL19Cre} mice.
4. As FRC constitute a major player in the induction of the adaptive immune response (Fletcher, Acton et al. 2015), LN of Notch1/2^{CCL19Cre} mice were investigated after immunization, to understand if Notch signaling in FRC could regulate T cell responses.
5. Notch signaling has been described to play an important role in embryonic and postnatal development (Hori, Sen et al. 2013). To distinguish between developmental versus homeostatic roles of Notch signaling in FRC, phenotypes of adult mice were compared to three weeks old Notch1/2 ^{CCL19Cre} mice.
6. As the above experiments led to many interesting findings, described in the following, we investigated the above questions also for mice lacking either Notch1 or Notch2 in FRC, to understand the relative roles of each Notch receptor in isolation. Then, to test whether activation of Notch1/2 in FRC uses the canonical Notch signaling pathway through the transcription factor RBP-Jκ, RBP-Jκ ^{CCL19Cre} mice (Han, Tanigaki et al. 2002) were generated and characterized similarly as Notch1/2^{CCL19Cre} mice.

Results

1. Naive pLN FRC express Notch receptors and target genes pointing to an active Notch signaling pathway in this cell type

In peripheral lymph nodes, three distinct stromal cell types can be distinguished according to their pdpn and CD31 expression among CD45- CD35- cells isolated from digested organs, CD31- Pdpn+ FRC, CD31+ Pdpn+ LEC and CD31+ Pdpn- BEC (**Fig. 7A**). FRC themselves can be further divided into three subsets according to their expression of MAdCAM and CD157: TRC (CD157+ MAdCAM-), MedRC (CD157- MAdCAM-) and MRC (CD157+ MAdCAM+) (**Fig. 7A**). A gene array was performed in the lab on sorted TRC and MedRC subsets from naive pLN of WT B6 mice which I searched for the different components of the Notch signaling pathway. We observed no striking difference for transcription expression of these different genes between naïve TRC and MedRC (**Fig. 7B**). *Notch1*, *Notch2* and *Notch3* transcripts are expressed at similar levels, with *Notch4* being expressed around 4-fold less. LN FRC also express transcripts for *RBP-Jκ* and the two Notch target genes, *Hes1* (Jarriault, Brou et al. 1995) and *Hey1* (Belandia, Powell et al. 2005) (**Fig. 7B**). The expression of these different actors of Notch signaling suggests the presence of an active Notch signaling pathway in pLN FRC.

In order to confirm the expression of Notch receptors at the protein level as well as at the single cell level, I measured Notch1, Notch2 and Notch3 surface expression by flow cytometry on pLN stromal cells from naive adult WT mice. I observed that FRC express higher levels of Notch1 than Notch2, with Notch3 expression being hardly detectable in FRC or EC (**Fig. 7C-D**). Notch1 and Notch3 antibodies were preliminary tested and validated on double negative (CD4- CD8-) thymic cells from WT mice. According to the gene arrays data from Malhotra et al., LEC express, at RNA level, a high expression of Notch2 (Malhotra, Fletcher et al. 2012). Therefore, Notch2 antibody was tested and validated on WT LEC. 78% of FRC express Notch1, and around 34% express Notch2 (**Fig. 7D**). In contrast, almost all LEC and BEC express high Notch1 levels with Notch2 expression being heterogeneous in LEC and absent in BEC (**Fig. 7C**). I observed a similarly high Notch-1 expression between MedRC (CD157-) and TRC/MRC (CD157+) populations with 75-80% of them expressing Notch-1 at their cell surface. More MedRC than TRC/MRC express Notch-2, with 50% versus 25% being positive, respectively. It appears as if Notch-2 expression levels on MedRC subset are heterogeneous with either a low or intermediate expression (**Fig. 7E**)**.**

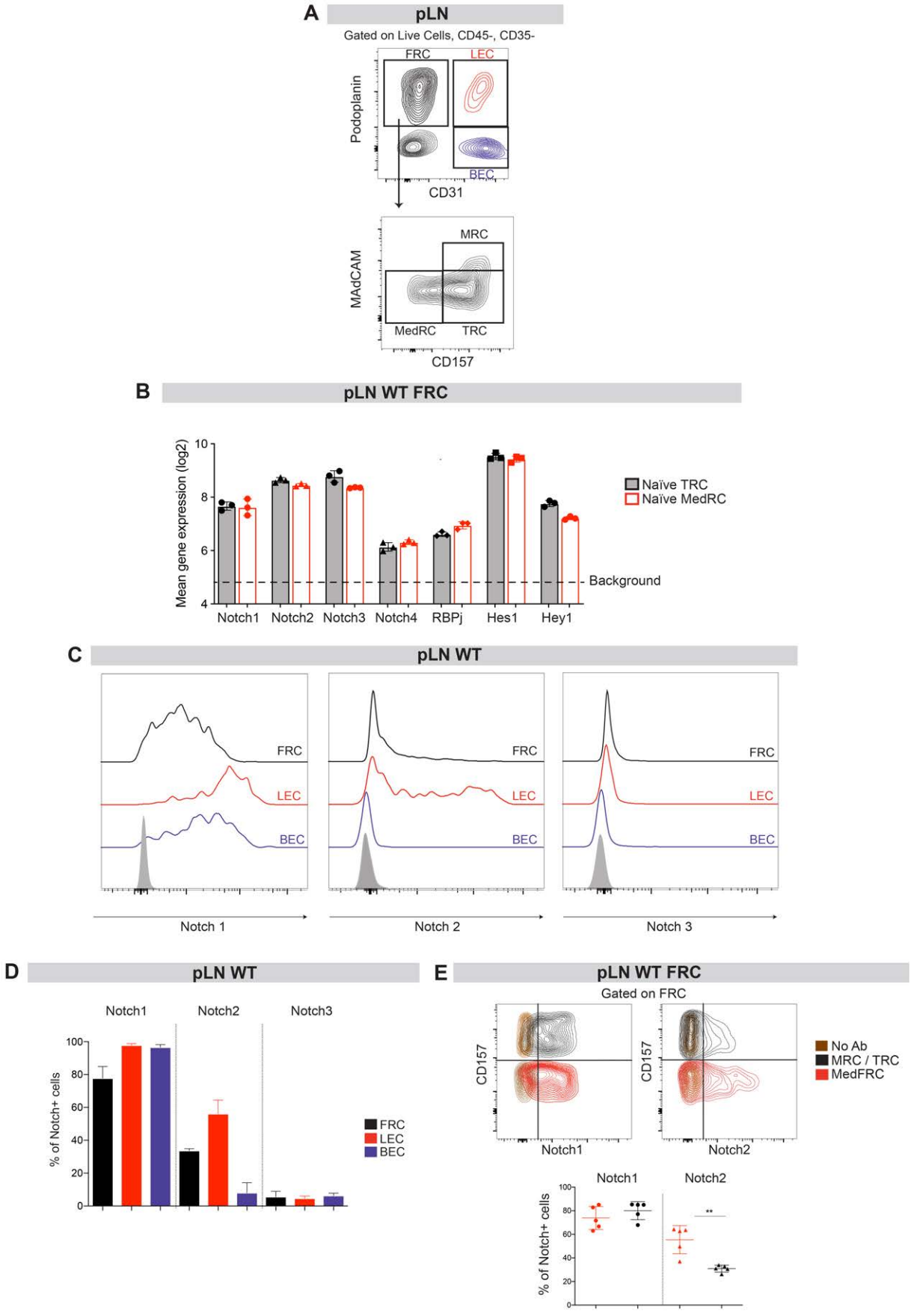
A
pLN
Gated on Live Cells, CD45-, CD35-
FRC
LEC
Podoplanin
BEC
CD31
MRC
MAdCAM
MedRC
TRC
CD157
B
pLN WT FRC
Mean gene expression (log2)
Naïve TRC
Naïve MedRC
Background
Notch1
Notch2
Notch3
Notch4
RBPj
Hes1
Hey1
C
pLN WT
FRC
LEC
BEC
Notch 1
Notch 2
Notch 3
D
pLN WT
Notch1
Notch2
Notch3
% of Notch+ cells
FRC
LEC
BEC
E
pLN WT FRC
Gated on FRC
CD157
Notch1
Notch2
No Ab
MRC / TRC
MedFRC
% of Notch+ cells

Figure 7: Lymph-node FRC express Notch 1 and Notch 2 receptors and show evidence of an active signaling pathway. A) Flow cytometric analysis of live CD45- and CD35- cells from enzymatically digested pLN of naïve C57BL/6 mice. The upper contour plot shows how the three stromal subsets (FRC, LEC and BEC) were distinguished according to their CD31 and pdpn (podoplanin) expression. Then contour plot below shows how FRC were divided into three subsets (TRC, MedRC and MRC) according to their expression of CD157 (BP-3) and MAdCAM: TRC (CD157+, MAdCAM-), MedRC (CD157-, MAdCAM-) and MRC (CD157+, MAdCAM+). **B)** mRNA expression analysis for Notch receptors, the main Notch transcription factor RBPj and two Notch target genes (Hes1 and Hey1) in naïve TRC and MedRC populations sorted from fully digested pLN of C57BL/6 mice. Dotted line indicates the background level with the expression of epithelial cell adhesion molecule, negative in FRC subsets. Log2 data were extracted from an Affymetrix 1.0 gene array dataset generated in our laboratory. Each sample (n=3) was derived from a pool of four naïve mice. **C-E)** Flow cytometric analysis of CD45-CD35- stromal cells from digested pLN from naïve WT mice. **C)** Histograms show Notch1, Notch2 and Notch3 protein expression profiles in stromal cells (FRC, LEC, BEC) **D)** Quantification of the proportion of these stromal cell subsets expressing these Notch receptors. Data are representative of three independent experiments (n=5). **E)** Contour plots on show the surface Notch 1 and Notch2 expression in MedRC (CD157- FRC) and TRC/MRC (CD157+); scatter plots show the quantification of Notch1- and Notch2-positive cells in these two FRC subsets. Data are representative of three independent experiments (n=5). P values are indicated as ** for $p< 0.01$.

To conclude, FRC express Notch1 and Notch2 receptors at the RNA and surface protein level. As transcripts for RBPj and well-known Notch target genes can be observed in FRC these data indicate that the Notch signaling pathway may be active in naive pLN FRC.

In order to investigate the function of Notch signaling in LN FRC *in vivo*, we established a mouse cross in which only lymphoid tissue FRC lack the expression of Notch1 and Notch2 receptors. We used a BAC transgenic mouse model that drives expression of the Cre-recombinase under the control of the CCL19 promoter, which is known to be active in pLN FRC (Onder, Scandella et al. 2011, Chai, Onder et al. 2013). We intercrossed this CCL19-cre mouse line with Notch1$^{lox/lox}$ (Radtke, Wilson et al. 1999) and/or Notch2$^{lox/lox}$ (Besseyrias, Fiorini et al. 2007) mice to obtain Notch1^{CCL19Cre}, Notch2^{CCL19Cre}, and Notch1/2^{CCL19Cre} mice (**Fig. 8A**). Initially, we investigated the double-floxed Notch1/2^{CCL19Cre} mice, as we expected these mice to have a stronger phenotype than the single floxed mice. Littermates lacking the Cre transgene (Notch1/2$^{fl/fl}$, or referred to as Notch1/2$^{CCL19Cre-)}$ were used as negative controls. Flow cytometric analysis of surface Notch1 and Notch 2 expression in pLN stroma indicated an efficient deletion of Notch 1 (deletion of around 73%) in Cre+ versus Cre- mice along with the loss of the low Notch 2 expression (deletion of around 46%) (**Fig. 8B, C**). Of note, while the Notch1 staining level on LN FRC allows to measure deletion efficiency in a reliable way, this is less the case for the low Notch2 staining intensity. To investigate the specificity of the deletion model, we analysed the surface expression of Notch1 and Notch2 in LEC and BEC which did not show any significant difference (**Fig. 8C**). We also did not observe a significant difference in percentage of Notch3+ cells in the three stromal cell subsets due to the deletion of the two other Notch receptors (**Fig. 8C**).

As the CCL19cre mouse line was reported to delete better in TRC/MRC versus MedRC (Huang, Rivas-Caicedo et al. 2018) we also investigated the deletion efficiency in the two major FRC subsets. The staining for Notch1+ cells in MedRC and TRC/MRC, revealed a reduction of 61% and of 71%, respectively, when cells from Cre+ versus Cre- mice were compared. For Notch2, a 34% versus 46% reduction of Notch2+ cells was observed cells in MedRC and TRC/MRC, respectively (**Fig. 8D**). In summary, Notch1/2^{CCL19Cre} mice allow to delete the majority of Notch1/2 expression on LN FRC.

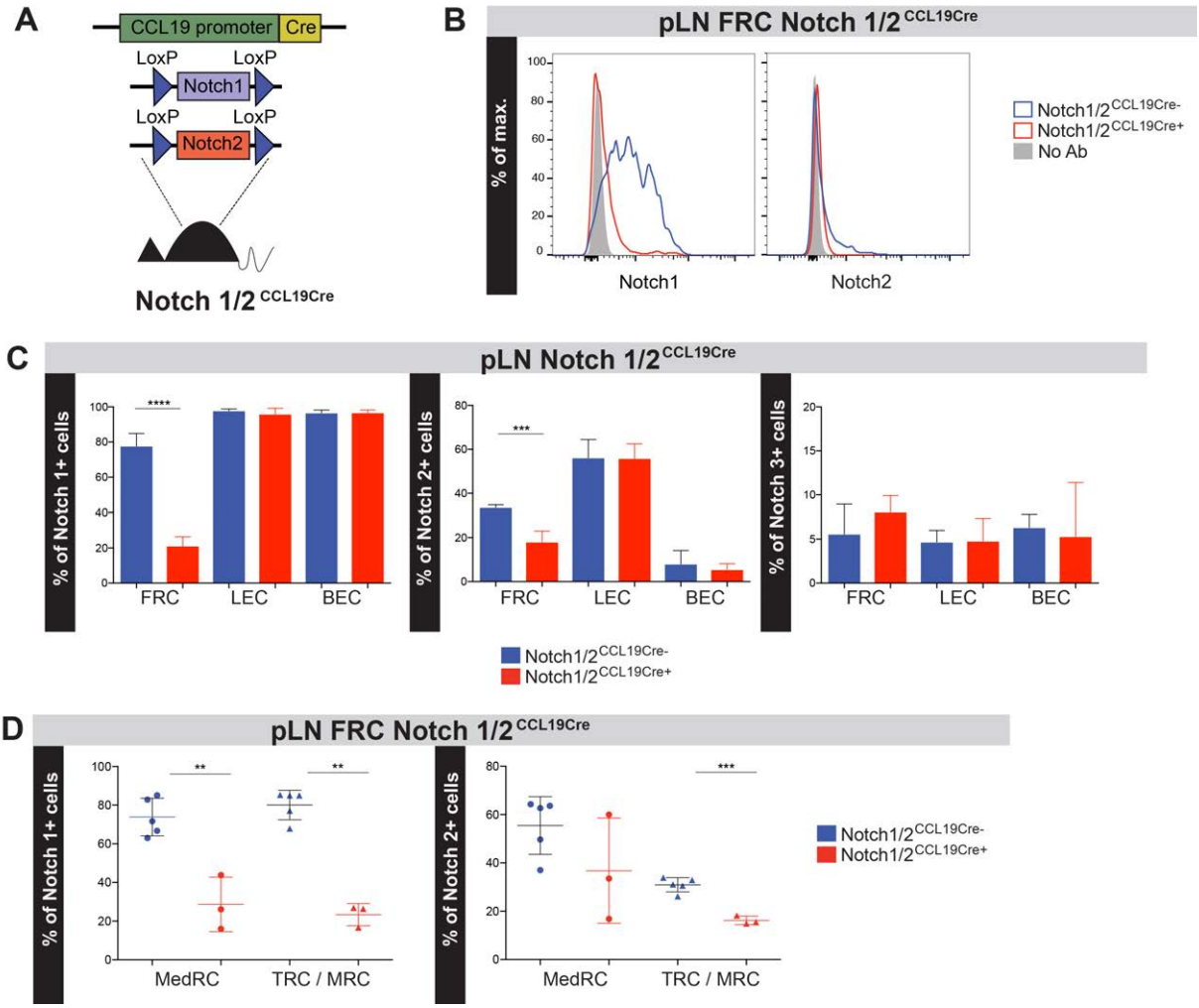

Figure 8: Notch1/2^{CCL19Cre} mice, a specific genetic tool to study by loss-of-function experiments the role of Notch signaling in pLN FRC. A) Simplified representation of the three mouse alleles that are needed to generate the new mouse model, Notch1/2^{CCL19Cre} , in order to study the role of combined absence of Notch1/2 in lymphoid tissue FRC. The Cre-recombinase is under constitutive control of the promoter responsible for CCL19 chemokine expression, which is largely restricted to FRC in LN, spleen and Peyer's patch. Two loxP sites flank both genes, Notch1 and Notch2, and when crossed to CCL19cre mice should allow to delete essential elements of Notch1/2 selectively in FRC using the Cre-lox recombination system. **B-D)** Flow cytometric analysis of Notch surface expression on stromal cells (CD45-CD35-) isolated from naive pLN of adult Notch1/2 $^{CCL19Cre-}$ and Notch1/2 $^{CCL19Cre+}$ mice to measure the efficiency and specificity of gene deletion. **B)** Histograms showing Notch1 and Notch2 expression in FRC of Cre+ vs Cre- mice. Data are representative of three independent experiments. **C)** Bar graphs showing the percentage of Notch1, Notch2 and Notch3 positive cells in FRC, LEC and BEC. Data are representative of three independent experiments (n=3-5). **D)** Scatter plot showing the percentage of Notch1 and Notch2 positive cells in MedRC (CD157-) versus TRC/MRC (CD157+). Data are representative of three independent experiments (n=3-5). P values are indicated as, ** for p< 0.01, *** for p<0.001, **** for p<0.0001.

2. Notch1/2 deletion in FRC impacts on FRC size, 3D organisation and function, including matrix and CCL19 production

To investigate the direct effect of Notch1/2 deletion in FRC, I started with flow cytometric analysis of stromal cells and FRC subsets from digested pLN of naive adult Notch1/2^{CCL19Cre} mice. This analysis revealed a 30% decrease in total cell numbers in Cre+ vs Cre- mice with no difference observed for the proportion of FRC, LEC and BEC (**Fig. 9A**).

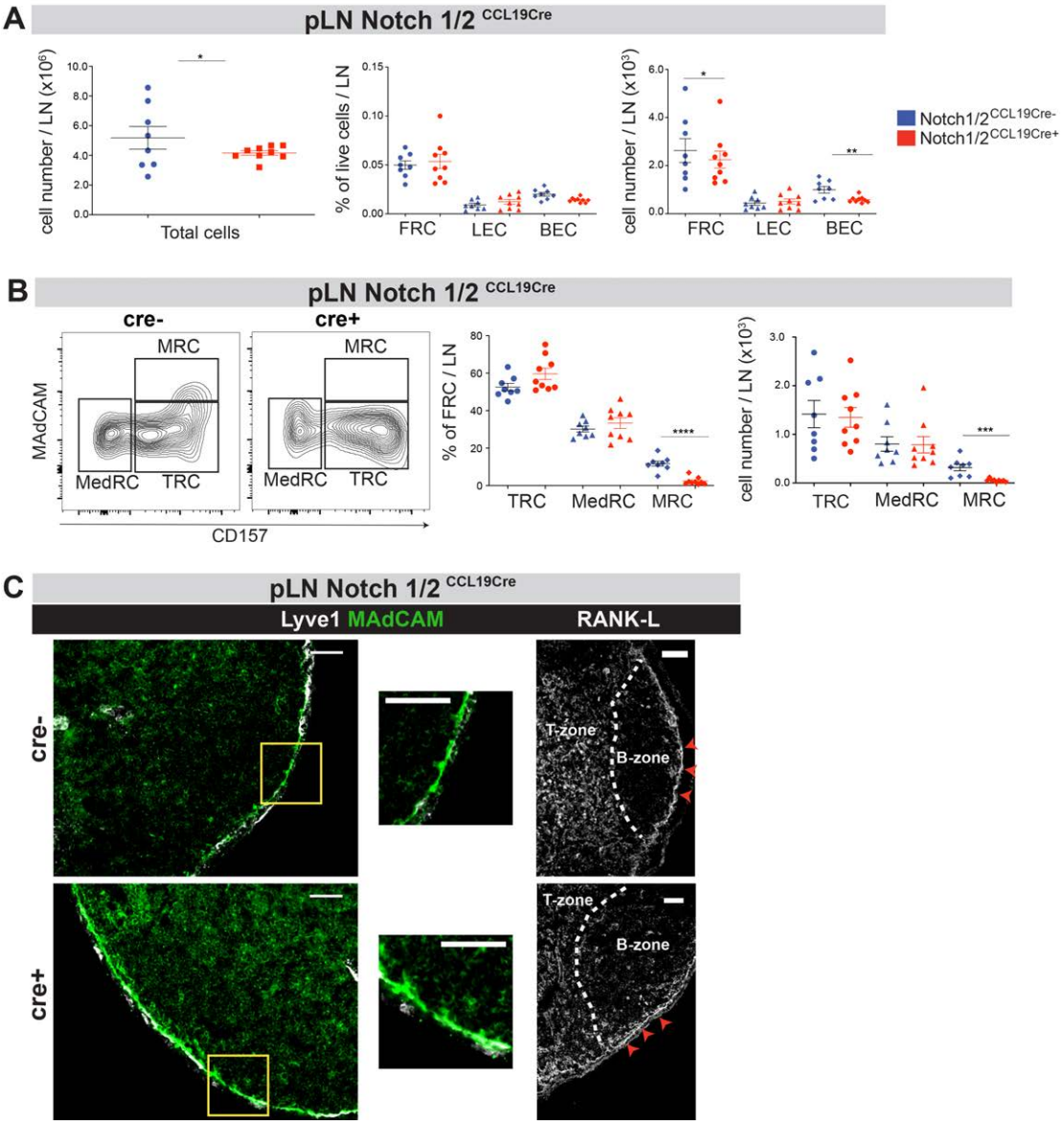

Figure 9: Notch1/2 deletion in FRC leads to a loss in total cell numbers. Naive pLN of adult Notch1/2^{CCL19Cre} mice were analyzed and we compared Cre- vs Cre+ littermate mice. **A-B)** Flow cytometry analysis of relative and absolute cell numbers for: total cells, stromal cells (FRC, LEC, BEC) and FRC subsets (TRC, MedRC, MRC) of digested pLN. Then contour plots (**B**) show how FRC were divided into FRC subsets according to their expression of CD157 and MAdCAM. Data are representative of three independent experiments (n=6-8). **C)** Immunohistological analysis of Cryostat sections of subcapsular region of pLN. Specialized stromal cells called MRC can be identified as MAdCAM+ RANK-L+ Lyve1- cells (red arrows) on the cortical side of the subcapsular sinus (SCS) lining, underneath the single layer of lyve1+ lymphatic endothelial cells. Scale bar, 50 µm. Data are representative of three independent experiments. P values are indicated as * for $p < 0.05$, ** for $p< 0.01$, *** for $p<0.001$ and **** for $p<0.0001$.

FRC themselves showed a significant 15% decrease in absolute cell numbers. Notch1/2 deletion in FRC also led to a decrease trend for BEC proportion, as well as a significant decrease (~ 51%) of absolute cell numbers for BEC, with no significant difference observed for LEC (**Fig.9A**). Analysis of FRC subsets did not reveal a difference for TRC and MedRC proportions or numbers in Notch1/2^{CCL19Cre} mice relative to littermate controls, but a striking decrease in relative (~ 79%) and absolute (~ 87%) cell numbers observed for the MRC subset (**Fig.9B**). The MRC population was further investigated by immunohistological analysis of pLN sections of Notch1/2^{CCL19Cre} mice. The outer region of the LN cortex is surrounded by the subcapsular sinus (SCS), that is formed by a layer of lymphatic endothelial cells marked by CD31, MAdCAM and lyve1. A thin layer of MRC is observed on the outer edge of the B-cell follicle region, underneath the SCS. MRC express MAdCAM and also RANKL/TRANCE (Katakai, Suto et al. 2008), a TNF family cytokine that is essential for LN development (Dougall, Glaccum et al. 1999). MAdCAM+ Lyve1- MRC were hardly visible in Cre- and Cre+ mice due to the thin MRC processes and due to the presence of the adjacent lymphatic layer (**Fig.9C**). Using the more MRC-restricted marker, RANK-L, we still observed the presence of the thin MRC layer in mice bearing a Notch1/2 deletion in FRC (**Fig.9C**). This histological finding is in contrast to the flow cytometry data, which are based only on MAdCAM staining to identify MRC (**Fig.9B**), as RANKL staining on digested tissues usually does not work.

In order to study FRC in more detail, analysis of the mean fluorescence intensity (MFI) of FRC subsets for size (FSC), granularity (SSC) and pdpn marker was assessed. All parameters, such as size (FSC) and granularity (SSC) showed an increase trend for all FRC subsets upon deletion of Notch1/2 in FRC (**Fig.10A**). TRC seems to be stronger affected with a significant 26% and 30% increase in size and granularity, compare to a 14% and 18% increase for MedRC and no difference and a significant 35% for MRC in size and granularity (**Fig.10A**). A significant 2-time increase of podoplanin MFI was observed in TRC, and no significant difference was observed for MedRC and MRC. Increase of TRC size, granularity and podoplanin expression suggest a higher activation state for TRC (Yang, Vogt et al. 2014) (**Fig.10A**). In conclusion, FRC activation state seems to be affected by Notch1/2 deletion, which a stronger effect on TRC population. Next, the cell network formed by FRC within pLN T zones was investigated in Notch1/2^{CCL19Cre} mice by immunohistological analysis and widefield microscopy, using the two FRC markers podoplanin and desmin. The podoplanin+ desmin+ TRC network did not show any striking difference in term of fluorescence intensity

for both markers (**Fig. 10B**) in contrary of previous flow cytometry data of pdpn expression level.

To study the structure of the TRC network of pLN in more detail, confocal microscopy was performed in 100um stacks to visualize the 3D structure at high resolution. The network of desmin+ T-zone FRC showed a somewhat altered 3D structure in Notch1/2^{CCL19Cre} mice, appearing less regular despite a comparable network density (**Fig.10C**). TRC are interconnected with special blood vessels called HEV that are the LN entry site of naïve lymphocytes and can be identified by their expression of PNAd (peripheral node addressin), a group of molecules including the CD34 molecule (von Andrian and Mempel 2003). The TRC appear to connect to and enwrap HEV normally (**Fig.10C**).

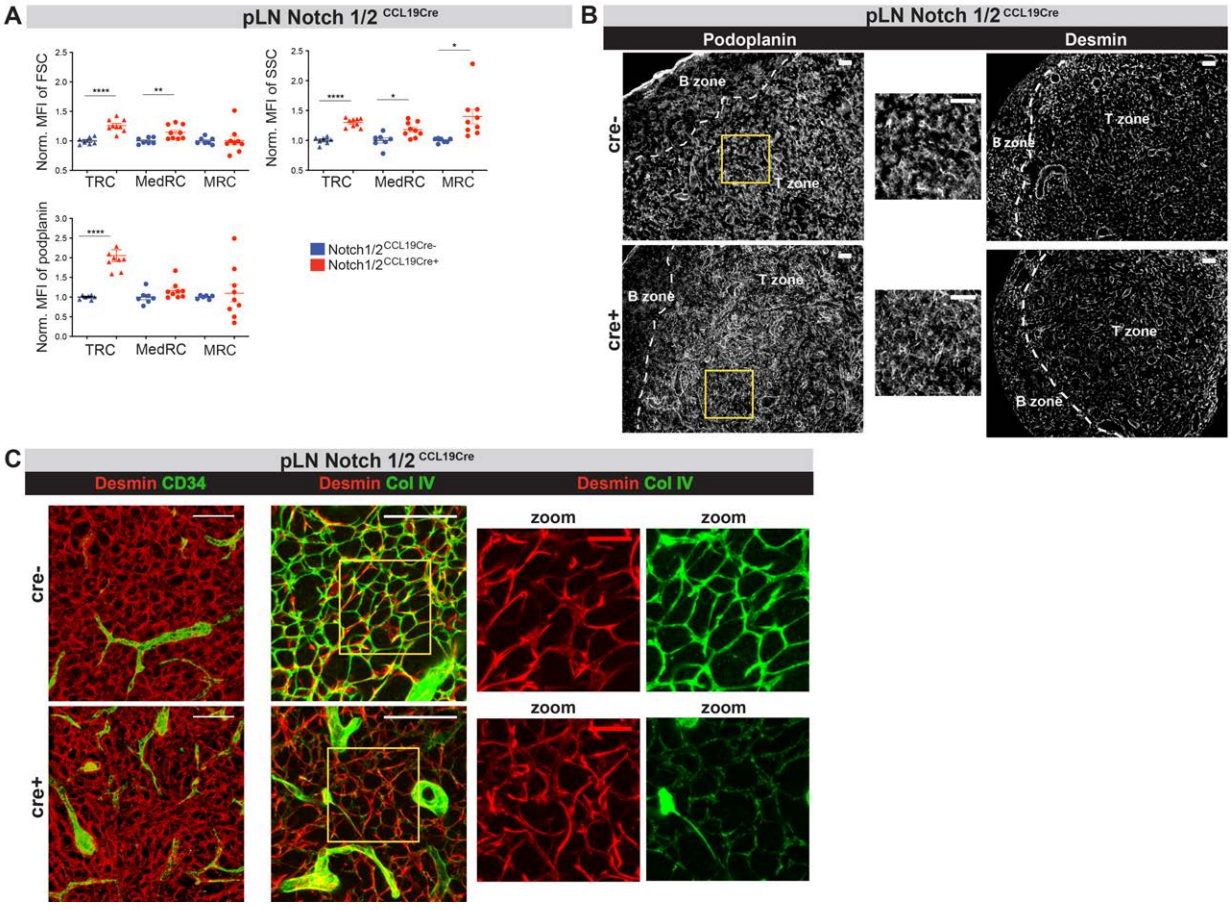

Figure 10: Notch1/2 deletion in FRC affects FRC size, activation state and TRC organization in pLN. A) Flow cytometric analysis of FRC subsets (TRC, MedRC and MRC) for FSC, SSC and podoplanin expression levels (MFI: mean fluorescence index) of digested pLN of Notch1/2^{CCL19Cre} mice. Data are representative of four independent experiments (n=9-10). **B)** Immunohistological analysis of cryostat sections stained for all FRC types using podoplanin and desmin as markers. Rectangles focus on T-zone FRC network that are shown also as zoom-in. Dashed lines indicate the limitations of B-cell follicles. Scale bar, 50 µm. Results are representative of three independent experiments. **C)** Confocal images of 100µm-vibratome sections. T-zone of pLN is stained for FRC (desmin), basement membranes of conduits and vessels (Collagen IV) and endothelial cells (CD34), including HEV. The rectangle focuses on the FRC network of the T-cell zone, shown in zoom-in in single color images. Scale bars: 50 µm for large images and 20 µm for the zoomed image area. Data are representative of two independent experiments. P values are indicated as * for $p < 0.05$, ** for $p< 0.01$, and **** for $p<0.0001$.

TRC produce extracellular matrix that they form into lymph-draining conduits that they enwrap almost completely. The basement membrane of these conduits was stained with collagen IV antibody, and this staining revealed a strongly reduced intensity on T zone conduits of Cre+ mice, in marked contrast to the normal collagen IV labelling of basement membranes around HEV (**Fig.10C**).

In summary, deletion of Notch1/2 in FRC does not strongly affect FRC numbers in adult pLN nor the generation of TRC or MedRC but leads to MRC alterations preventing their enzymatic isolation. FRC show an increase in size, granularity and most notably TRC show an increase of pdpn expression along with alterations in network organization. Most strikingly, collagen IV expression within T zone conduits appeared to be strongly reduced pointing to changes in FRC function, such as matrix production, assembly or turnover.

The matrix proteins TRC produce are virtually all assembled into the conduit structures that have a core of collagen fibers (collagen I and III) associated with fibrils (ERTR7) which are surrounded by a single basement membrane layer (collagen IV, fibronectin and laminin) (Gretz, Norbury et al. 2000, Roozendaal, Mebius et al. 2008) (**Fig.11A**). Therefore, ECM proteins produced by TRC were studied by immunohistological labeling of pLN sections. Analysis of the collagen I core revealed no difference in terms of staining intensity in Cre+ vs Cre- mice suggesting the existence of conduits despite the reduction of collagen IV staining. We noted an abnormal conduit network structure with an increased frequency of linear unbranched collagen fibers in Cre+ mice (**Fig. 11B, C**).

ECM proteins of the basement membrane, such as laminin and fibronectin, and of the microfibrillar zone, such as ERTR7, were strongly reduced in their amount as seen by the important decrease in signal intensity in pLN T zones of Notch1/2^{CCL19Cre} mice, with basement membranes around blood vessels showing normal laminin expression levels (**Fig.11B**). High-resolution images, through airyscanning acquisition, of ERTR-7 staining revealed the disrupted conduit structure of the microfibrillar zone with Notch1/2 deletion (**Fig.11D**) Quantification of signal intensities representative for matrix proteins founds within conduits showed significant decreases of 42% and 32% for laminin and ERTR7 signals, respectively, while the the collagen I signal in the conduit core was not affected by Notch1/2 deletion in FRC (**Fig.11E**). The latter finding was confirmed by RT-PCR analysis showing no difference in *collagen 1a1* and *collagen 1a2* transcripts on stroma-enriched pLN fractions in Cre+ versus Cre- mice (**Fig.11F**).

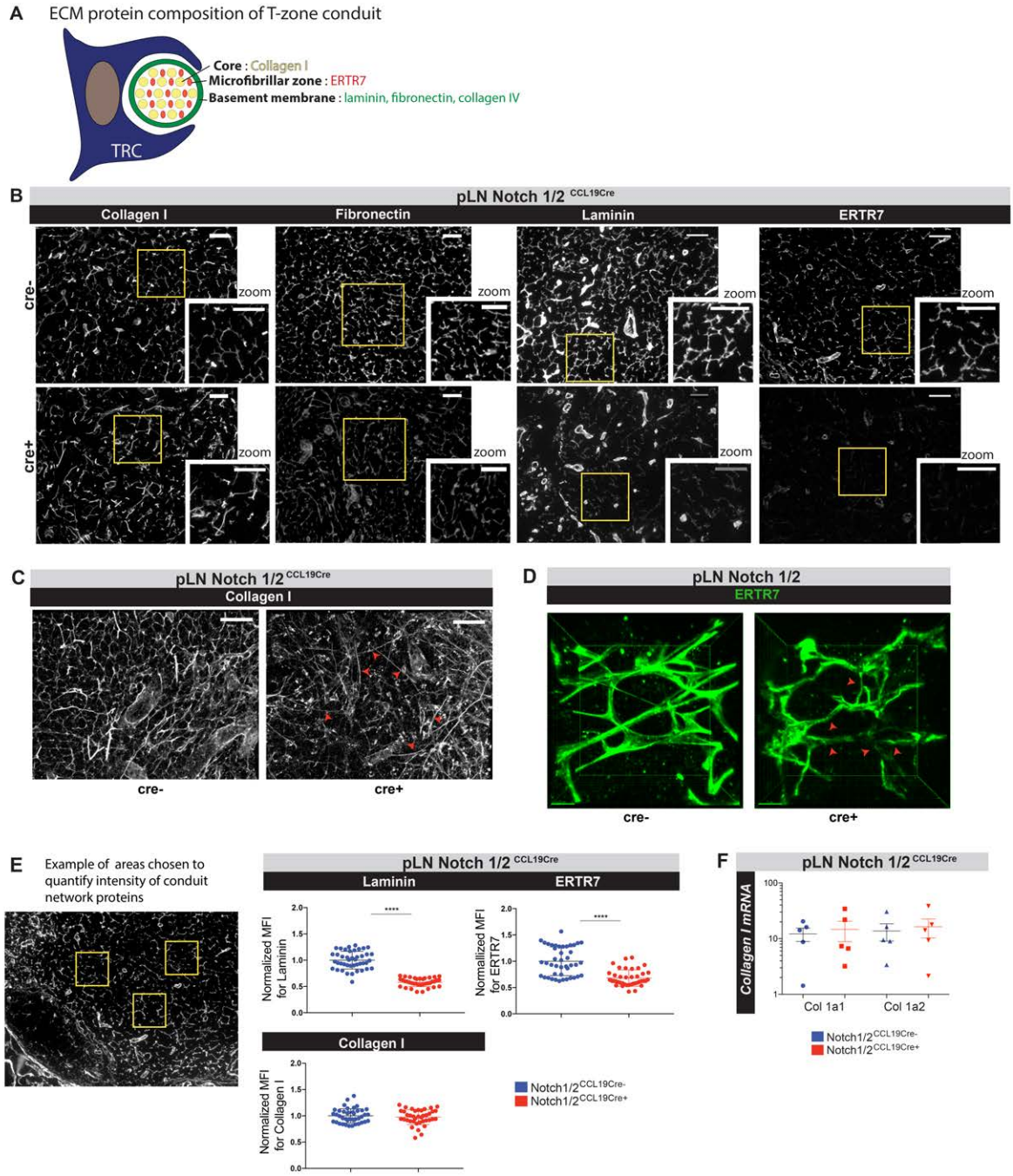

Figure 11: Notch1/2 deletion in pLN FRC results in conduits showing aberrant ECM protein expression and structure. A) Simplified representation of the ECM composition and structure of conduits within pLN T-zones. **B)** Immunofluorescence microscopy of cryostat sections of pLN from naïve Notch1/2^{CCL19Cre} stained for the indicated ECM protein markers. Data shown are representative images for the conduit networks of the T-cell zone. (Scale bar, 50 µm). Data are representative of three independent experiments. **C-D)** Confocal image stacks (100µm) of pLN vibratome sections from naïve adult Notch1/2^{CCL19Cre} mice **C)** Vibratome sections stained with collagen I and imaged within the central T-cell zone. Arrow points to the increased presence of long unbranched collagen I fibers in Cre+. Scale bar, 20 µm. Data are representative of two independent experiments. **D)** Vibratome sections stained with ERTR-7 and imaged with airyscanning acquisition within the central T-cell zone. Arrow points to the discontinued ERTR-7 conduit structure in Cre+. Scale bar, 5 µm. Data are representative of two independent experiments. **E)** Image on left side: Representative example showing how three areas (150 x 150 pixels; yellow squares) per image were chosen within the T zone while avoiding vessels. The MFI of ECM protein labels within these areas was quantified and is shown in the scatter plots on the right side. MFI values from Notch1/2$^{CCL19Cre+}$ sections have been normalized to values from Notch1/2$^{CCL19Cre-}$ sections. Data are representative of 3 independent experiments (n=6). P values are indicated as, **** for p<0.0001.F) qRT-PCR analysis on non-soluble fractions (stroma-enriched) of naïve pLN from Notch1/2^{CCL19Cre} mice. Shown is a scatter plot with levels of Col1a1 and Col1a2 normalized to two housekeeping genes (mean ± SD) (n=5).

In summary, deletion of Notch1/2 in pLN FRC decreases the expression of basement membrane and microfibrillar zone proteins found within T-zone conduits. Interestingly, the core shows a normal collagen I protein content but the structure seems to be altered. To conclude, pLN FRC and Notch signaling within these cells play a key role in ECM protein expression or turnover leading ultimately to proper T- zone conduit formation.

Besides ECM production, FRC are also well known for their production of cytokines such as IL-7, CCL19 and CCL21, especially by T zone FRC (Link, Vogt et al. 2007, Huang, Rivas-Caicedo et al. 2018). To this end, we analyzed transcripts levels in stroma-enriched pLN fractions from Notch1/2^{CCL19Cre} mice.

A 50% decrease of *ccl19* transcripts was observed in cre+ versus Cre- mice while no difference was observed for the second CCR7 ligand, *ccl21,* or for the T cell survival factor *il-7* (**Fig. 12A**). No striking difference was observed for two other stromal cell-derived factors: *cxcl13*, the principal chemokine organizing B cell follicles, and *il-33,* an alarmin present in FRC and LEC and previously proposed to be Notch dependent in endothelial cells (Sundlisaeter, Edelmann et al. 2012) (**Fig.12A**). *Il-6* transcripts, however, were 2-fold increased in Cre+ pLN (**Fig. 12A**)**.** As HEV and not only FRC produce large amounts of CCL21 (Gunn, Tangemann et al. 1998), I assessed the intracellular CCL21 protein expression in pLN FRC by flow cytometry. I observed no significant difference in the proportion of FRC expressing CCL21 nor in the CCL21 staining intensity (**Fig.12B**) suggesting Notch1/2 deletion in FRC impacts selectively CCL19 but not CCL21 expression.

To understand if the decrease of *ccl19* transcripts translates into reduced CCL19 protein expression within pLN, we took an indirect approach by investigating whether naive T cells encounter less CCL19 protein within pLN T zones. CCL19 binding to CCR7 leads to the efficient internalization of CCR7, and as consequence T cells from CCL19-/- pLN show an increased surface CCR7 expression, with CCL19+/- mice showing an intermediate phenotype (Britschgi, Link et al. 2008). Two different reagents were used to label surface CCR7 expression: An anti-CCR7 monoclonal antibody which detects all CCR7 expressed, independent of bound ligand, while the CCL19-Fc fusion protein binds to CCR7 via the CCL19 ligand-binding site and therefore is an indirect readout of CCR7 occupancy by CCL19 (Britschgi, Link et al. 2008). CCL19-Fc staining was strongly enhanced on naive lymphocytes from Cre+ versus Cre- mice, with a 2-fold increase on B cells, a close to 5-fold increase for T cells, with a slighly higher increase for CD8+ (5.7 times) compared to CD4+ (4.6 times) T cells (**Fig.12C-D**).

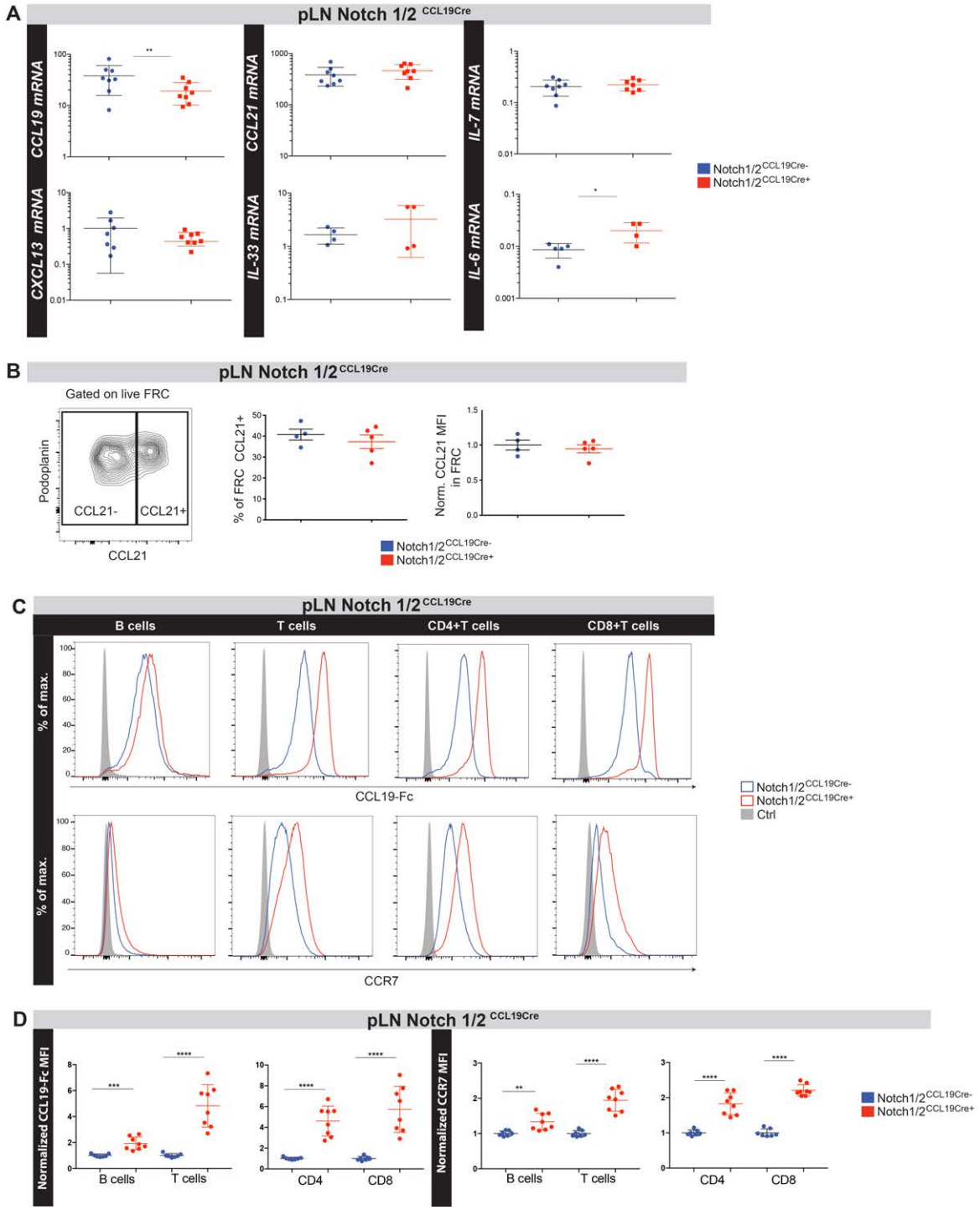

Figure12: Notch1/2 expression by pLN FRC is required for high expression levels of the T cell chemoattractant CCL19 but not CCL21. Shown are analysis of naive pLN from adult Notch1/2^{CCL19Cre} mice with littermates as control. **A)** qRT-PCR analysis on non-soluble fractions (stroma-enriched) of pLN for the normalized transcript levels of the indicated cytokines (mean ± SD) (n=4-8). **B)** Flow cytometric analysis of FRC from enzymatically digested pLN with the contour plot on the left side showing the intracellular expression of CCL21 protein, with the quantification in the scatter plots on the right side showing either the fraction of CCL21+ cells among FRC (top) or the normalized MFI for CCL21 signals within FRC. Data are representative of two independent experiments (n=4-5). C-D) Flow cytometric analysis of CCL19-Fc, anti-CCR7, or isotype control stainings on naïve T (CD19- TCRb+ CD44^{low}), CD4+ T / CD8+ T (CD19- TCRb+ CD44^{low}) and B (CD19+ TCRb-) lymphocytes. CCL19-Fc recognizes CCR7 free of bound CCL19, while anti-CCR7 antibodies label all surface CCR7 independent of bound ligands. Shown in **(C)** are representative histograms and in **(D)** scatter plots with the quantification of the MFI for the CCL19-Fc and anti-CCR7 stainings on the indicated cell types from Cre+ mice normalized to the signals from cells of Cre- mice. Data are representative of two independent experiments (n=7-8). P values are indicated as, ** for p< 0.01, *** for p<0.001, **** for p<0.0001.

As expected (Britschgi, Link et al. 2008), the anti-CCR7 staining intensity level was lower than the one for CCL19-Fc, with B and T cells from cre+ pLN showing an increase of 1.3-times and 2-times, respectively, relative to cells from Cre- pLN (**Fig. 12C-D**). Again a slightly stronger increase was observed for CD8+ (2.2-times) compared to CD4+ (close to 1.8-times) T cells (**Fig.12C-D**). Together, these data demonstrate that pLN of Notch1/2$^{CCL19Cre+}$ mice contain lower amounts of CCL19 protein detectable for recirculating T cells which leads to less CCR7 downregulation and more CCR7 able to bind CCL19. Therefore, my data indicate that Notch1/2 signaling in pLN FRC may be a new pathway regulating CCL19 expression (**Table1**).

3. Combined deletion of Notch1/2 in FRC leads to reduced T lymphocyte accumulation and less well demarcated B-cell follicles in pLN

CCL19 produced by FRC is believed to participate alongside CCL21 in the attraction of naive T cells and mature dendritic cells into T-zones of SLO (Link, Vogt et al. 2007) and their retention, motility, and survival in that microenvironment (Kaiser, Donnadieu et al. 2005) (Asperti-Boursin, Real et al. 2007). To test if the decreased CCL19 expression by Notch1/2-deleted FRC affects T cell accumulation in pLN, we studied lymphocyte populations by flow cytometric analysis. pLN from Notch1/2^{CCL19Cre} mice showed a decrease in relative (14%) and absolute numbers (32%) of T lymphocytes with this decrease being linked to an increase (30%) of relative but not absolute B cell numbers (**Fig.13A**). This T cell accumulation defect is stronger for CD8 than CD4 T cells, as seen in the shift for the relative cell numbers, with absolute numbers of CD8+ and CD4+ T cells in naive pLN of Cre+ versus Cre- mice being reduced by 41% and 27%, respectively. Both naive (CD44low CD62L+) and effector (CD44high CD62L-) CD8 T cells appear to be similarly decreased in percentage but not absolute numbers (**Fig.13A**).

To assess the global structure and T/B segregation in pLN from Notch1/2^{CCL19Cre} mice, immunohistological analysis was performed on tissue sections. A good segregation of T and B- lymphocytes with distinct T and B-cell zones was observed in both Cre+ and Cre- pLN (**Fig.13B**). However, the T cell staining appeared less dense in Cre+ mice, which could be due to the decrease of T lymphocyte numbers observed by flow cytometry (**Fig.13B**).

The B cell staining indicated an altered B-cell follicle shape in Cre+ pLN with follicles appearing less polarized and often fused together, in contrast to the separated and polarized follicles observable in Cre- pLN (**Fig.13B**)

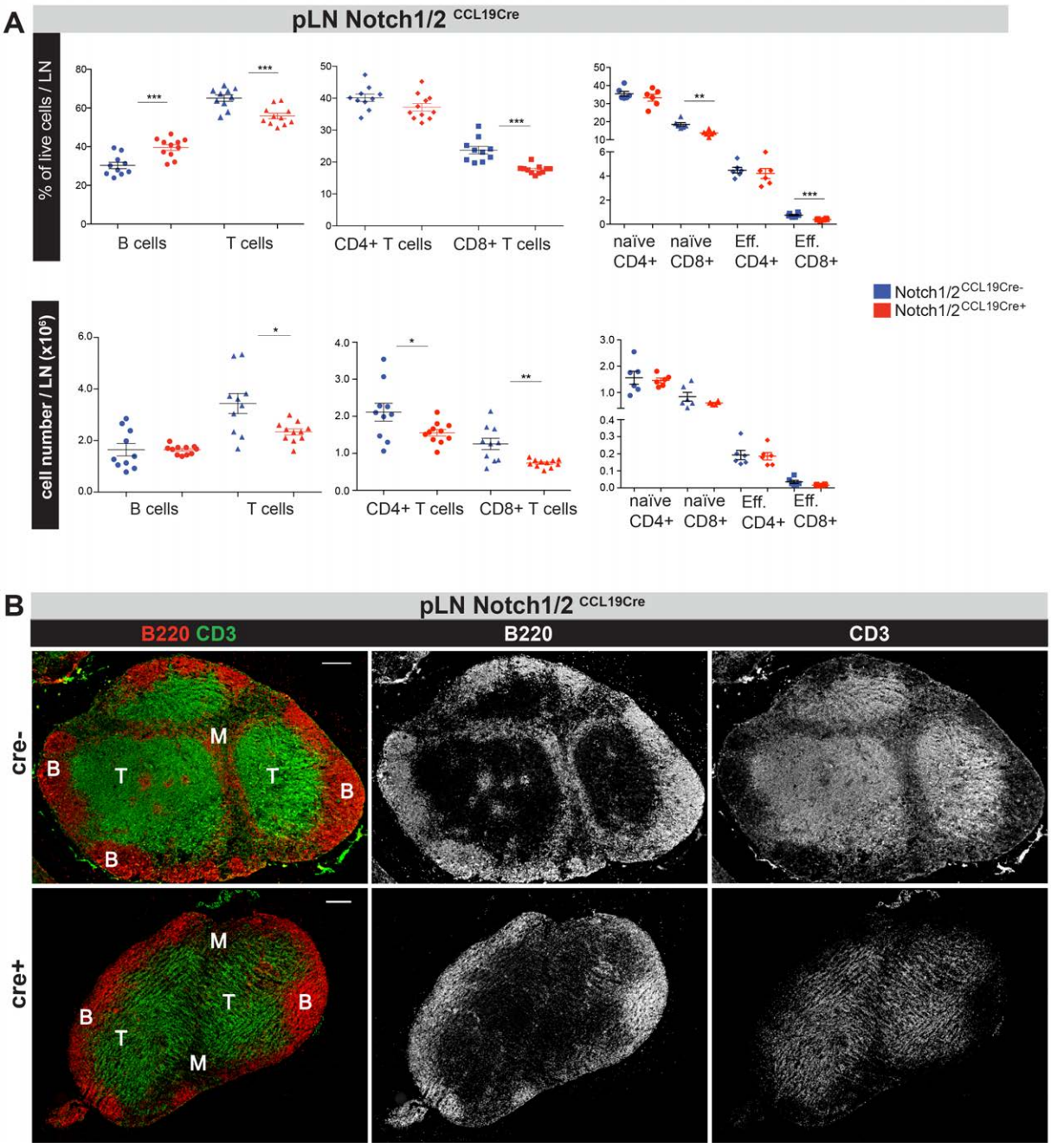

Figure 13: Notch1/2 deletion in FRC reduces naive T cell but not B cell accumulation in naive pLN. Analysis of naive pLN from adult Notch1/2^{CCL19Cre} mice. **A)** Flow cytometric analysis of the following lymphocyte populations: B cells (CD19+, TCRb-), T cells (CD19-, TCRb+), CD4+ or CD8+ T cells (TCRb+, CD4+/CD8+), subdivided into naive (CD44-, CD62L+) or effector (CD44+, CD62L-) T cell phenotypes with both subsets including presumably small memory populations. Data are representative of four independent experiments (n=10-11). P values are indicated as * for $p < 0.05$, ** for $p< 0.01$, *** for $p<0.001$. **B)** Immunofluorescence microscopy of pLN cryostat sections stained for CD3+ T cells and B220+ B cells. B, B cell zone (follicle); M, medulla; T, T-cell zone. Scale bar, 200 µm. Data are representative of two independent experiments.

In summary, lymphocytes are indirectly affected by the deletion of Notch1/2 in FRC, with T cells being present in reduced numbers and B cells segregating well from T cells but not forming proper follicular structures (**Table1**).

4. Combined deletion of Notch1/2 in splenic FRC also impairs CCL19 expression and T cell accumulation

To understand if the defects observed in pLN of Notch1/2^{CCL19Cre} are limited to these SLO, we also investigated the spleen which is the biggest SLO in the body but with blood and not lymph filtering function. Immunohistological analysis of the splenic white pulp architecture, and more precisely T zone FRC, showed no striking difference for the podoplanin+ TRC, as the staining intensity and reticular structure looked comparable in Cre+ and Cre- mice (**Fig14A**). However, we noted the existence of possibly smaller WP cords.

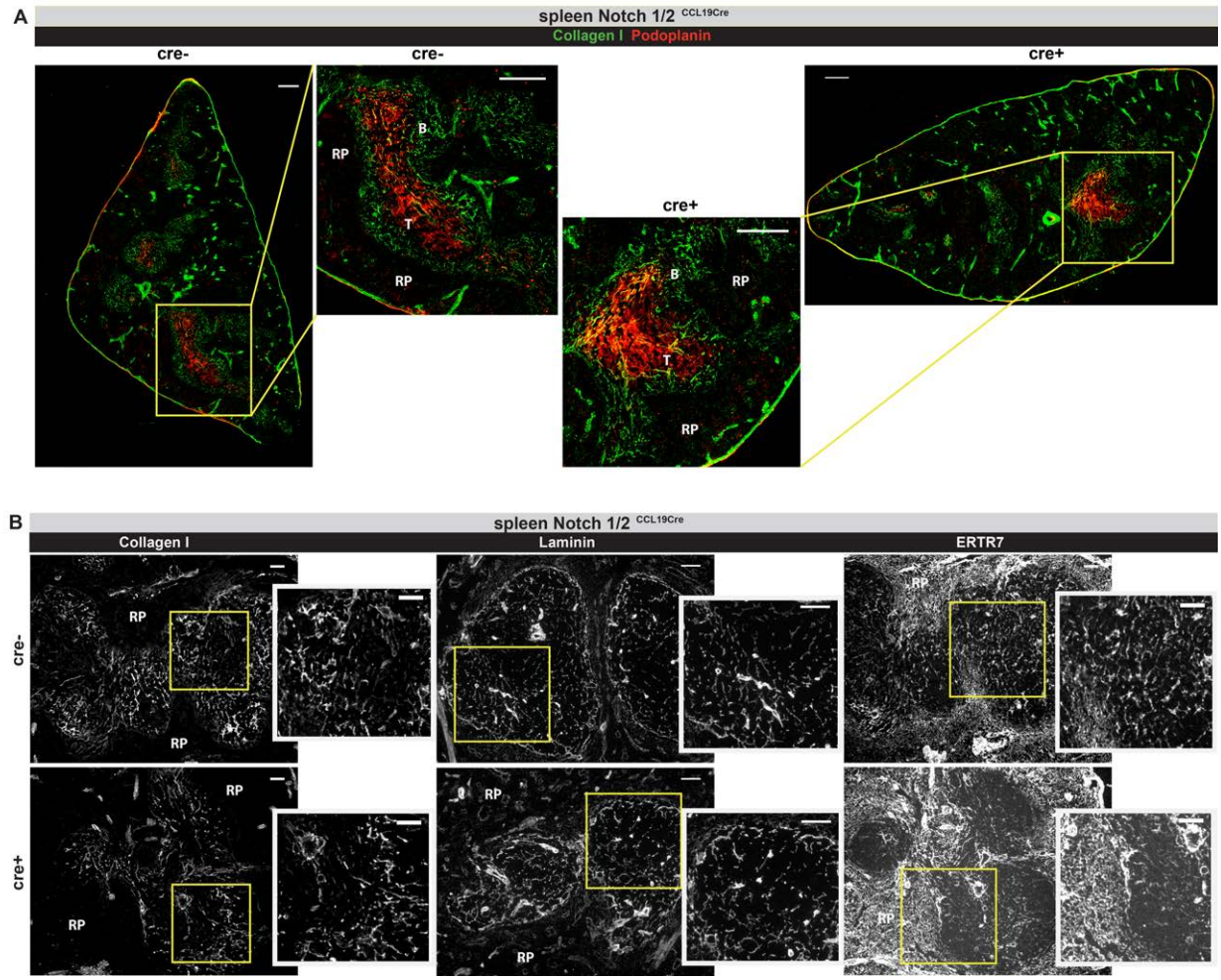

Figure 14: Notch1/2 deletion in FRC does not impair FRC development and ECM protein expression within the splenic white pulp cords. Immunofluorescence microscopy analysis of naïve spleen cryostat sections from adult Notch1/2^{CCL19Cre} mice, with a focus on white pulp areas (B, B zone; T, T zone; RP, red pulp) shown at higher magnification for the areas with a yellow rectangle. **A)** Representative images showing the labeling for the ECM component collagen I and podoplanin+ FRC. Scale bar, 200µm. Data are representative of two independent experiments**. B)** Representative images of the T/B zones stained for the indicated ECM components to highlight the conduit network of splenic white pulps. Scale bar, 50 µm. Data are representative of two independent experiments (RP, red pulp).

Next, we studied the expression of conduit network proteins, as pLN from naïve Notch1/2^{CCL19Cre} mice had shown a strong deficiency. However, no striking difference was observed for various ECM protein stainings of splenic T zone conduits (**Fig14.B**), although we have not quantified the expression level.

To study other functional properties of splenic FRC different cytokine transcripts were measured in stroma-enriched fractions from Notch1/2^{CCL19Cre} spleens.

No striking difference was observed for *cxcl13, ccl21, il33 and il-6* mRNA levels in Cre+ versus Cre- splenic stroma, however, we observed a 50% decrease in *ccl19* transcripts (**Fig15A**), similar to findings in pLN. In contrast to pLN, splenic *il-7* transcripts were decreased by 50% in Cre+ spleen stroma (**Fig15A**). In pLN, IL-7 is a crucial cytokine for the maintenance of the naive T cell pool (Link, Vogt et al. 2007) (Surh and Sprent 2008). TRC are a strong IL-7 source (Link, Vogt et al. 2007), but recently LEC have also been described to express some IL-7 within pLN (Onder, Narang et al. 2012). Therefore, our reduction of *il-7* transcripts seen in Cre+ pLN may be due to either an FRC or LEC defect. Several lines of evidence argue for an FRC-specific effect: First, IL-7 levels are much higher in pLN FRC than EC (Link, Vogt et al. 2007)(Hara, Shitara et al. 2012). Second, adult spleens harbor very few LEC with IL-7 reporter mice showing that most IL-7 transcription is found within TRC (Hara, Shitara et al. 2012); notably in Notch1/2-deficient spleens we have reproduced the pLN findings. Finally, having targeted Notch deletion principally within FRC using CCL19cre mice makes a direct effect in TRC more likely while obviously not excluding indirect effects in LEC.

In order to understand if the *ccl19* transcript reduction observed in Cre+ spleens leads also to decreased CCL19 protein sensing by splenic lymphocytes, similar to pLN, we investigated again surface CCR7 expression levels using CCL19-Fc fusion proteins and anti-CCR7 antibodies. A significant increase in CCL19-Fc staining levels was observed for B cells (1.6-times) as well as T cells (3-times) with both CD4+ and CD8+ T cells showing a similar increase. Also similar to pLN, the CCR7 labeling using the monoclonal antibody showed an increased staining intensity on all lymphocyte subsets in Notch1/2$^{CCL19Cre+}$ spleens, with B cells as well as T cells showing a 1.3-time and 1.7-time increase, respectively, with naive CD4+ and CD8+ T cells behaving similarly (**Fig.15B-C**). Therefore, we conclude that T cells encounter much less CCL19 protein in spleens of Notch1/2$^{CCL19Cre+}$ mice.

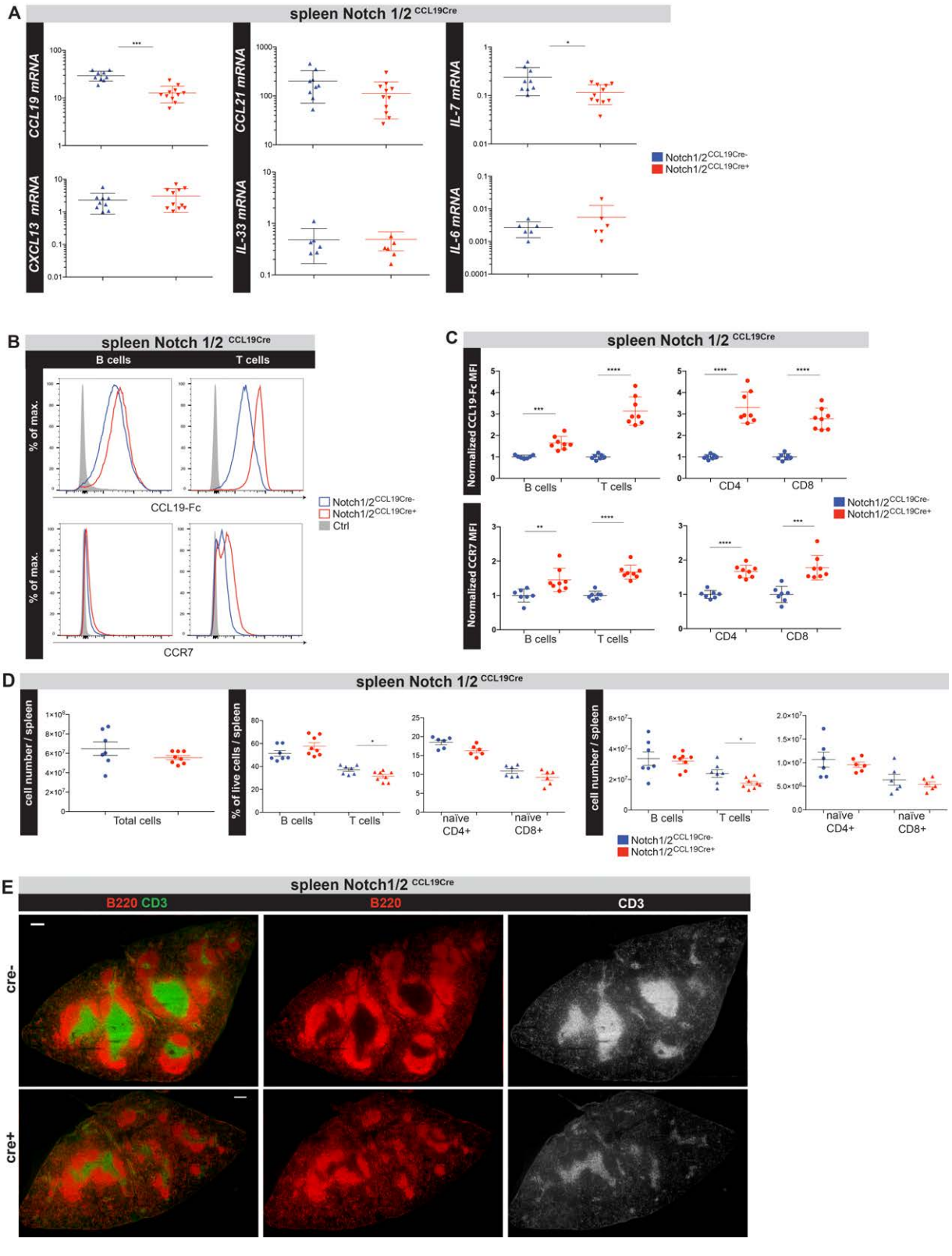
A
spleen Notch 1/2 CCL19Cre
CCL19 mRNA
CCL21 mRNA
IL-7 mRNA
CXCL13 mRNA
IL-33 mRNA
IL-6 mRNA
Notch1/2CCL19Cre-
Notch1/2CCL19Cre+
B
spleen Notch 1/2 CCL19Cre
B cells
T cells
% of max.
CCL19-Fc
CCR7
Ctrl
C
spleen Notch 1/2 CCL19Cre
Normalized CCL19-Fc MFI
Normalized CCR7 MFI
B cells
T cells
CD4
CD8
D
spleen Notch 1/2 CCL19Cre
cell number / spleen
Total cells
% of live cells / spleen
naïve CD4+
naïve CD8+
E
spleen Notch1/2 CCL19Cre
B220 CD3
B220
CD3
cre-
cre+

Figure 15: Notch1/2 deletion in FRC dampens CCL19 expression and T lymphocyte accumulation also in splenic white pulp cords. Analysis of naive spleens isolated from adult Notch1/2$^{CCL19Cre+}$ mice or their littermate controls. A) qRT-PCR analysis for transcript levels of the indicated cytokines in non-soluble spleen fractions (stroma-enriched); values were normalized to two housekeeping genes (mean ± SD) (n=6-11). **B-C)** Flow cytometric analysis of CCL19-Fc, anti-CCR7, or isotype control staining on naïve T (CD19- TCRb+ CD44-) and B (CD19+ TCRb+) lymphocytes. CCL19-Fc recognizes CCR7 free of bound CCL19, and anti-CCR7 recognizes all surface CCR7. Data are representative of two independent experiments. Shown in (B) are representative histograms and in **(C)** quantification of the MFI of these stainings, normalized to the littermate controls in each of the two independent experiments shown (n=7-8). **D)** Scatter plots showing the flow cytometric analysis of various lymphocyte populations, either as proportion or absolute numbers: B cells (CD19+, TCRb-), T cells (CD19-, TCRb+), and naive (CD44-,CD62L+) CD4+ or CD8+ T cells. Data are representative of three independent experiments (n=6**). E)** Immunofluorescence microscopy images of cryostat sections stained for CD3+ T cells and B220+ B cells. Scale bar, 200 µm. Data are representative of three independent experiments.

The decrease of two cytokines, *ccl19* and *il-7*, important in migration and survival of naive recirculating T cells (Link, Vogt et al. 2007)(Surh and Sprent 2008), suggested that T cell populations may be reduced in size within spleens of naïve Notch1/2^{CCL19Cre} mice. By flow cytometric analysis a significant decrease in relative (15%) and absolute (27%) T cell numbers was observed in Cre+ relative to Cre- spleens, with both CD4+ and CD8+ T cells being similarly affected (**Fig.15D**). To assess lymphocyte compartmentalization in spleens of Notch1/2^{CCL19Cre} mice, we localized B and T cells by histology. First, we noted that the total white pulp area may be reduced in mice with Notch1/2 deletion in FRC but this aspect has not been properly assessed yet. Second, while T cells localized correctly within the T zone, the T cells stained by CD3 antibodies appeared to be less densely grouped in Cre+ mice (**Fig.15E**) which most likely reflect the decreased splenic T-cell numbers isolated from Cre+ spleens. The B cell staining indicated that B cells localize correctly and form well polarized follicles.

5. Notch1/2 deletion in FRC does not affect T lymphocyte homing to pLN but is associated with altered blood and lymph vessels

The reduction in T cell numbers localizing to pLN and spleen of Notch1/2 $^{CCL19Cre+}$ mice may be explained by a problem in thymic T cell development, especially as CCL19cre is active in thymic fibroblasts and some medullary epithelial cells (Ueno, Hara et al. 2002). To formally test this possibility, thymocyte development was assessed in these mice by flow cytometry. No striking difference was observed for the different maturation stages of thymocytes, going from the double negative cells (DN; CD4-, CD8-) to the double positive cells (DP; CD4+CD8+) and finally the single positive cells (SP; CD4+CD8- or CD4-CD8+), neither in proportions nor in absolute numbers (**Fig.16A**). These thymic data point to a problem in peripheral T cell maintenance or migration which may be linked to the reduced IL-7 levels in the spleen or the reduced CCL19 levels in pLN and spleen.

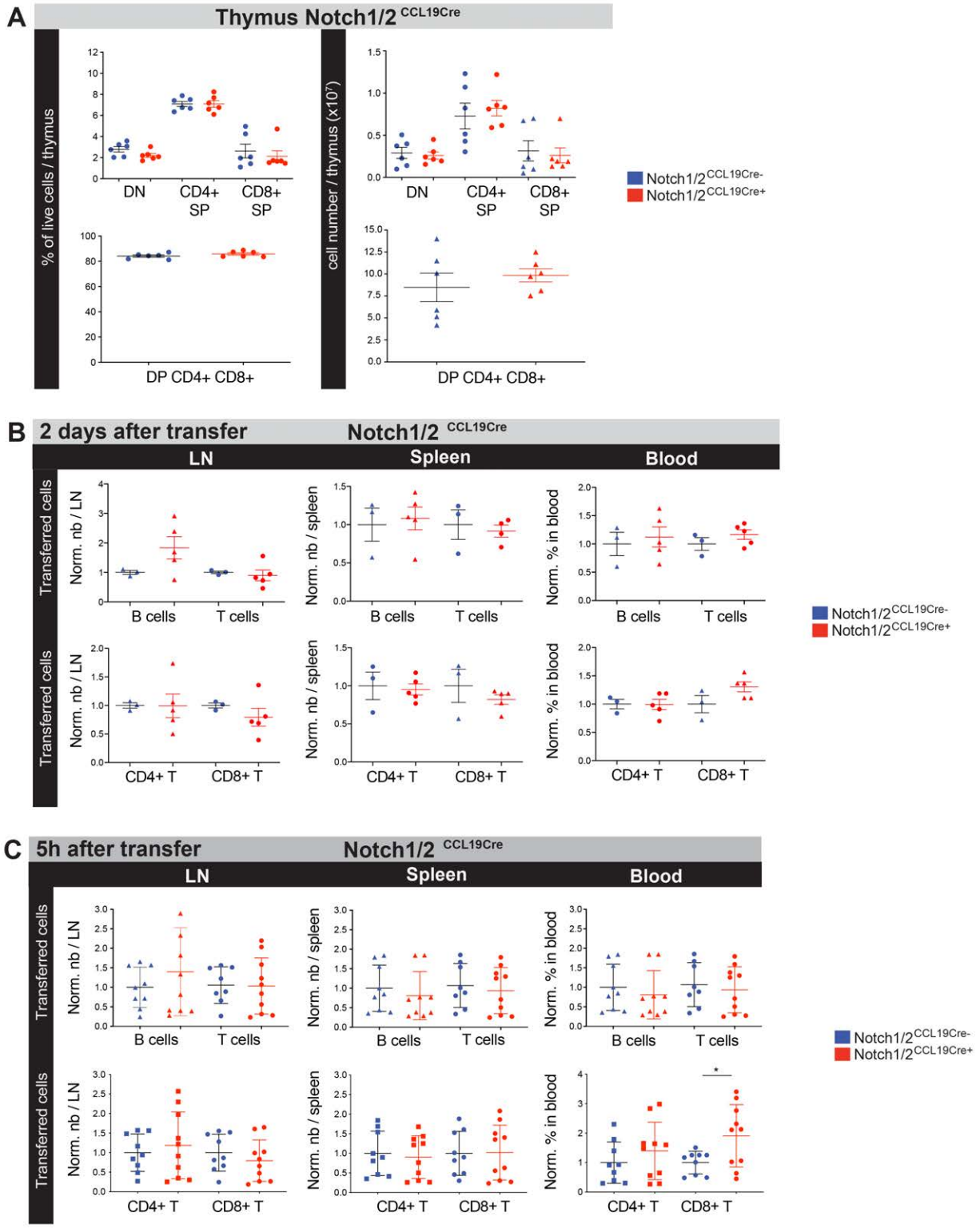

Figure 16: Notch1/2 deletion in FRC does not affect T lymphocyte maturation or T cell homing to pLN and spleen. Scatter plots showing the quantification of flow cytometric data of the indicated organs or blood isolated from naive adult Notch1/2$^{CCL19Cre+}$ mice or their littermate controls. **A)** Analysis of 9 week old mice for the following thymocyte populations: DN (CD4-, CD8-), DP (CD4+ CD8+), SP (CD4+/CD8- or CD4-/CD8+). Data shown are pooled from three independent experiments (n=6). **B-C)** WT T and B cells marked with the eFluor670 dye and adoptively transferred into naive adult Notch1/2^{CCL19Cre} mice were measured in their number either 2 days **(B)** or 5h **(C)** later in the pLN, spleen or blood. Data are representative of one (B; n=3-5) or three (C; n=9-10) experiments. P value indicated as, * for $p < 0.05$.

So far, I have not tested a role for Notch1/2 signaling in FRC for T cell survival but have evaluated a potential difference in short-term homing into SLO. To address this point, we marked WT lymphocytes with the eFluor670 dye, then adoptively transferred them into Notch1/2^{CCL19Cre} mice and then tracked these cells in pLN, spleen and blood two days after transfer by means of flow cytometry. No significant difference was observed in the number of transferred B and T cells recovered within pLN, spleen or blood of Cre+ versus Cre- recipients, but a trend was visible suggesting a slightly reduced CD8+ T cell homing to pLN and spleen, with more of them remaining within the blood (**Fig.16B**). Therefore, these transfer data show the same trend as visible for endogenous CD8+ T cells that are reduced in SLO and show a trend of an increased frequency in the blood.

In order to test whether entry into the SLO is altered in these Notch1/2^{CCL19Cre} mice, lymphocyte homing was assessed 5 hours after transfer into Notch1/2^{CCL19Cre} mice. While the values in each group were highly variable, possibly due to this early time point, no statistically significant difference could be observed in pLN, spleen or blood, except for an increased presence (1.9-times) of transferred CD8+ T cells in blood in Cre+ mice, with CD4+ T cells showing a non-significant trend towards an increase (1.4 times) (**Fig.16C**). CD8 T cells have been shown to migrate significantly less than CD4+ T cells towards low CCL19 concentrations (Britschgi, Link et al. 2008), suggesting their attraction to retention within SLO are slightly impaired.

In summary, homing or retention issues may contribute to the T cell accumulation defect observed in pLN and spleen of Notch1/2^{CCL19Cre} mice. At present, we cannot exclude that this signaling pathway also impacts naive T cell survival processes which may be coupled to the dwell time in lymphoid tissue T zones.

CCL19/CCL21 expression by FRC is not only important for attracting and retaining CCR7+ T cells within T zones, but also allows the attraction of mature CCR7+ DCs into T zones (Luther, Tang et al. 2000) (Seth, Oberdorfer et al. 2011). To determine whether SLO of Notch1/2^{CCL19Cre} mice have alterations in myeloid cells, these populations were measured in enzymatically digested pLN using flow cytometry.

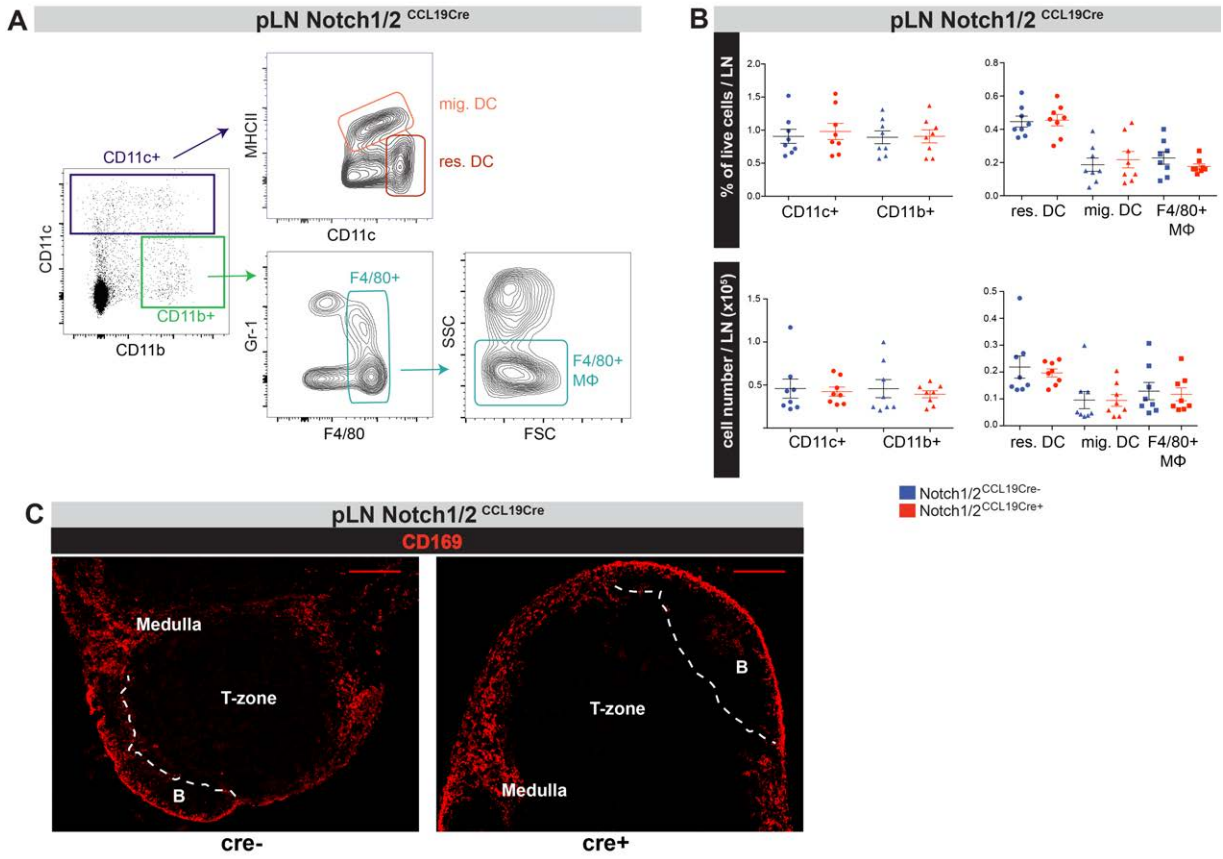

Figure 17: Notch1/2 deletion in FRC does not affect myeloid cell populations in pLN. A-B) Flow cytometric analysis of enzymatically digested pLN of naïve adult Notch1/2$^{CCL19Cre+}$ mice and their littermate controls. **A)** In the left dot plot two myeloid cell populations can be distinguished among TCRb- CD19- cells according to their CD11c and CD11b expression profile as indicated by the colored rectangular gates. In the upper contour plot the CD11c+ gated population was further divided into two subsets according to their expression of MHCII and CD11c: migratory DC (MHCII^{hi} CD11c$^{int/hi}$) and resident DC (MHCII^{int} CD11c^{hi}). In the lower contour plot the CD11b+ population was analysed more precisely for the expression level of Gr-1 and F4/80 markers with the F4/80+ population identified as F4/80+ macrophages according to their low granularity (SSC) in the adjacent contour plot. **B)** Scatter plots showing the relative and absolute numbers for each population shown in A. Data were pooled from three independent experiments (n=8). **C)** Cryostat sections of naïve Notch1/2^{CCL19Cre} pLN stained for CD169+ macrophages found at sites of antigen drainage, the subcapsular lymphatic sinuses in the back of the follicle or the medullary lymphatic sinuses. B, B-cell follicle. Dashed lines surround the limitation of B-cell follicles. Scale bar, 200 µm. Data are representative of two independent experiments.

Two populations can be distinguished according to their CD11c and CD11b expression profile: CD11c^{high} cells with variable CD11b levels, containing mostly dendritic cells, and CD11b+ cells with absent or low CD11c levels, containing most macrophages (**Fig.17A**). CD11c+ cells were further subdivided according to their MHCII expression levels in order to distinguish resident DC (MHCII^{int} CD11c^{hi}) from migratory DC (MHCII^{hi} CD11c$^{int/hi}$) (**Fig.17A**). In contrast, CD11b+ CD11c^{low} cells were analysed for their expression of the surface markers Gr-1 and F4/80. While Gr-1^{high} cells are enriched for granulocytes, F4/80-expressing cells of low granularity (SSC) represent F4/80+ macrophages (Rose, Misharin et al. 2012)(**Fig.17A**).

Relative and absolute numbers of these different myeloid populations were analysed in pLN of Notch1/2^{CCL19Cre} mice but no significant difference was observed between Cre+ an Cre- mice (**Fig.17B**). This could be explained by the fact that CCL19, which is decreased in Notch1/2$^{CCL19Cre+}$, has been described as a molecule dispensable for DC migration if CCL21 is still present (Britschgi, Link et al. 2008). Another type of macrophages present in pLN are SCS and medullary sinus macrophages, characterized by the metallophilic macrophage marker CD169. These macrophages have been characterized as specialized antigen-presenting cells that deliver antigens to antigen-specific B cells (Phan, Green et al. 2009). MRC might be involved in the function of these macrophages (Katakai 2012). Due to the decrease of MAdCAM+ MRC observed by flow cytometry but not confirmed by histology, we decided to check for the presence of CD169+ SCS macrophages by immunohistological stainings. No striking difference was observed for SCS and medullary macrophages expressing CD169 in Cre+ versus Cre- pLN (**Fig.17C**). In conclusion, the different myeloid populations studied do not appear to be affected by the deletion of Notch1/2 in pLN FRC.

In pLN, LEC are identified by their expression of lyve1 and their location in the SCS, where the afferent lymph enters the tissue, and the medulla. When we studied the global pLN structure by immunohistological analysis we observed an aberrant presence of lyve1+ structures within the T-cell zone in Notch1/2$^{CCL19Cre+}$ mice but not Cre- littermates (**Fig.18A**). Lyve1, or lymphatic vessel hyaluronan receptor 1, identifies lymph vessels and sinuses, such as the ones in the subcapsular region where the lymph enters the LN, and in the medulla where the lymph leaves again the LN. Lymph vessels are typically not found within T zones of naive pLN in mice, but only after LN activation (Randolph, Angeli et al. 2005, Huang, Rivas-Caicedo et al. 2018). These lyve1+ T zone structures also expressed the endothelial marker CD31, but at levels far below blood vessels (**Fig. 18A**), again consistent with a lymph vessel identity. Further, these vessels displayed a thin laminin+ basement membrane, in contrast to the thicker counterpart seen with blood vessels, again supporting the notion that these are misplaced lymph vessels (data not shown). Quantification of the % area covered by lyve1+ pixels within pLN T zones of Notch1/2^{CCL19Cre} mice revealed a variable but in average significant 5-fold increase of these vessels in Cre+ versus Cre- mice (**Fig. 18B**).

As we observed in cryostat sections that also CD31^{hi} blood vessels were more often localizing within the central T zone in Cre+ compared to Cre- pLN (**Fig. 18A**), we decided to assess the blood vasculature by labeling thick vibratome sections of Notch1/2^{CCL19Cre} pLN followed by their confocal imaging in 3D allowing a better visualization of these large structures. Both endothelial markers investigated, CD31 and CD34, pointed to a higher density of CD31/34^{hi} blood vessels within the central T zone (**Fig. 18C**).

This finding was supported by the increased presence in central T zones of vessel-associated basement membranes labelled by both collagen IV and ERTR7 (**Fig. 18C**).

In addition, we could confirm that the intensity of the Collagen IV and ERTR7 signals was fairly normal on vessel-associated basement membranes but strongly decreased in the much thinner conduit structures. To summarize, deletion of Notch1/2 in FRC not only affects the lymph draining conduits but also changes the arrangement of both blood and lymph vessels within the pLN T zones (**Table1**).

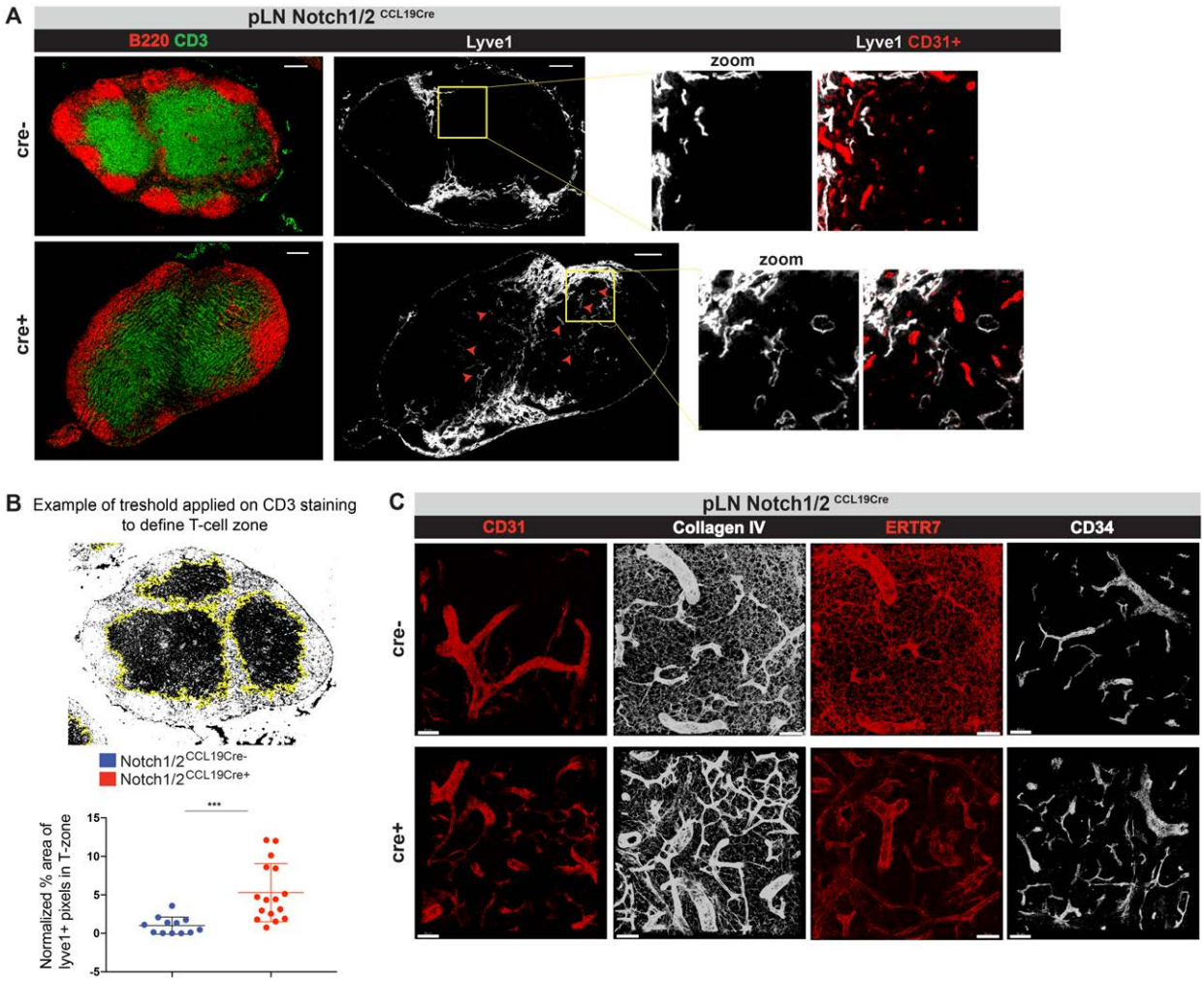

Figure 18: Notch1/2 deletion in FRC increases lymph and blood vessel presence within the pLN T-zone. Histological analysis of tissue sections from naive pLN of adult Notch1/2^{CCL19Cre} mice for the presence of lymphatic vessels (Lyve1+, CD31^{low}) or blood vessels (Lyve1-, CD31^{high}). **A)** Cryostat sections of pLN stained for CD3+ T cells and B220+ B cells to highlight the compartments, for lymphatic vessels (lyve1+) and blood vessels (CD31^{high}). Arrows point to lyve1+ lymphatic endothelial cells within the T cell-zone. Magnified regions of the T zone show the presence of lyve1+ lymph vessels in Cre+ but not Cre- mice. Representative of 3 independent experiments. Scale bar, 200µm. **B)** Example of the automized delimitation of the T-cell zone with a threshold applied to the CD3 staining. The zone obtained was then transferred to the lyve1 staining on the same section in order to quantify the presence of lyve1+ lymphatic vessels within the gated T zone. The percentage of the T-zone area covered by lyve1+ pixels was calculated and normalized to the Cre- control tissues. Data were pooled from three independent experiments (n=6). P values are indicated as, *** for p<0.001. **C)** Confocal image stacks (100µm) of vibratome sections labeled for the indicated endothelial cell markers (CD31, CD34) or ECM/basement membrane markers (collagen IV, ERTR7) showing both vessels and conduits. The areas chosen represent the central T-cell zone. Scale bar, 50µm. Data are representative of two independent experiments.

6. pLN lacking Notch1/2 in FRC are competent to mount a CD4+ and CD8+ T cell response

To evaluate if the deletion of Notch1/2 in FRC and the various alterations observed could influence T cell responses, we immunized Notch1/2^{CCL19Cre} mice subcutaneously with a model vaccine, ovalbumin (OVA) protein in clinical grade Montanide (Mont) adjuvant, known to induce a strong LN swelling and T cell response (Yang, Vogt et al. 2014, Huang, Rivas-Caicedo et al. 2018). As gene arrays had been previously performed in the lab on sorted pLN FRC subsets from naïve versus OVA/Mont-immunized (day8.5) WT B6 mice I searched this dataset for Notch-related transcripts. No striking difference was observed for transcript levels between naïve and activated FRC, neither for Notch receptors (Notch1-4), the transcription factor RBPj nor the two Notch target genes Hes1 and Hey1 (**Fig.19A**).

Between the different FRC subsets, no clear transcriptional differences were observed regarding this pathway (**Fig.19A**), while hundreds of other genes were differentially expressed (data not shown). Therefore, based on these mRNA data, also activated FRC appear to have an active Notch signaling pathway with no obvious regulation observed by this vaccination approach.

Using the same vaccination scheme, I immunized Notch1/2^{CCL19Cre} mice subcutaneously with OVA/montanide and analyzed draining pLN 4.5 and 8.5 days later using flow cytometry. At both time points I did not observe any striking and consistent difference in the three major stromal cell subsets, FRC, LEC and BEC, in Cre+ versus Cre- mice (**Fig. 19B-C**), suggesting the stromal cell expansion occurs normally in mice lacking Notch1/2 signaling in FRC. More detailed analysis of FRC subsets showed a trend towards more TRC in Cre+ pLN after immunization, while the MedRC subset showed no difference (**Fig. 19B-C**). As previously seen for naive pLN, MadCAM+ MRC were significantly decreased in Cre+ compared to Cre- pLN, both in relative (~80%) and absolute (~85%) numbers (**Fig. 19B-C**). As we had previously observed MRC by histology in naive pLN, we performed also immunohistology on d8.5 activated pLN from Notch1/2^{CCL19Cre} mice. RANK-L+ MRC were equally present in the back of the follicle of Cre+ and Cre- pLN (**Fig. 19D**), again suggesting that MRC are present in Notch1/2$^{CCL19Cre+}$ mice, but most likely altered in their viability or MAdCAM-1 expression level. Investigation of podoplanin+ FRC in the T zone revealed a similar cell density and organization in the two groups (**Fig. 19D**). Together, these findings suggest that Notch1/2 signaling in FRC may be dispensable for stromal cell expansion during immune response.

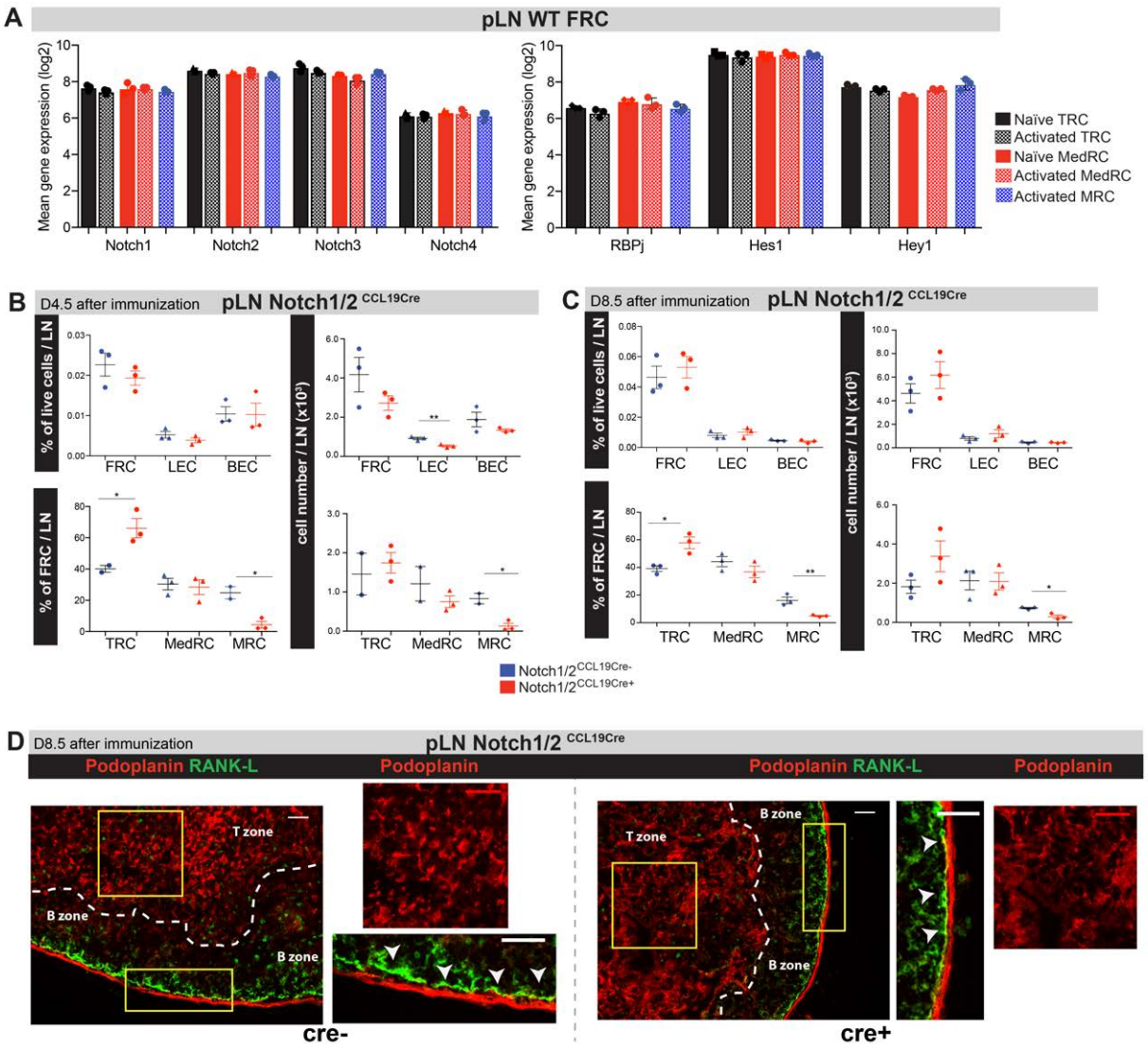

Figure 19: Notch1/2 deletion in FRC still allows stromal cells to expand normally during immune response induction in draining pLN. Adult B6 mice having received ova-specific OT-1 and OT-2 T cells by adoptive cell transfer were immunized subcutaneously with ova protein in Montanide adjuvant followed by draining pLN analysis at the indicated time point after immunization. **A)** Analysis of the expression of Notch receptors, RBPj and two Notch target genes (Hes1 and Hey1) in naïve TRC/MedRC versus d8.5 activated TRC/MedRC/MRC populations sorted from fully digested pLN isolated from wt B6 mice. Log2 data were extracted from our unpublished Affymetric 1.0 gene array analysis. **(B-D)** Adoptive cell transfer and immunization as in A, but in Notch1/2^{CCL19Cre} mice. **(B-C)** Flow cytometric analysis of digested pLN for total cells, stromal cells (FRC, LEC, BEC) and FRC subsets (TRC, MedRC, MRC), in relative and absolute numbers, on d4.5 (B) or d8.5 (C) after immunization. Data are representative of one preliminary experiment per time point (n=2-3). P values are indicated as * for $p < 0.05$, ** for $p< 0.01$**. D)** Immunofluorescence microscopy of pLN cryostat sections stained for the podoplanin+ FRC network (TRC and MRC) and RANKL+ MRC. The two rectangles and magnifications show the podoplanin+ TRC of the T-zone and the RANK-L+ MRC layer at the cortical side of the subcapsular sinus. Arrows point to the MRC layer present in both Cre+ and Cre- mice. Dashed lines indicate the boundary of the B-cell follicle. Scale bar, 50 µm. Results are representative of one experiment.

To look for alterations in the immune response in Notch1/2-deficient FRC, I measured the total and ova-specific lymphocyte populations on d4.5 and 8.5 after vaccination. At both time points, a similar lymphocyte composition was observed as in naïve Notch1/2^{CCL19Cre} mice, namely a decrease of relative T cell numbers in Cre+ compared to Cre- pLN which led to a relative increase in B cell numbers (**Fig. 20A**).

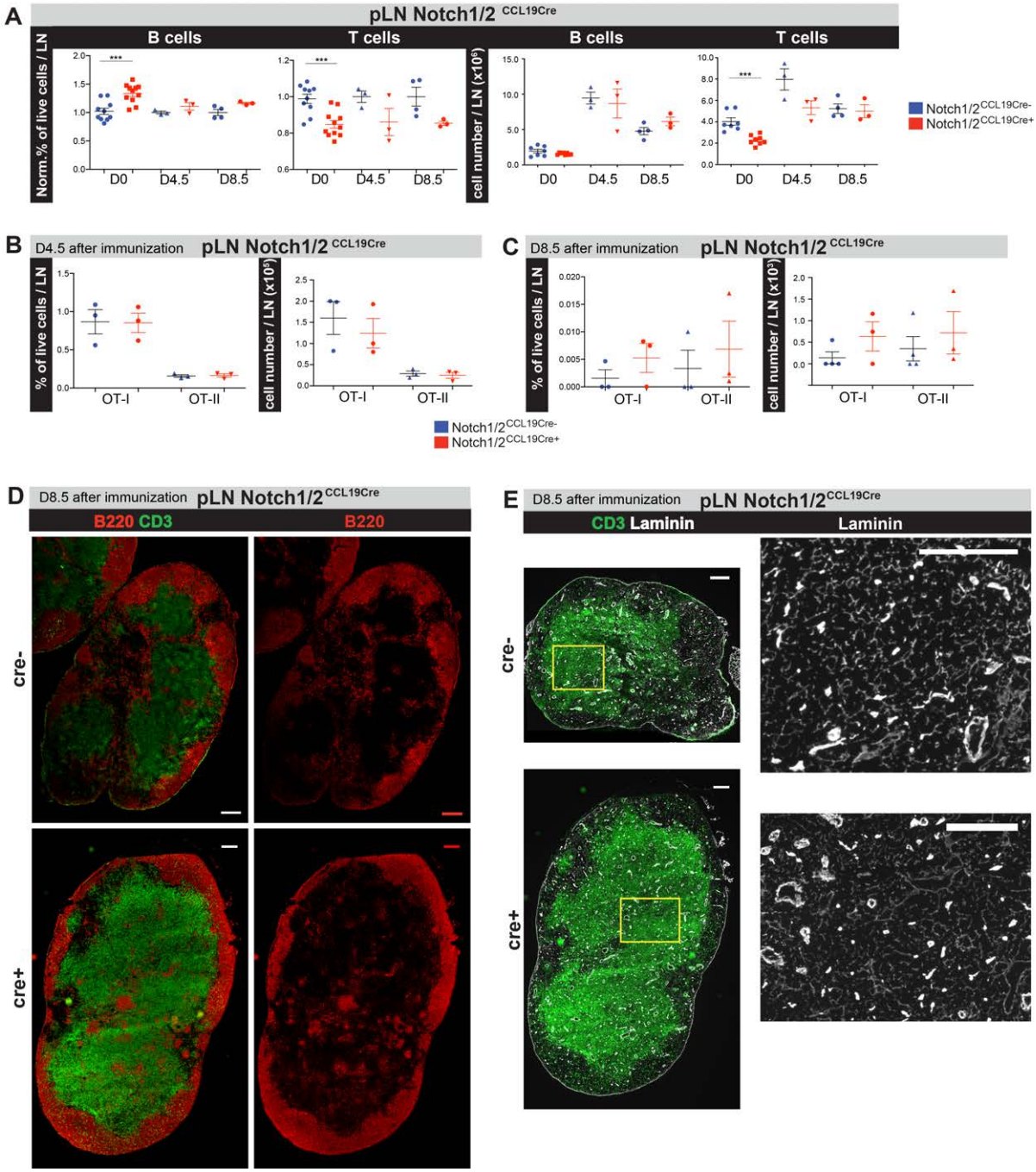

Figure 20: Notch1/2 deletion in FRC allows a normal pLN swelling and ova-specific T cell response. Adult Notch1/2^{CCL19Cre} mice having received ova-specific CD8+ OT-1 and CD4+ OT-2 T cells by adoptive cell transfer were immunized subcutaneously with ova protein in Montanide adjuvant followed by draining pLN analysis at the indicated time point after immunization. **A-C)** Flow cytometric analysis of cell frequencies and numbers in enzymatically digested pLN, either total B and T cells **(A),** or ova-specific T cells on d4.5 **(B)** or d8.5 **(C)** after immunization. The immunization data are representative of one experiment per time point of activation (n=2-3) and are therefore preliminary while the d0 data are a pool of 10-11 mice. P values are indicated as *** for p<0.001. **D-E)** Immunofluorescence microscopy of pLN cryostat sections stained for CD3+ T cells and B220+ B cells **(D)** or CD3 and laminin as basement membrane marker **(E),** with magnified areas showing the conduit network of the T-cell zone. Scale bar, 200 µm. Data are representative of one experiment.

In absolute numbers, the decreased T cell pool observed on d0 appeared to be less striking during immune response with B cells being comparable in absolute numbers between the two groups (**Fig. 20A**). To be able to track antigen-specific T cell responses, these mice had received an adoptive transfer of ova-specific CD8+ (OTI) and CD4+ (OTII) T cells marked by the CD45.1 allele, as previously described (Yang, Vogt et al. 2014). On day4.5 after immunization, ova-specific CD8+ and CD4+ T cells were present in similar relative and absolute numbers in both groups, suggesting an unimpaired T cell priming and early expansion in Cre+ mice (**Fig.20B**). At day8.5 after immunization, the ova-specific T cell response did not show a significant difference between the two groups (**Fig.20C**). Of note, relatively few transgenic T cells were observed in d8.5 LN in general, suggesting many of the activated T cells may have left the organ already, or rather, the adoptive transfer had not worked efficiently.

Next, we assessed whether the immune response had an effect on the global LN organization where we had previously observed alterations in naive Notch1/2^{CCL19Cre} mice. By immunohistological analysis, the T-B cell segregation appeared similar in Cre+ and Cre- mice on d8.5 of the response, but as in naïve Cre+ mice, the shape of B-cell follicles was different giving the impression of a continuous follicle without clear interfollicular regions (**Fig.20D**). Also the conduit defect appears to be preserved in immunized LN, based on the reduced laminin staining for T zone conduits in Cre+ compared to Cre- mice (**Fig.20E**). In summary, the defects observed in naive pLN of Notch1/2^{CCL19Cre} mice were still present in activated LN, including the MRC decrease, the altered conduit structure and the abnormal B cell follicles, suggesting these changes may be imprinted onto the stromal cell architecture. Importantly, these various defects did not seem to have a strong impact on T cell immunity, but more work is needed to evaluate T and B cell immunity in more depth.

In summary, we observed similarities and differences in the phenotype of pLN and spleens in Notch1/2$^{CCL19Cre+}$ mice (see **table1**). While the decrease in CCL19 expression and T cell accumulation was observed in both organs, the splenic white pulp did not show the striking alterations in conduit and FRC structure seen in pLN of Notch1/2$^{CCL19Cre+}$ mice.

Phenotypes – adult Notch1/2 ^{CCL19Cre}	pLN	Spleen
Stromal cells		
FRC number (FACS)	-	N.D.
BEC number (FACS)	--	N.D.
MRC number (FACS)	---	N.D.
TRC size - granularity	+	N.D.
TRC – pdpn expression	++	N.D.
TRC network organization	≠	N.D.
FRC functions		
Collagen I conduit structure	≠	wt
Basement membrane of conduits	--	wt
Microfibrillar zone of conduits	--	wt
Ccl19 transcripts	--	--
CCL19-Fc staining (T cells)	+++	++
CCR7 staining (T cells)	++	+
Il-6 transcripts	++	wt
Il-7 transcripts	wt	---
Neighboring cells		
T cell number	--	-
B-cell follicle shape	≠	wt
BEC inside the central T-zone	++	wt
LEC inside the T zone	+++	wt

Table 1: Summary of the different phenotypes observed in naïve pLN and spleen of adult Notch1/2^{CCL19Cre} mice. ('-' : decrease ; '+ ': increase ; '≠' :different ; 'wt ' : no difference). N.D.: not determined. -/+ : 10-30% or 1.5-2 times for transcript/MFI analysis; --/++ : 30-50% or 2-5 times for transcript/MFI analysis; ---/+++ : more than 50% or more than 5 times for transcript/MFI analysis.

7. Notch2 and not Notch1 is responsible for the different phenotypes observed in Notch1/2^{CCL19Cre} mice

To better dissect the connections between the various phenotypes observed in Notch1/2$^{CCL19Cre+}$ mice we wondered whether some defects are fully Notch1-dependent while others are fully Notch2-dependent, with the third possibility being that the two receptors work together in these processes. In order to understand the relative importance of the two Notch receptors on FRC we studied the role of each receptor in isolation by using single floxed Notch1^{CCL19Cre} and Notch2^{CCL19Cre} mice. Flow cytometric analysis of digested pLN of Notch1^{CCL19Cre} mice showed no statistically significant difference between Cre+ and Cre- mice for total cells, nor for absolute and relative numbers of FRC, LEC and BEC, or for the three FRC subsets (**Fig.21A**). No striking difference was observed for TRC and MedRC size, granularity as well as podoplanin expression level in Notch1^{CCL19Cre} mice (**Fig.21B**).

The same flow cytometric analysis performed on Notch2^{CCL19Cre} pLN showed a trend towards lower total cell numbers, with a reduced absolute numbers for LEC (~ 40 %), BEC (~ 40 %) but not FRC (**Fig. 21C**). The only FRC subset that was reduced were MRC, showing a 35 % decrease of relative number and a trend towards reduced absolute numbers (**Fig. 21C**). A significant increase of TRC and MedRC size (1.2 and 1.1-time respectively) and granularity (1.2 and 1.1 respectively) was observed (**Fig. 21D**). Podoplanin expression was also upregulated in TRC (2-times) and MedRC (1.4-time) (**Fig. 21D**). Immunohistological analysis confirmed the presence of MAdCAM+podoplanin+RANK-L+ MRC in pLN of Notch2$^{CCL19Cre+}$ mice (**Fig. 21E**).

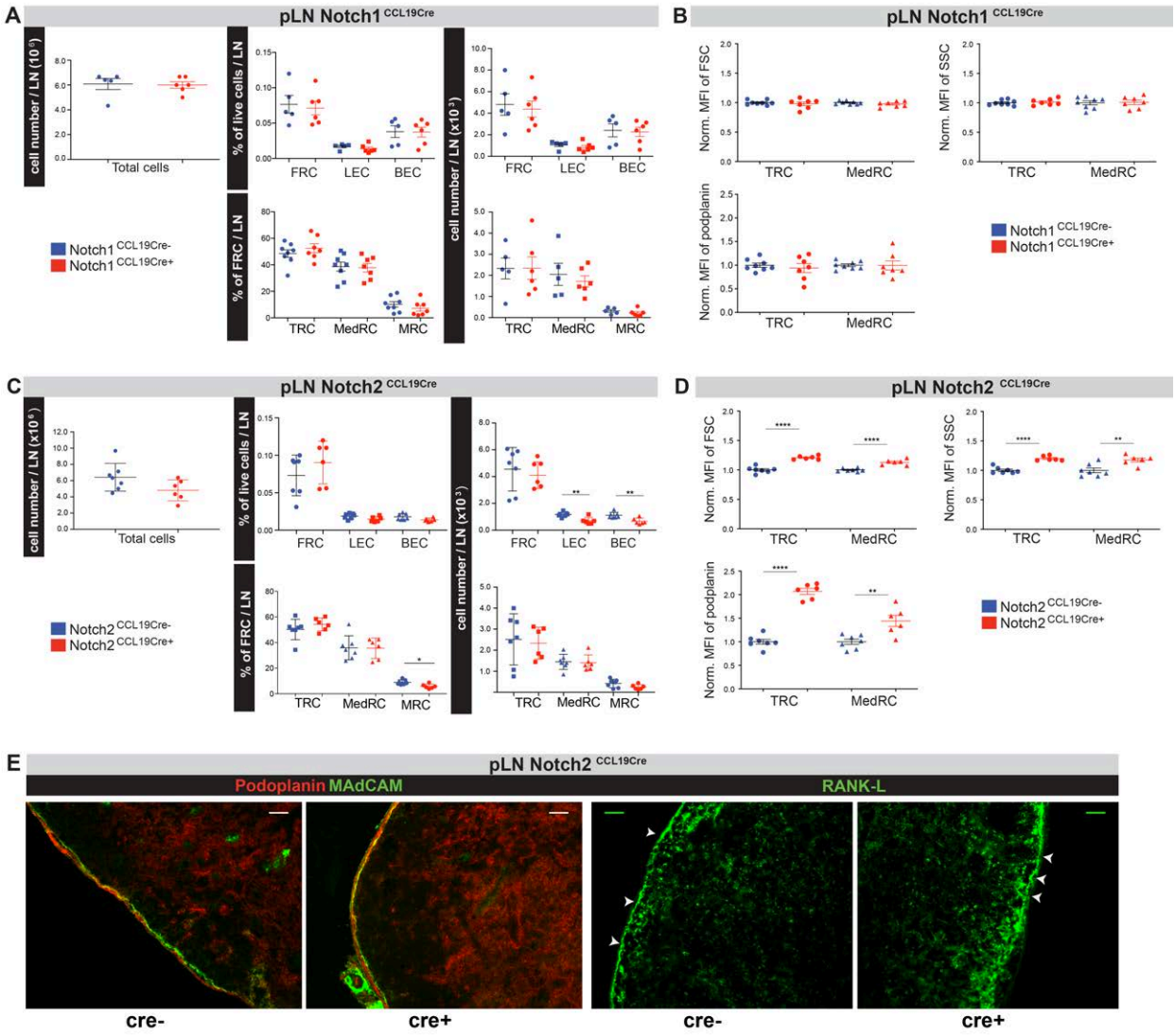

Figure 21: Notch2 but not Notch 1 receptor is required in pLN FRC to regulate FRC size, activation state. (A-D) Flow cytometric analysis of naive digested pLN from adult Notch1^{CCL19Cre} and/or Notch2^{CCL19Cre} mice for total cells, stromal cells (FRC, LEC, BEC) and FRC subsets (TRC, MedRC, MRC) both in relative and absolute numbers in either Notch1^{CCL19Cre} (A; n=5-7) or Notch2^{CCL19Cre} mice (C; n=6-7). Analysis of TRC and MedRC size (FSC), granularity (SSC) and podoplanin expression levels (MFI) in either Notch1^{CCL19Cre} (B; n=7) or Notch2^{CCL19Cre} mice (D; n=6-7). **E)** Immunofluorescence microscopy analysis of pLN cryostat sections labeled with the indicated markers. Scale bar, 50µm. Presence of podoplanin+ MAdCAM+ RANK-L+ MRC in of pLN from Notch2$^{CCL19Cre+}$ pLN, with arrows pointing to the MRC layer. Data are representative of two independent experiments. P values are indicated as * for $p < 0.05$, ** for $p<0.01$,*** for $p<0.001$.

Next, we labelled ECM proteins by immunohistology to assess the composition and structure of the T zone conduit network. pLN from Notch1^{CCL19Cre} and Notch2^{CCL19Cre} mice showed no difference in the staining intensity for collagen I highlighting the presence of conduit cores (**Fig. 22A-D**). However, only pLN of Notch2^{CCL19Cre} mice showed more unbranched, stick-like collagen I fibers (**Fig. 22C**), similar to observations in Notch1/2^{CCL19Cre} mice. Similarly, only Notch2^{CCL19Cre} but not Notch1^{CCL19Cre} mice reproduced also the lower staining intensity for laminin and ERTR-7 antibodies seen in double deficient mice (**Fig. 22C-D**). These data demonstrate that Notch2 but not Notch1 is required for proper ECM matrix production and conduit formation, while normal MRC development may possibly depend on both receptors (**Table2**).

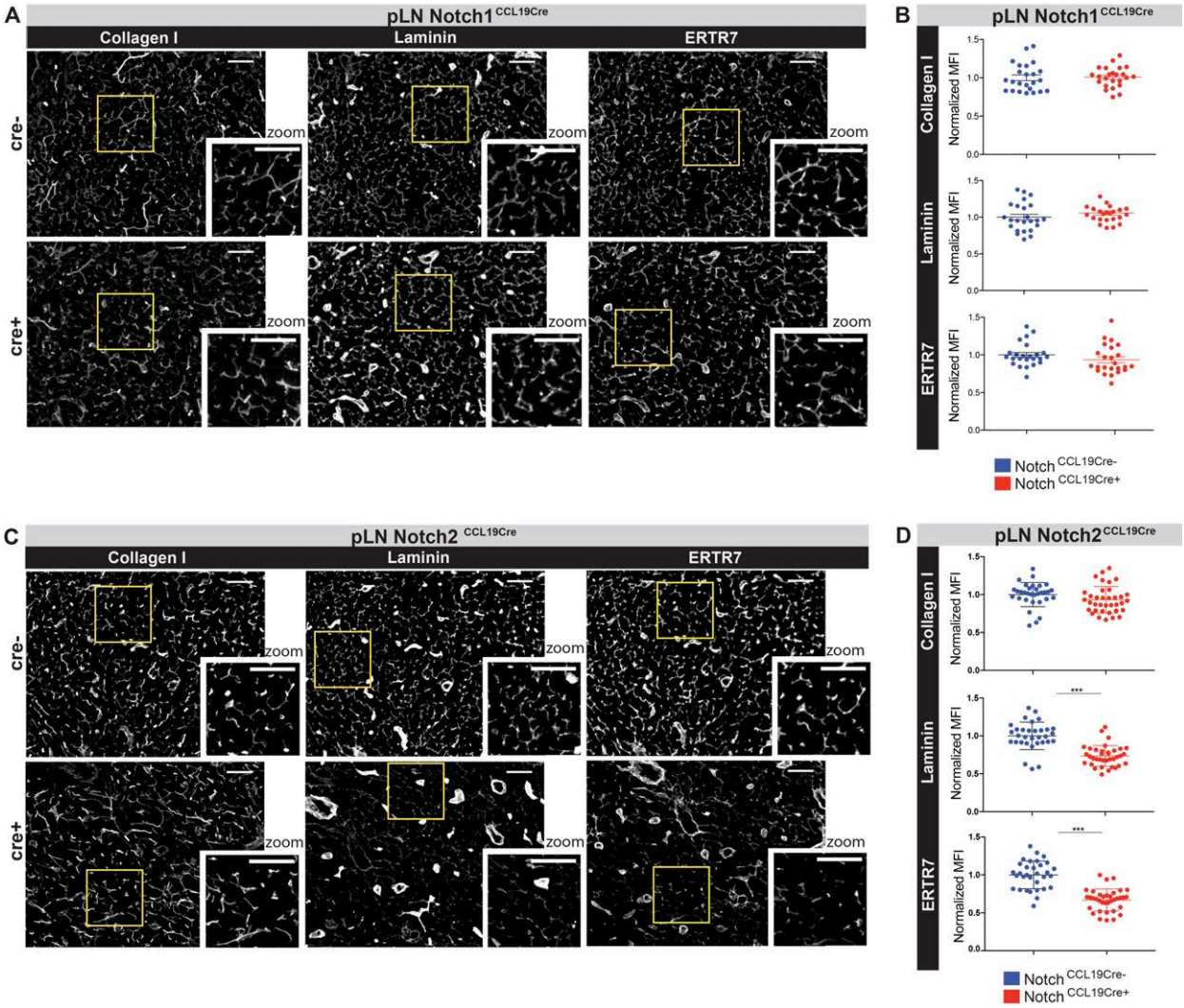

Figure 22: Notch2 but not Notch 1 receptor is required in pLN FRC for matrix expression and proper conduit formation. (A-D) Immunofluorescence microscopy analysis of pLN cryostat sections labelled with indicated markers of ECM proteins. Scale bar, 50µm. pLN of Notch1^{CCL19Cre} mice **(A, B)** and Notch2^{CCL19Cre} **(C, D).** Representative images are shown for the T zone along with magnified views of T zone conduits. To quantify the ECM protein staining of the conduit network the MFI was measured in three areas (squares of 150 x 150 pixels) per image and normalized to littermate controls. Data are representative of one (A, B; n=2) or two (C, D; n=4) experiments. P values are indicated as *** for p<0.001.

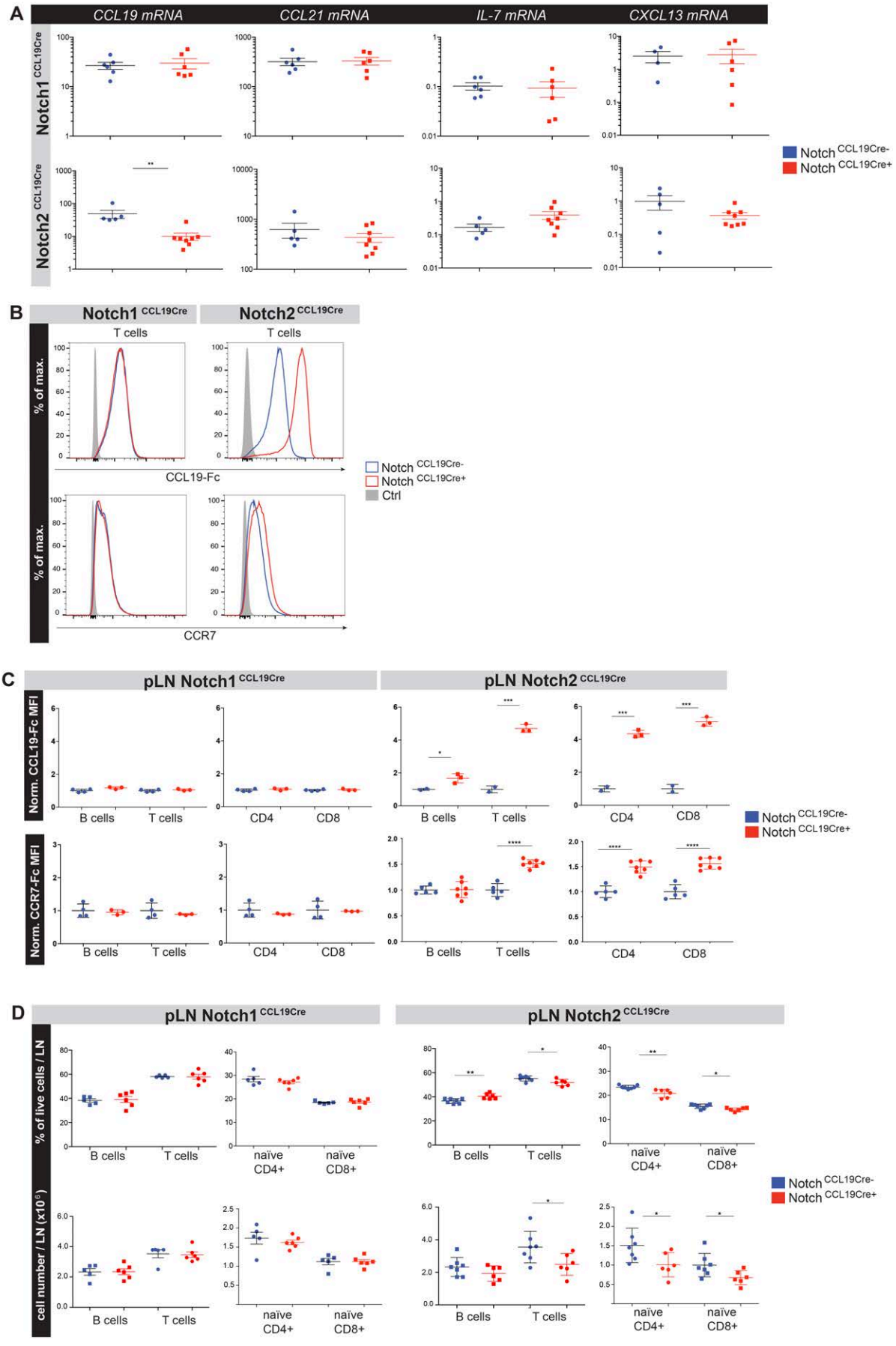
A
CCL19 mRNA
CCL21 mRNA
IL-7 mRNA
CXCL13 mRNA
Notch1 CCL19Cre
Notch2 CCL19Cre
Notch CCL19Cre-
Notch CCL19Cre+
B
Notch1 CCL19Cre
Notch2 CCL19Cre
T cells
% of max.
CCL19-Fc
CCR7
Notch CCL19Cre-
Notch CCL19Cre+
Ctrl
C
pLN Notch1 CCL19Cre
pLN Notch2 CCL19Cre
Norm. CCL19-Fc MFI
Norm. CCR7-Fc MFI
B cells
T cells
CD4
CD8
Notch CCL19Cre-
Notch CCL19Cre+
D
pLN Notch1 CCL19Cre
pLN Notch2 CCL19Cre
% of live cells / LN
cell number / LN (x10⁶)
naïve CD4+
naïve CD8+
Notch CCL19Cre-
Notch CCL19Cre+

Figure 23: Notch2 but not Notch1 in FRC regulates CCL19 expression. Analysis of naive pLN from adult Notch1^{CCL19Cre} and Notch2^{CCL19Cre} mice for cytokines and lymphocyte populations. **A)** qRT-PCR analysis on non-soluble fractions (stroma-enriched) of pLN for the normalized transcript levels of the indicated cytokines (mean ± SD) (n=4-8). **B-C)** Flow cytometric analysis of CCL19-Fc, anti-CCR7, or isotype control stainings on TCRb+ T cells from the indicated mouse strains, with representative histograms shown in **B** and scatter plots of the MFI from several mice shown in **C**. Data are representative of one (Notch1^{CCL19Cre}) or two experiments (Notch2^{CCL19Cre}) (n=3-7). **D)** Flow cytometric analysis of lymphocyte populations in the indicated strains. B cells (CD19+, TCRb-), T cells (CD19-, TCRb+), and naive CD4+ or CD8+ (CD44-, CD62L+) T cells. Data are representative of two experiments per mouse strain (n=5-7). P values are indicated as, * for $p < 0.05$, ** for $p< 0.01$, *** for $p<0.001$, **** for $p<0.0001$.

Next, we tested the expression of the different cytokine transcripts in stroma-enriched pLN fractions. No difference in *ccl19*, *ccl21*, *il-7* and *cxcl13* transcript levels was observed in Notch1^{CCL19Cre} mice, while mice with Notch2-deficient FRC showed a significant 80% decrease in *ccl19* transcripts relative to Cre- control mice, with the other three cytokines not showing a different expression (**Fig. 23A**). Consistent with the qRT-PCR data, CCL19-Fc and anti-CCR7 stainings showed an increased MFI only on pLN lymphocytes derived from Notch2^{CCL19Cre} but not Notch1^{CCL19Cre} mice (**Fig. 23B-C**). In Notch2$^{CCL19Cre+}$ pLN, CCL19-Fc signal intensities were significantly increased on B cells (1.6-times), CD8+ and CD4+ T cells (4-5-times), with also a 1.5-fold increase seen for anti-CCR7 stainings in both T cell subsets (**Fig. 23B-C**). In summary, these data demonstrate that naive T cells in pLN of Notch2$^{CCL19Cre+}$ mice encounter much less CCL19 protein, to an extent that is very comparable to the situation in Notch1/2$^{CCL19Cre+}$ pLN.

To study the possible impact of this altered CCL19 expression, I used again flow cytometry to study the various lymphocyte populations in naive pLN of adult Notch1^{CCL19Cre} and Notch2^{CCL19Cre} mice. No difference was observed for B and T cell populations in Notch1$^{CCL19Cre+}$ pLN relative to littermate controls while T but not B cells showed significantly reduced absolute numbers in Notch2^{CCL19Cre} mice, with the reduction being around 30% (**Fig. 23D**), similar to our previous findings in Notch1/2^{CCL19Cre} mice where the reduction was around 40% (**Table1**).

Next, I determined whether another aspect previously observed in Notch1/2^{CCL19Cre} pLN, namely the presence of lymph vessels within the T-cell zone (**Table1**), was due to either Notch 1 or 2 expression in FRC. Immunohistological staining of pLN sections from adult Notch1^{CCL19Cre} and Notch2^{CCL19Cre} mice showed the augmented presence of Lyve1+ LEC in T zones only in the Notch2-deficient mice, with the increase being 3.4-times fold (**Fig. 24A-D**), again similar to Notch1/2^{CCL19Cre} mice.

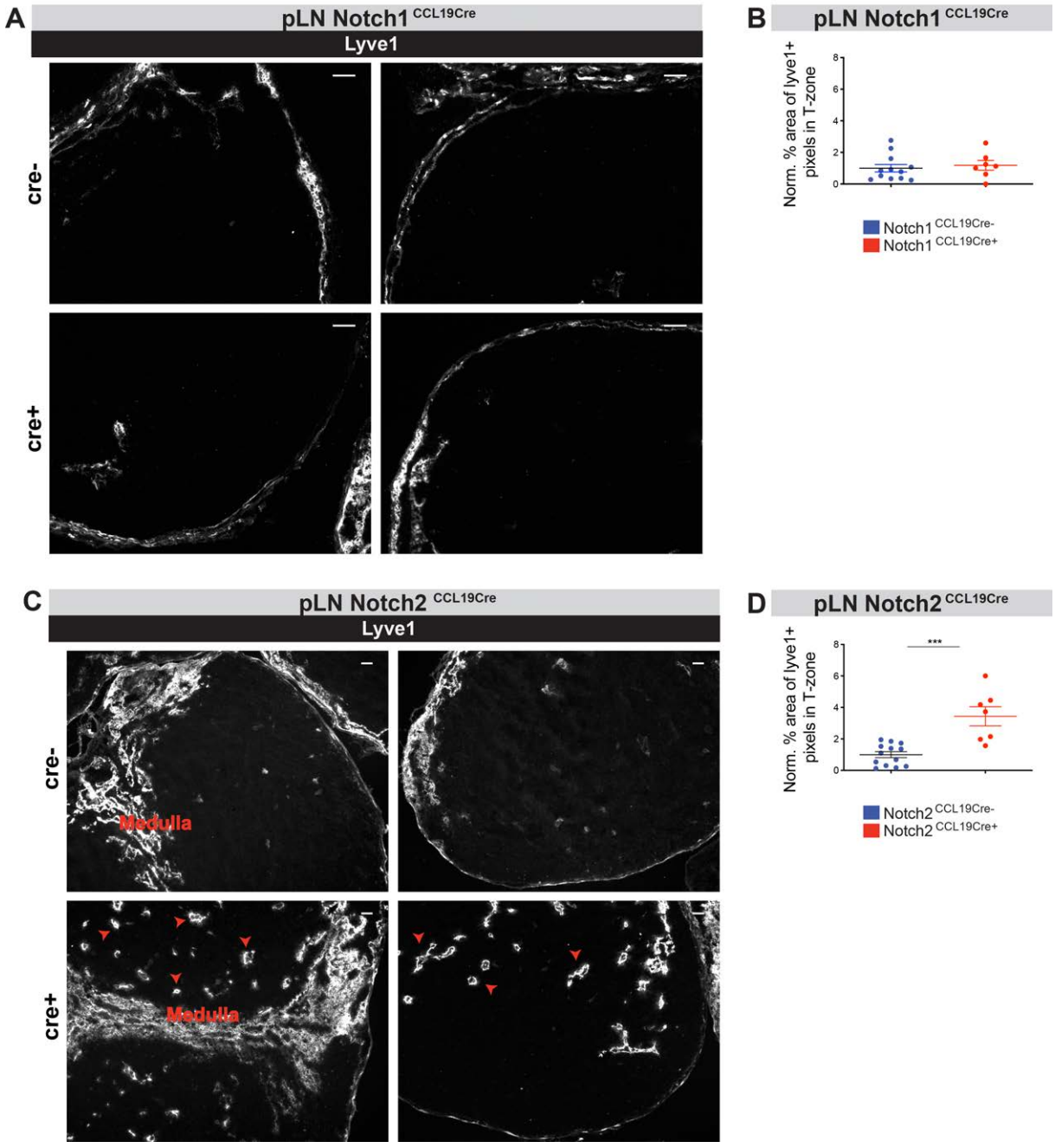

Figure 24: Notch2 but not Notch 1 in FRC is responsible for lymphatic vessel presence within pLN T zones. Cryostat sections of naïve pLN from adult Notch1^{CCL19Cre} (**A-B**) and Notch2^{CCL19Cre} (**C-D**) mice were stained for the lymphatic endothelial cell marker Lyve1. Representative histology images are shown for Cre- and Cre+ pLN (**A, C**) and quantified as percentage of the T-zone area covered by lyve1+ pixels normalized to the Cre- control (B, D). Arrows point to Lyve1+ lymphatic endothelial cells within the T cell-zone identified by CD3 co-staining (data not shown). Data are representative of one (n=2; **A, B**) or one (n=2; **C,D**) experiment. Scale bar, 50 µm. P values are indicated as, *** for p<0.001.

To summarize, surprisingly Notch1$^{CCL19Cre+}$ mice did not show any phenotype, except for a potential weak contribution to MRC development (**Table2**). On the contrary, Notch2$^{CCL19Cre+}$ mice showed similar defects or alterations as observed in Notch1/2$^{CCL19Cre+}$ mice, such as activation state of TRC, altered conduit and lymph vessel formation as well as reduced

CCL19 expression and decreased T cell accumulation (**Table2**). Only the striking defect in MRC numbers isolated from Notch1/2^{CCL19Cre} pLN was not fully reproduced in Notch2-deficient mice possibly suggesting a role for both Notch receptors in MRC development. So clearly, Notch2 seems to be much more important than Notch1 in pLN FRC under the conditions tested, with roles in FRC themselves and indirect effects on the neighbouring immune and non-immune cells sharing the same pLN microenvironments (**Table2**).

8. Notch function in FRC is dependent to a large extent on the canonical signaling pathway acting via RBPj

The DNA-binding protein RBPj has been described as the principal transcription factor collaborating with the activated and cleaved Notch receptor, NICD, in what is referred to as the canonical Notch pathway (Bray 2006, Radtke, Fasnacht et al. 2010). However, several Notch-receptor driven biological processes seem to be RBPj-independent (Siebel and Lendahl 2017), raising the possibility that studying its role in FRC may allow to segregate into two groups the many phenotypes previously observed in Notch1/2$^{CCL19Cre+}$ and Notch2$^{CCL19Cre+}$ pLN and thereby gain a better insight into the linked phenotypes. To this end, a new genetic mouse model was generated by intercrossing CCL19cre with RBPj$^{lox/lox}$ mice (Han, Tanigaki et al. 2002) to obtain RBPj^{CCL19Cre} mice (**Fig. 25A**). We also expected that this tool would allow us to gain a better understanding of Notch-driven transcriptional events in FRC as a large number of human gene promoters have been identified to be bound by RBPj, including those of several cytokines and ECM proteins also highlighted in our study (Procopio, Laszlo et al. 2015). Of note, RBPj-deficiency in FRC may also reveal roles that go beyond Notch1/2-mediated effects, as Notch3 may signal via RBPj, and as RBPj also acts as transcriptional repressor in absence of Notch signaling (Hori, Sen et al. 2013) (Oswald, Winkler et al. 2005). Thus, naive pLN of adult RBPj^{CCL19Cre} mice were analyzed for the different phenotypes observed in the other mouse strains. Flow cytometric analysis of stromal cells in RBPj$^{CCL19Cre+}$ pLN revealed a statistically significant 50% decrease in percentage and 37% decrease in absolute numbers of FRC (**Fig. 25B**). We also observed a trend to lower LEC and BEC numbers (**Fig. 25B**). Regarding FRC subsets, I saw a significant 30% decrease in relative TRC numbers and a 60% decrease in absolute numbers of TRC in Cre+ versus Cre- mice. While MedRC numbers stayed constant, we noted a trend to lower MRC numbers, although the low percentage of MRC in this isolation did not allow to get very robust data (**Fig. 25B**).

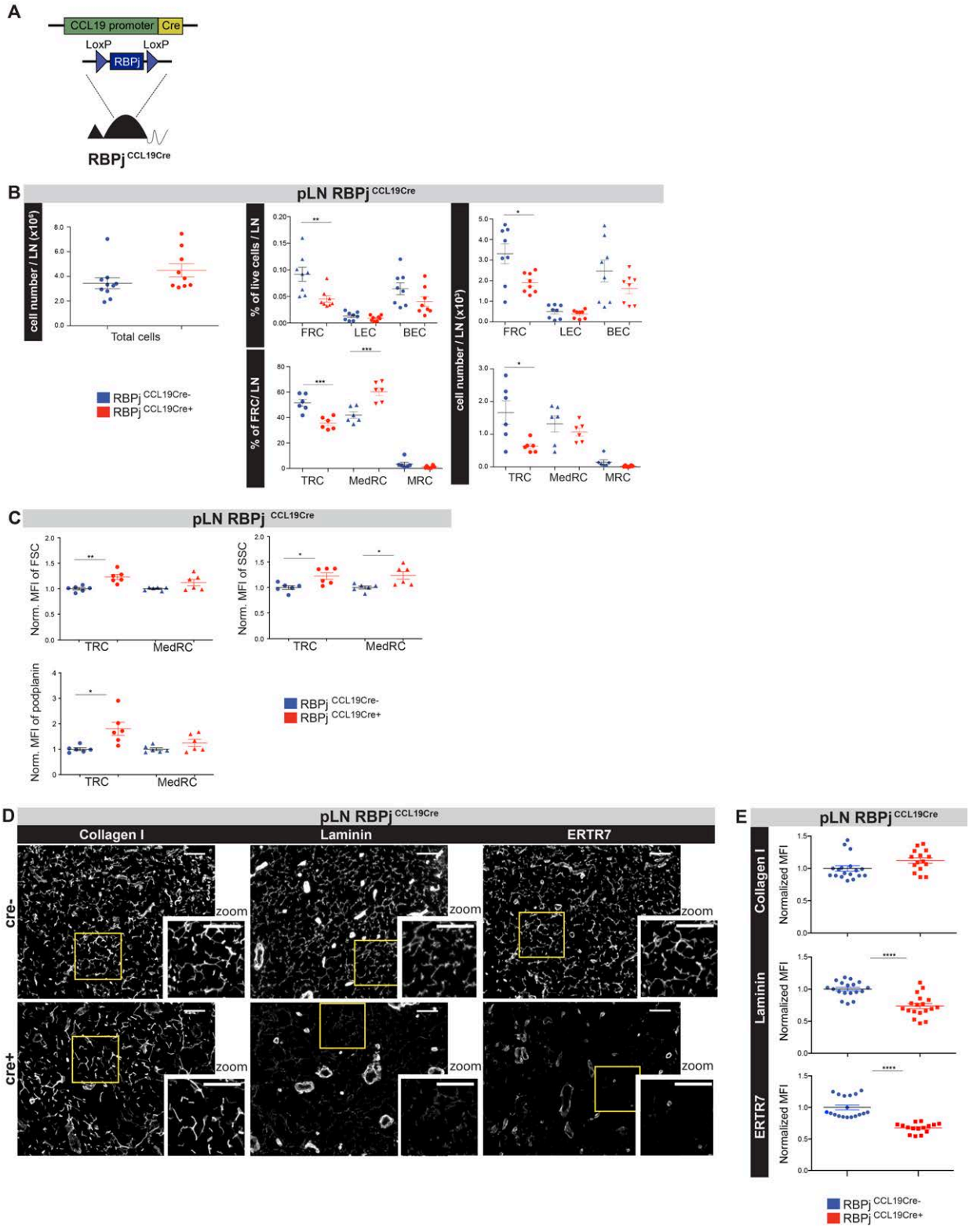
A
CCL19 promoter
Cre
LoxP
LoxP
RBPj
RBPj CCL19Cre
B
pLN RBPj CCL19Cre
cell number / LN (x10⁶)
Total cells
% of live cells / LN
FRC
LEC
BEC
cell number / LN (x10³)
% of FRC/ LN
TRC
MedRC
MRC
RBPj CCL19Cre-
RBPj CCL19Cre+
C
pLN RBPj CCL19Cre
Norm. MFI of FSC
Norm. MFI of SSC
Norm. MFI of podplanin
TRC
MedRC
RBPj CCL19Cre-
RBPj CCL19Cre+
D
pLN RBPj CCL19Cre
Collagen I
Laminin
ERTR7
cre-
cre+
zoom
E
pLN RBPj CCL19Cre
Collagen I
Laminin
ERTR7
Normalized MFI
RBPj CCL19Cre-
RBPj CCL19Cre+

Figure 25: Canonical Notch signaling via RBPj regulates FRC development and matrix expression within pLN. Stromal cell analysis of naive pLN from adult RBPj^{CCL19Cre} mice. **A)** Drawing illustrating the novel generation of RBPj^{CCL19Cre} mice by intercrossing two existing mouse strains, one expressing conditional RBPj alleles (gene flanked by loxP sites) and the other expressing Cre-recombinase under control of the CCL19-gene promoter active in FRC of SLO. **(B-C)** Flow cytometric analysis digested pLN from adult RBPj^{CCL19Cre} mice. Data are representative of two independent experiment (n=6-8) **B)** Analysis of total cells, stromal cells (FRC, LEC, BEC) and FRC subsets (TRC, MedRC, MRC) plotted in relative or absolute cell numbers. **C)** Analysis of TRC and MedRC size (FSC), granularity (SSC) and podoplanin expression level (MFI). **D-E)** Immunofluorescence microscopy of cryostat pLN sections stained for the indicated ECM components. **D**) Representative images are shown for the T zone along with magnified views of T zone conduits. Data are representative of one experiment (but confirmed on a second experiment with 3-week old mice). Scale bar, 50 µm. **E)** To quantify the ECM protein staining of the conduit network the MFI was measured in three areas (squares of 150 x 150 pixels) per image and normalized to littermate controls. Data are representative of one experiment (n=2). P values are indicated as, * for $p < 0.05$, ** for $p< 0.01$, *** for $p<0.001$, **** for $p<0.0001$.

A significant increase of TRC size (1.2-time) and granularity (1.2-time) was observed (**Fig. 25C**). Only a significant increase of MedRC granularity (1.2-time) was observed (**Fig. 25C**). Podoplanin expression was significantly upregulated (1.8-time) in TRC, but no significant difference was observed for MedRC (**Fig. 25C**). In conclusion, RBPj-deficient mice reproduce the defects in stromal cell numbers and TRC activation state previously seen in Notch1/2$^{CCL19Cre+}$ mice (**Table2**).

Analysis of the T zone conduit network by immunohistology in RBPj$^{CCL19Cre+}$ pLN revealed a normal collagen I staining intensity, however again with longer and more unbranched conduit structures (**Fig.25D-E**). A marked decrease in laminin and ERTR7 staining intensities was observed for the conduit network (**Fig.25D-E**). Therefore, the Notch2-dependent ECM regulation by FRC is also RBPj dependent, pointing to canonical Notch 2 signaling (**Table2**).

Analysis of cytokine transcripts in stroma-enriched pLN fractions of RBPj^{CCL19Cre} mice did, much to our surprise, not show any significant difference for *ccl19* transcript levels, although the data were quite variable, with no differences for *ccl21*, *il-7* and *cxcl13* in Cre+ versus Cre- mice (**Fig.26A**). Using our indirect readout for CCL19 protein levels encountered by T cells, we observed only a 1.5-fold increase in MFI for the CCL19-Fc staining for both T cell subsets but not B cells in Cre+ versus Cre pLN (**Fig.26B-C**). Similarly, the MFI of the anti-CCR7 staining showed no difference for B cells and only a 1.3-1.6-time increase in MFI for the two T cell subsets in Cre+ pLN (**Fig.26B-C**). Thus, the small differences observed at the CCL19 protein level in RBPj^{CCL19Cre} mice are consistent with the low or absent differences in CCL19 transcripts between the two groups, suggesting that RBPj is not the major regulator of CCL19 expression. These findings are markedly different from Notch1/2$^{CCL19Cre+}$ mice where CCL19 transcripts were reduced by 60% along with a 2-fold higher CCR7 and 5-fold higher CCL19-Fc staining on T lymphocytes, with even B-lymphocytes showing increased staining intensities for both reagents (**Fig.12**).

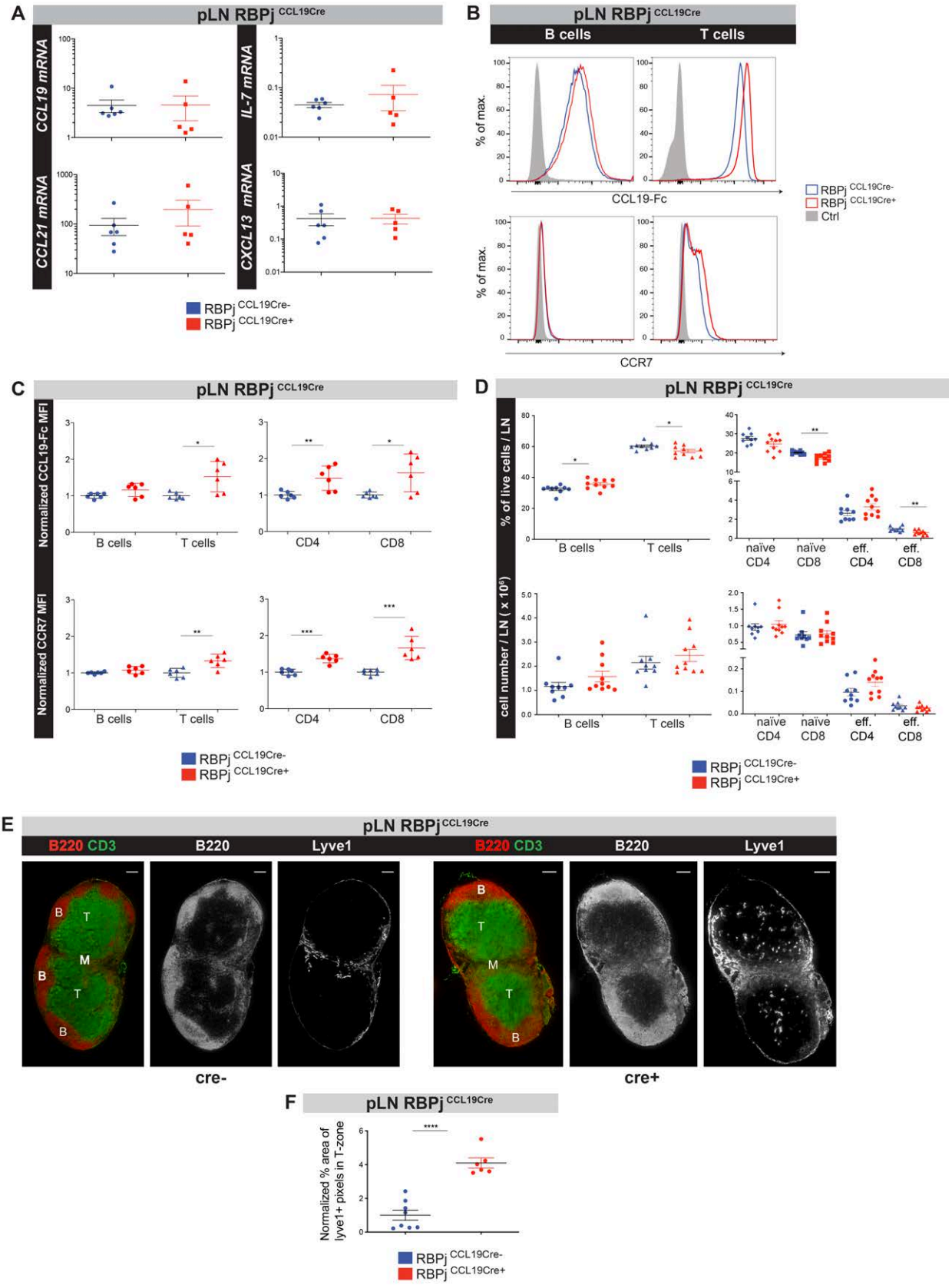
A
pLN RBPj CCL19Cre
CCL19 mRNA
IL-7 mRNA
CCL21 mRNA
CXCL13 mRNA
RBPj CCL19Cre-
RBPj CCL19Cre+
B
pLN RBPj CCL19Cre
B cells
T cells
% of max.
CCL19-Fc
CCR7
RBPj CCL19Cre-
RBPj CCL19Cre+
Ctrl
C
pLN RBPj CCL19Cre
Normalized CCL19-Fc MFI
Normalized CCR7 MFI
B cells
T cells
CD4
CD8
RBPj CCL19Cre-
RBPj CCL19Cre+
D
pLN RBPj CCL19Cre
% of live cells / LN
cell number / LN (x 10⁶)
B cells
T cells
naïve CD4
naïve CD8
eff. CD4
eff. CD8
RBPj CCL19Cre-
RBPj CCL19Cre+
E
pLN RBPj CCL19Cre
B220 CD3
B220
Lyve1
B
T
M
cre-
cre+
F
pLN RBPj CCL19Cre
Normalized % area of lyve1+ pixels in T-zone
RBPj CCL19Cre-
RBPj CCL19Cre+

Figure 26: RBPj deletion in FRC only weakly affects CCL19 expression but leads to lymphatic vessel presence within pLN T zones. Analysis of naive pLN from adult RBPj^{CCL19Cre} mice for cytokines and lymphocyte populations. **A)** qRT-PCR analysis on non-soluble fractions (stroma-enriched) of pLN for transcript levels of the indicated cytokines normalized to two housekeeping genes (mean ± SD) (n=5-6). **B-C)** Flow cytometric analysis of CCL19-Fc, anti-CCR7, or isotype control stainings on TCRb+ T cells and CD19+ B cells, with representative histograms shown in B and scatter plots of the MFI from several stainings/mice shown in C, including for CD4+ and CD8+ T cells. Data are representative of two independent experiments (n=6). **D)** Flow cytometric analysis of lymphocyte populations: B cells (CD19+, TCRb-), T cells (CD19-, TCRb+), and naive CD4+ or CD8+ (CD44-, CD62L+) T cells. Data are representative of four independent experiments (n=9-10). **E-F)** Immunofluorescence microscopy of pLN cryostat sections stained for CD3+ T cells, B220+ B cells and lyve1+ lymphatic endothelial cells. Representative images of two independent experiments (n=4) are shown in E with magnified regions of the T zone showing the presence of lyve1+ lymph vessels in Cre+ but not Cre- mice. B, B cell zone (follicle); T, T-cell zone; M, medulla. Scale bar, 200 µm. **F)** Scatter plot showing the percentage of T-zone area covered by lyve1+ pixels after normalization to the Cre- control tissues. Data are representative of one independent experiments (n=2). P values are indicated as, * for $p < 0.05$, ** for $p< 0.01$, *** for $p<0.001$.

To test whether the CCL19 levels correlate again with the number of T cells accumulating inside pLN, as previously seen in Notch1/2$^{CCL19Cre+}$ and Notch2$^{CCL19Cre+}$ mice, where both parameters were reduced, we assessed lymphocyte population of RBPj^{CCL19Cre} pLN using flow cytometry. While relative frequencies showed a small decrease in CD8+ T cells in Cre+ compared to Cre- mice, absolute numbers of lymphocyte subsets were comparable between the two groups (**Fig.26D**). In conclusion, RBPj deletion in FRC affects pLN lymphocyte numbers only marginally, much in contrast to the marked defect observed in mice with deletions of Notch1/2 or Notch2 (**Table2**).

Histological analysis of the global pLN structure in RBPj$^{CCL19Cre+}$ mice showed a normal T/B segregation with preliminary evidence again pointing towards less polarized B-cell follicles compared to Cre- mice (**Fig.26E**). Cre+ mice also showed a 4-times higher frequency of T zone LEC compared to Cre- mice (**Fig. 26E-F**).

In summary, Notch1/2 $^{CCL19Cre+}$ and RBPj$^{CCL19Cre+}$ mice share several pLN phenotypes, such as reduced FRC numbers, altered conduit protein composition and network structure, along with aberrant lymph vessels within the T-zone indicating that these processes are dependent on canonical Notch signaling. Interestingly, Notch1/2 $^{CCL19Cre+}$ but not RBPj$^{CCL19Cre+}$ mice show differences in CCL19 transcript levels that go along with a defect in T cell accumulation (see **Table 2**).

Phenotypes – adult pLN	N1/2^{CCL19Cre}	N1^{CCL19Cre}	N2^{CCL19Cre}	RBPj^{CCL19Cre}
Stromal cells				
FRC number (FACS)	-	wt	wt	--
BEC number (FACS)	--	wt	--	wt
MRC number (FACS)	---	wt	--	wt
TRC size-granularity	+	wt	+	+
TRC – pdpn expression	++	wt	+	+
FRC functions				
Collagen I structure	≠	wt	≠	≠
Basement membrane (conduits)	--	wt	--	--
Microfibrillar zone (conduits)	--	wt	--	--
Ccl19 transcripts	--	wt	---	wt
CCL19-Fc staining (T cells)	+++	wt	+++	+
CCR7 staining (T cells)	++	wt	++	+/-
IL-6 transcripts	++	N.D.	N.D.	N.D.
Neighboring cells				
T cell number	--	wt	-	wt
B-cell follicle shape	≠	N.D.	N.D.	≠
Aberrant LEC in T cell-zone	+++	wt	++	++

Table 2: Summary of the multiple phenotypes observed for the different mouse strains. ('-' : decrease ; '+ ': increase ; '≠' :different ; 'wt ' : no difference). N.D.: not determined. -/+ : 10-30% or 1.5-2 times for transcript/MFI analysis; --/++ : 30-50% or 2-5 times for transcript/MFI analysis; ---/+++ : more than 50% or more than 5 times for transcript/MFI analysis.

9. Defects due to Notch1/2 deletion in FRC are already present during postnatal development of pLN

The results presented so far are all derived from the analysis of pLN and spleens in adult animals and do not distinguish between a developmental versus a homeostatic role of Notch signaling in FRC. By investigating pLN of 2-3 weeks old mice we thought we could shed light onto this question as well as possibly getting an idea of the sequence of events. Finally, Notch2 expression was only found in a smaller FRC subset in adult pLN in contrast to the more prominent Notch1 expression in FRC while paradoxically our genetic evidence pointed to a dominant role of Notch2 for virtually all our defects observed in Notch1/2-deficent mice. Therefore, we wished to test first whether during development more FRC express Notch 2 with possibly less FRC expressing Notch1.

To that end, we analyzed pLN stromal cells from 3 weeks old WT mice for Notch receptor expression and to our surprise did not see any difference in the fraction of FRC expressing Notch1 and Notch2 compared to pLN FRC from adult wt mice, with the surface expression of Notch1 being apparently much more prominent than the one of Notch2, both in MFI and percentage of expressing cells (**Fig.27A,** and data not shown). Next, we investigated pLN stromal cells of 3 weeks old Notch2 ^{CCL19Cre} mice to get an estimate for the efficiency and

specificity of the Cre-mediated deletion. Notch1 expression was unaltered in FRC, LEC and BEC of Cre+ compared to Cre- pLN, as expected, with all three subsets showing relatively high expression levels (**Fig.27B-C**). Surface Notch2 levels were again rather low on FRC with 20% being positive in Cre- pLN FRC but in Cre+ mice they showed a trend towards a lower expression level, reminiscent of our findings in adult Notch1/2 ^{CCL19Cre} mice (**Fig.8B-C**) where this level of deletion triggered many biological effects. Similar to the adult mice, the deletion seemed to be specific for FRC with no significant difference seen for Notch-2 expressing LEC, with BEC being Notch2-negative (**Fig.27B-C**).

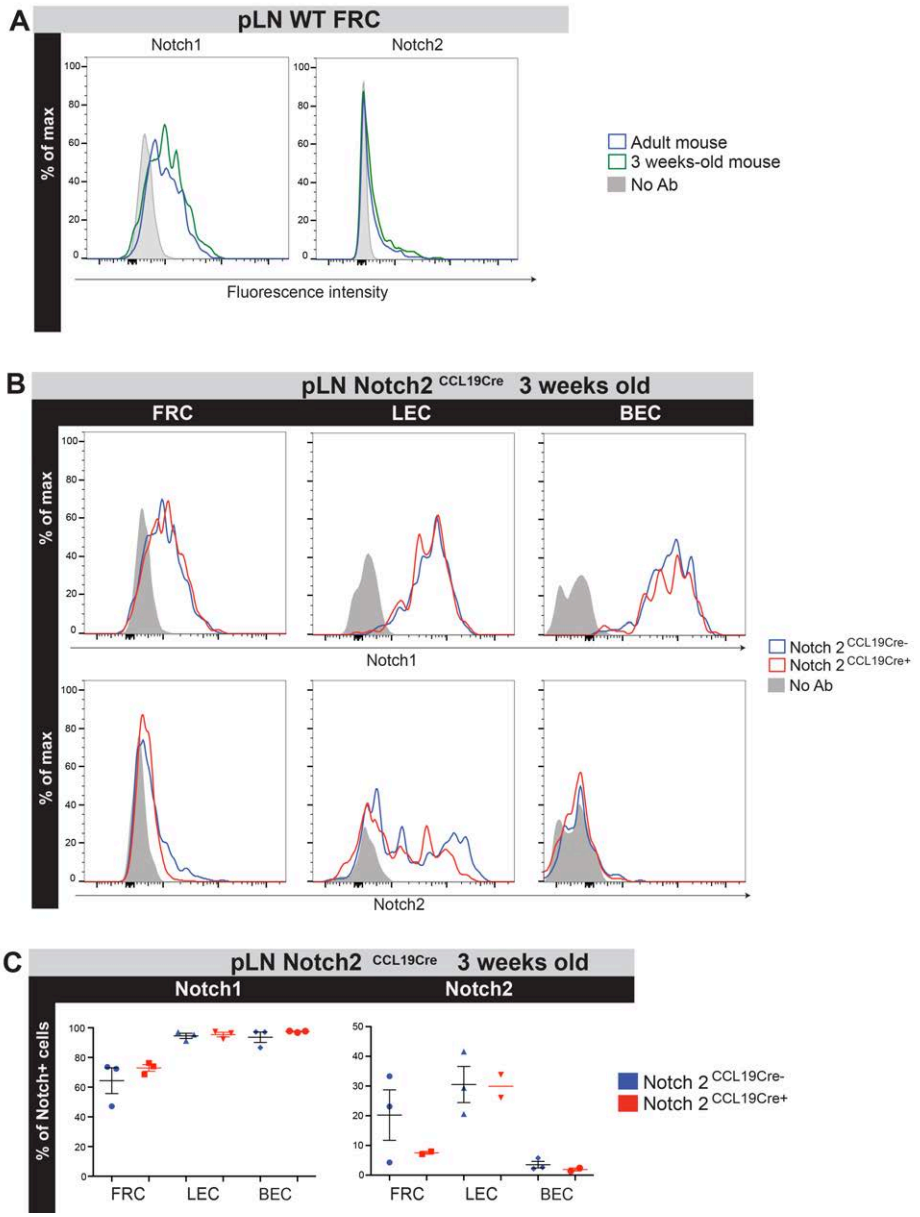

Figure 27: No difference in Notch1 and Notch2 expression in FRC postnatal mouse development. Analysis of naive pLN from 3-weeks old mice, either of wt, Notch2^{CCL19Cre} or Notch1/2^{CCL19Cre} background. **A-C)** Flow cytometric analysis of stromal cells from enzymatically digested pLN. Analysis of surface Notch1 and Notch2 expression levels either on wt FRC (3 weeks old), with adult wt FRC shown as comparison (histograms showing in **A)** to measure postnatal Notch expression, or from FRC, LEC and BEC of 3-weeks old Notch2^{CCL19Cre} mice with representative histograms shown in **B** and scatter plot analysis of multiple mice shown in C to assess the Notch2 deletion efficiency and specificity. Data are representative of two (A, n=4) or one (B-C, n=3) experiment.

Next, we investigated the stromal cell composition in pLN of 3 weeks-old mice and did not observe any major difference in relative and absolute numbers of FRC, LEC and BEC in Notch1/2 $^{CCL19Cre+}$ versus Cre- littermate controls, with comparable findings obtained also for 3 weeks-old Notch2 ^{CCL19Cre} mice (**Fig. 28A**). Also the analysis of FRC subsets did not reveal alterations between Cre+ versus Cre- pLN of both strains that translated into differences in absolute numbers (**Fig.28A**). Of note, MRC numbers were not reduced in any of these Cre+ postnatal pLN, in contrast to our findings with adult Cre+ pLN. Interestingly, 3 weeks-old pLN already had adult numbers of the various stromal cells, with all investigated subsets being present (**Fig. 28A**), despite the smaller LN size suggesting their expansion and differentiation is already complete at this stage (**Table3**).

We then analyzed FRC functions. Doing ECM protein stainings of T zone conduits in pLN sections of 3 weeks-old mice revealed that the collagen I core did not show any difference in term of intensity but the structure was impaired with “longer” fibers in Cre+ compared to Cre- mice of both strains (**Fig. 28B-C;** and data not shown). The labeling with antibodies to laminin and ERTR7 showed a significant decrease in intensity for both Cre+ strains (**Fig. 28B-C**), again reproducing the findings from adult Cre+ pLN, indicating this phenotype develops early and is not due to altered TRC numbers (**Table3**).

Figure 28: The Notch2-dependent ECM expression defect in pLN FRC is already present during postnatal mouse development. Flow cytometry analysis of digested pLN from 3-weeks old naïve mice, either Notch2^{CCL19Cre} or Notch1/2^{CCL19Cre} background**. A)** Scatter plots showing the relative and absolute pLN numbers in 3 weeks old Notch1/2^{CCL19Cre} and Notch2^{CCL19Cre} mice: for total cells, stromal cells (FRC, LEC, BEC) and FRC subsets (TRC, MedRC, MRC). Data are representative of two independent experiments (n= 2-7 for Notch1/2^{CCL19Cre}, n=5-6 for Notch2^{CCL19Cre} mice). **B-C)** Immunofluorescence microscopy of pLN cryostat sections from 3 weeks old Notch2^{CCL19Cre} mice stained for the indicated ECM components. Representative images are shown in **B** with magnified regions of the T zone to highlight the conduit defect in Cre+ mice. Scale bar, 50 µm. **C)** Scatter plots showing the quantification of the ECM protein staining intensity (MFI) of the conduit network measured in three T zone areas (squares of 150 x 150 pixels) per image and normalized to littermate controls. Data are representative of one (B, n=4) and two (C, n=4-6) experiments. P values are indicated as, * for $p < 0.05$, ** for $p< 0.01$, **** for $p<0.0001$.

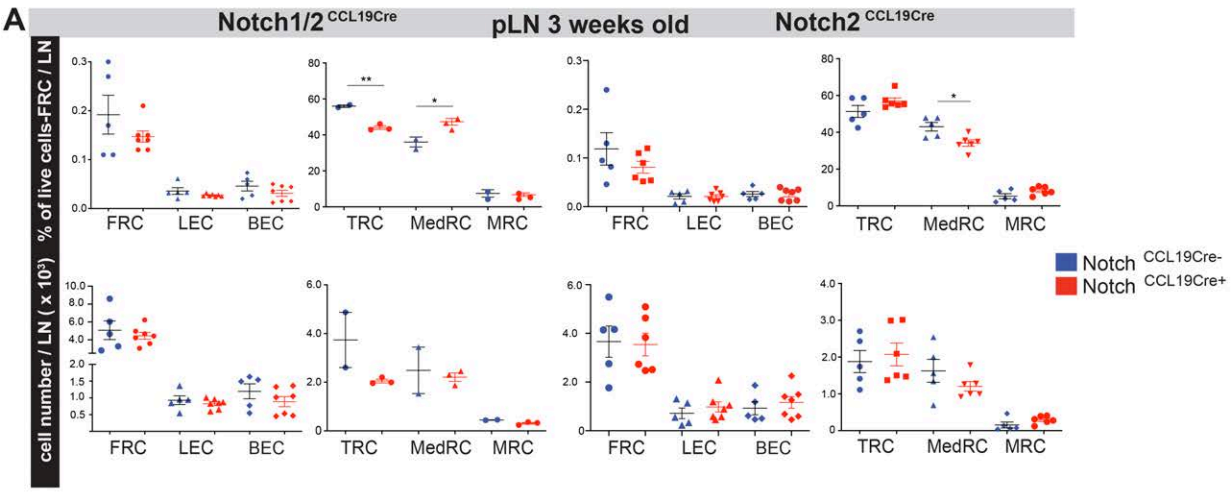
A
Notch1/2 CCL19Cre
pLN 3 weeks old
Notch2 CCL19Cre
% of live cells-FRC / LN
cell number / LN (x 10³)
FRC
LEC
BEC
TRC
MedRC
MRC
Notch CCL19Cre-
Notch CCL19Cre+

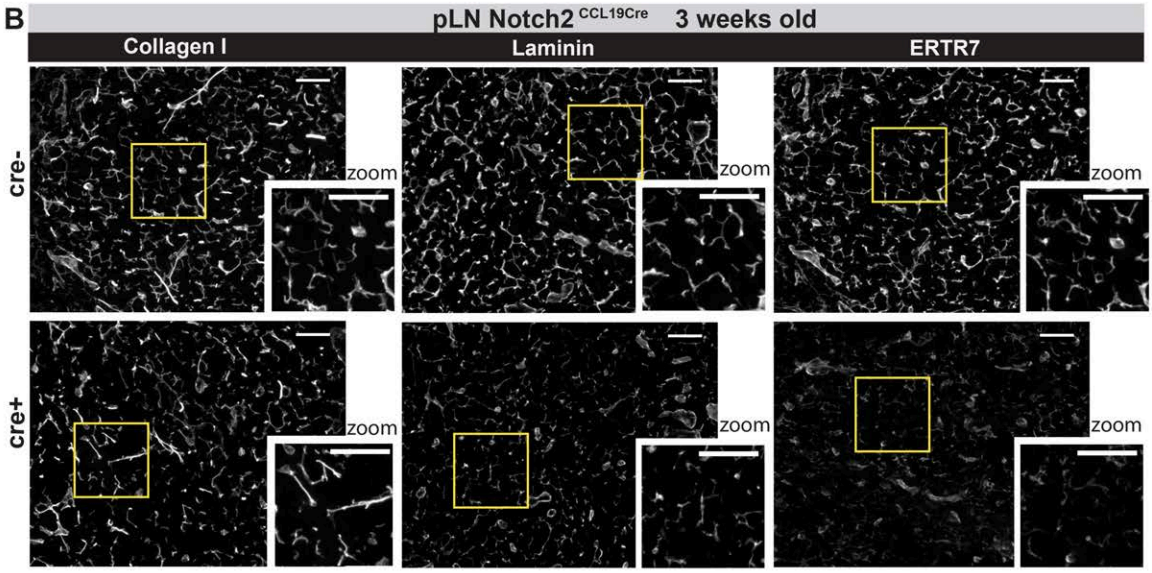
B
pLN Notch2 CCL19Cre 3 weeks old
Collagen I
Laminin
ERTR7
cre-
cre+
zoom

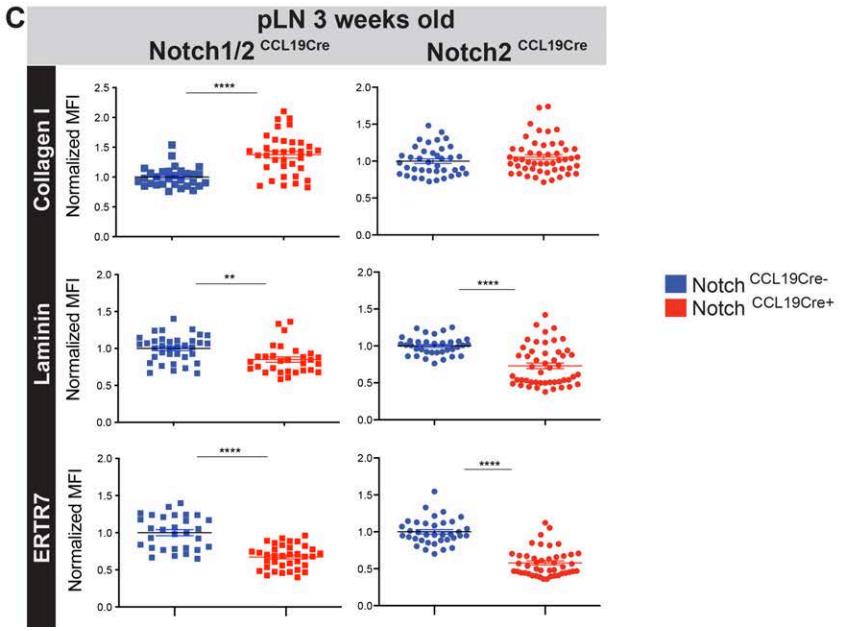
C
pLN 3 weeks old
Notch1/2 CCL19Cre
Notch2 CCL19Cre
Collagen I
Laminin
ERTR7
Normalized MFI
Notch CCL19Cre-
Notch CCL19Cre+

To investigate cytokines typically expressed in naive pLN FRC we analyzed this time whole pLN due their smaller size at 3 weeks of age. pLN of young Notch1/2 $^{CCL19Cre+}$ and Notch2 $^{CCL19Cre+}$ mice showed a significant decrease of *ccl19* transcripts for both strains, with the reduction being around 70% for Notch1/2 and 50% for Notch2 deletion, comparable to adult Cre+ pLN (**Fig.29A**). In contrast, I did not observe any statistically significant difference for *ccl21*, *il-7* and *cxcl13* transcripts (**Fig.29A**). Given the reduced CCL19 transcript levels we expected to see increased levels of surface CCR7 staining on naive lymphocytes. Indeed, CCL19-Fc stainings on 3 weeks-old Notch2 $^{CCL19Cre+}$ pLN cells showed a 1.6 time increased MFI on B cells from Cre+ versus Cre- pLN, with the two T cell subsets showing a similarly increased MFI (**Fig.29B-C**). However, no striking difference was observed for CCR7 staining in B and T cells of Notch2 ^{CCL19Cre} pLN (**Fig.29B-C**). These data are preliminary but indicate that there is probably already a difference in the CCL19 protein levels sensed by lymphocytes, but that the CCR7 modulation is not yet as pronounced as in adult mice.

Flow cytometric analysis of lymphocyte populations of Notch1/2^{CCL19Cre} and Notch2^{CCL19Cre} mice at 3weeks of age showed no difference in T cell numbers in both strains, but an increase in B cells in Cre+ relative to Cre- pLN, both in relative (~5-20%) and absolute numbers (~ 35-45%) (**Fig. 29D**).

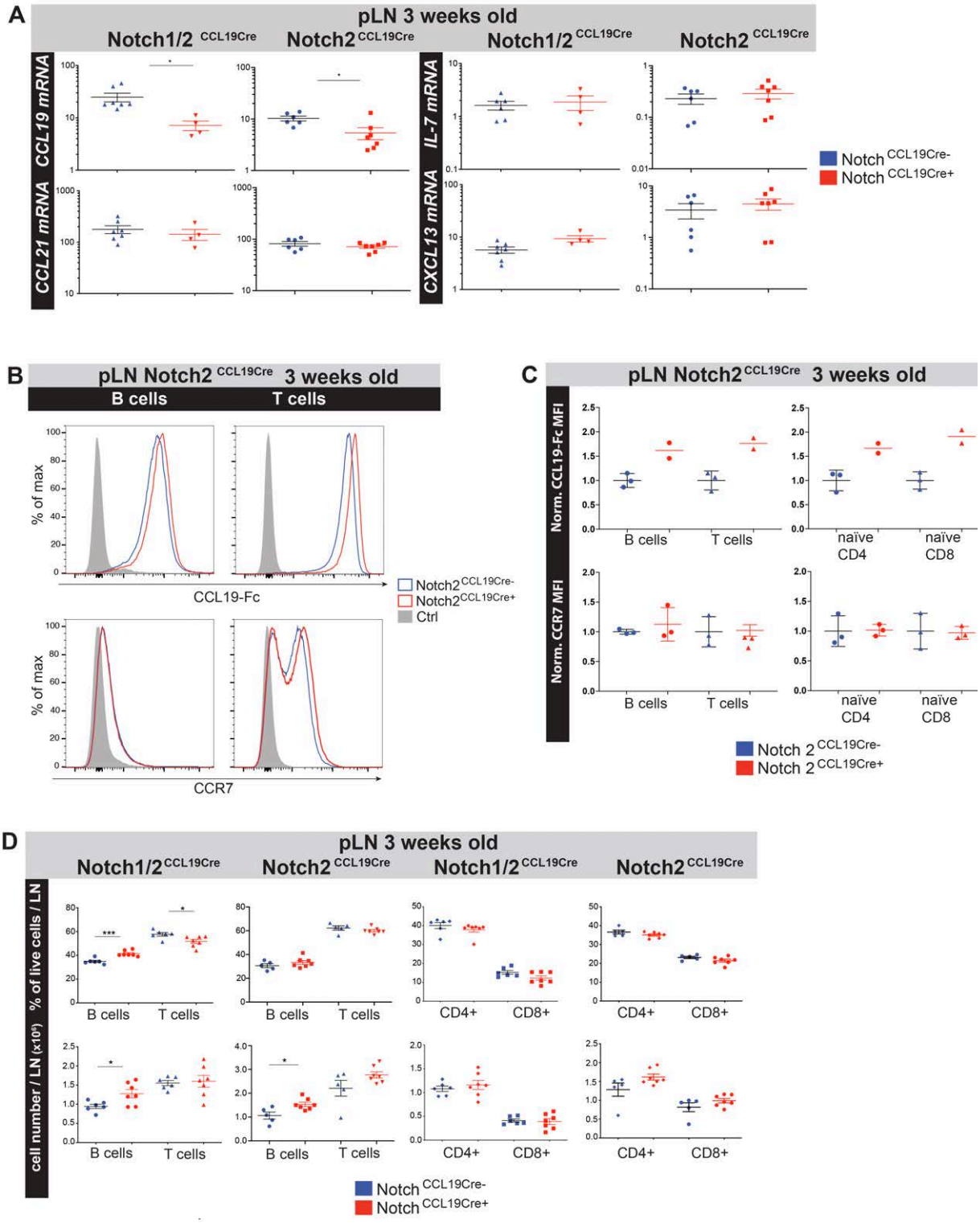

Figure 29: The Notch2-dependent defects in CCL19 expression is already present during postnatal mouse development. Analysis of naive pLN from 3-weeks old Notch1/2^{CCL19Cre} or Notch2^{CCL19Cre} mice for cytokines, lymphocytes and lymphatic vessels. **A)** qRT-PCR analysis of whole pLN from the two mouse strains for transcript levels of the indicated cytokines normalized to two housekeeping genes (mean ± SD)(n=6-7). B-C) Flow cytometric analysis of CCL19-Fc, anti-CCR7, or isotype control stainings on CD19+ B cells and TCRb+ T cells from Notch2^{CCL19Cre} mice, with representative histograms shown in **B** and scatter plots of the MFI from several stainings/mice shown in **C**, including for naive (CD44-) CD4+ and CD8+ T cells. Data are representative of one experiment (n=2-3). **D)** Flow cytometric analysis of lymphocyte populations in pLN from Notch1/2^{CCL19Cre} and Notch2^{CCL19Cre} mice: B cells (CD19+,TCRb-), T cells (CD19-,TCRb+), and naive CD4+ or CD8+ (CD44-, CD62L+) T cells. Data are representative of two independent experiments (n=5-7). P values are indicated as, *for $p<0.05$.

As a next step we assessed the pLN structure by immunohistology in both strains at 3 weeks of age. Notch1/2^{CCL19Cre} mice showed similar phenotypes as adult mice, with an altered B-cell follicle shape and a 4.5-time increase in T zone lymph vessels only in Cre+ but not Cre- mice (**Fig. 30A-B**). Young Notch2$^{CCL19Cre+}$ mice a similarly altered B-cell follicle shape with 5.3-fold more T zone lymph vessels (**Fig.30C-D**). Staining of the lymphatic vessel-specific transcription factor Prox-1 confirmed that these Lyve1+ structures present in the T-cell zone are indeed of the lymphatic cell lineage (**Fig. 30C**).

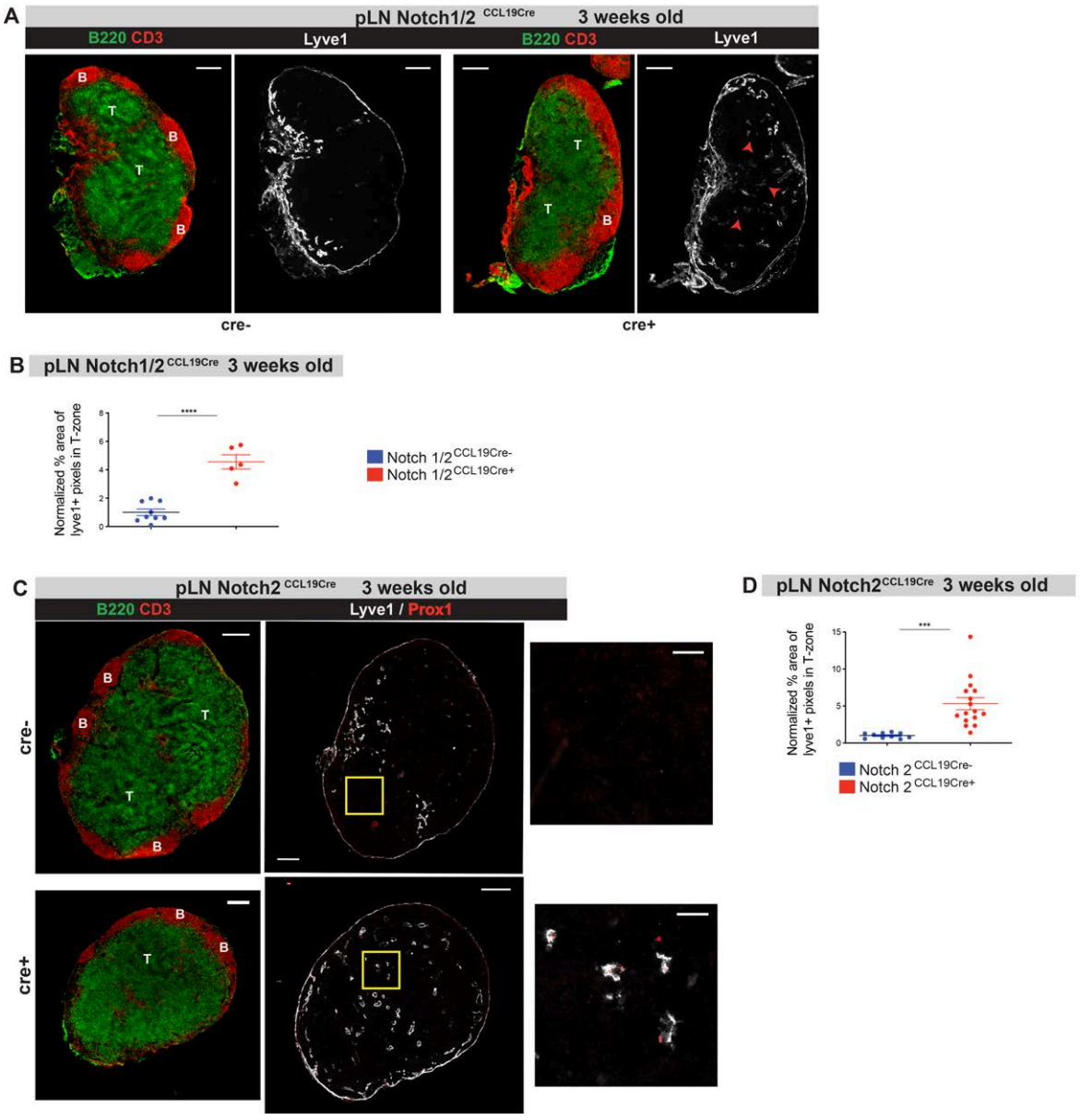

Figure 30: The Notch2-dependent defects in lymph-vessels is already present during postnatal mouse development. A-D) Immunofluorescence microscopy analysis of pLN cryostat sections from 3-weeks old Notch1/2^{CCL19Cre} (**A, B**) and Notch2^{CCL19Cre} mice (**C, D**) stained for CD3+ T cells, B220+ B cells and Lyve1+ lymphatic endothelial cells. Representative images are shown (**A, C**) with magnified regions of the T zone showing the presence of Lyve1+ Prox-1+ lymph vessels in Cre+ but not Cre- mice. B, B cell zone (follicle); T, T-cell zone. Scale bar, 200 µm. B, **D)** Scatter plots showing the percentage of T-zone area covered by lyve1+ pixels after normalization to the Cre- control tissues. Data are representative of one (A, B: n=4) and two (C, D: n=4-6) experiments. P values are indicated as, *** for p<0.001.

In summary, the defects seen in adult mutant mice regarding matrix-based conduit, ccl19 expression, and aberrant follicles and LEC positioning, are phenotypes already present during postnatal pLN development. In the **table 3** below, the various pLN phenotypes of adult versus 3-weeks old mice are summarized highlighting that also most other defects observed in adult Cre+ mice are seen already in juvenile mice, except for the reduction in numbers of FRC, BEC and T cells that only becomes apparent in adult mice.

Phenotypes – pLN	N1/2^{CCL19Cre} Adult	N2^{CCL19Cre} Adult	N1/2^{CCL19Cre} 3weeks old	N2^{CCL19Cre} 3weeks old
Stromal cells				
FRC number (FACS)	-	wt	wt	wt
BEC number (FACS)	--	--	wt	wt
MRC number (FACS)	---	--	wt	wt
TRC size-granularity	+	+	N.D.	N.D.
TRC – pdpn expression	++	+	N.D.	N.D.
FRC functions				
Collagen I conduit structure	≠	≠	≠	≠
Basement membrane (conduits)	--	--	-	--
Microfibrillar zone (conduits)	--	--	--	--
Ccl19 transcripts	---	---	---	---
CCL19-Fc staining (T cells)	+++	+++	N.D.	+
CCR7 staining (T cells)	++	++	N.D.	wt
IL-6 transcripts	++	N.D.	N.D.	N.D.
Neighboring cells				
T cell number	--	-	wt	wt
B-cell follicle shape	≠	N.D.	≠	≠
Aberrant LEC in T cell-zone	+++	++	++	+++

Table 3: Summary of the multiple phenotypes observed for N1/2^{CCL19Cre} and N2^{CCL19Cre} in adult and 3-weeks old mice. ('-' : decrease ; '+ ': increase ; '≠' :different ; 'wt ' : no difference). N.D.: not determined. -/+ : 10-30% or 1.5-2 times for transcript/MFI analysis; --/++ : 30-50% or 2-5 times for transcript/MFI analysis; ---/+++ : more than 50% or more than 5 times for transcript/MFI analysis.

Discussion

I. Notch signaling in FRC

RNA expression analysis of different Notch signaling factors in naive pLN FRC suggested the presence of an active Notch signaling . The aim of my thesis work was to understand the role of this Notch signaling pathway in FRC during development, homeostasis and immunity, by analyzing mostly pLN.

By using loss-of-function approaches, we characterized the function downstream of Notch1 and Notch2 signaling in FRC (**Table1**). We identified several functions of Notch signaling in pLN FRC. The first group of effects we referred to as “direct functions” as they affect FRC, their 3D organization and their secreted products, namely ECM and chemokines (**Table 4**). Notch signaling in FRC also regulates neighboring cells, such as vascular endothelial cells and lymphocyte populations, with mechanisms not yet identified. We referred to these effects on neighboring cells as “indirect effects” (see **Table 4**).

Direct effects	Indirect effects
↘ FRC number	↘ T cell number
↗ Activation state of FRC / FRC network	≠ follicular B zone shape
↘ MRC / MAdCAM expression	↘ BEC number
↘ ECM production (conduits)	↗ Aberrant LEC positioning within T zones
↘ CCL19 production	

Table 4: Summary of the different functions of Notch signaling in FRC, observed in the different mouse strains studied, classified in two categories: “direct effects” that focus on FRC and their functions; and “indirect effects” which identifies functions of Notch signaling in FRC affecting neighboring cells.

In our study, the phenotypes observed were mainly Notch2 dependent despite a weaker Notch2 expression in FRC relative to Notch1. However, endocytosis as well as enzymatic receptor cleavage have been shown to regulate ligand and receptor availability at the cell surface, especially after the binding of Notch ligand to the Notch receptor (Kopan and Ilagan 2009). Therefore, Notch2 expression in pLN FRC may be be under-estimated when assessing it by surface staining and flow cytometry, due to an ongoing Notch2 signaling leading to its cleavage of the intracellular and extracellular domains. Absence of active Notch1 signaling could render Notch1 more accessible to antibodies and therefore lead to higher staining levels on FRC.

Therefore, future attempts should assess Notch 2 surface expression in settings where this cleavage is blocked using inhibitors, either *in vitro* or *in vivo*. Currently it is also unclear how efficiently Notch2 is deleted given the low detection level by flow cytometry, with MedRC expected to give a lower deletion efficiency than TRC. In order to assess the approximate Notch 2 deletion efficiency in the various cell types when using the CCL19Cre model, we are generating Notch2^{CCL19cre} mice carrying also an allele of a fluorescent cre reporter (ROSA26-EYFP), allowing to identify cells with Cre activity. This mouse model can then also be used to sort EYFP+ TRC and MedRC and compare their transcriptome in order to identify Notch2-dependent transcripts and potential direct Notch2 targets. The strong decrease observed for the ECM within the T-zone as well as for CCL19 point to an important role for Notch2 in TRC, with the precise role for MedRC remaining elusive.

The study of RBPj-deficiency in FRC revealed phenotypes similar to those previously observed with Notch1/2 and Notch2 deficiency, leading us to conclude that Notch2 receptors in FRC signal through the canonical-RBPj signaling. The predominant role for canonical Notch2 versus Notch1 signaling is in contrast which what was previously described in the literature on Notch signaling roles in peripheral tissue fibroblasts, such as in bleomycin-induced pulmonary fibrosis in mice (Hu, Wu et al. 2015), skin fibroblasts in case of systemic sclerosis (Kim, Lee et al. 2014) and in some kidney chronic disease in humans (Murea, Park et al. 2010) where Notch1 appears to be the major Notch signaling pathway. These data also suggest that Notch3 signaling in FRC plays a lesser role, except if it does not signal via a RBPj-dependent pathway.

II. Direct effects

1. Notch signaling: an important player in FRC activation state and cell network organization

Absolute FRC numbers, as assessed by flow cytometry after pLN digestion, were slightly decreased in adult mice with Notch1/2 deletion (**Table1**). Although the 3D network organization looked different by histology, no striking difference was observed in terms of cell density within T zones which was consistent with the fairly normal FRC numbers. Modifications of FRC size, network organization or fitness may affect the efficiency of our digestion and therefore lead to a decrease in FRC number, especially for MRC that were poorly isolated from Notch1/2$^{ccl19cre+}$ mice despite their presence in pLN sections.

Notch signaling has been described to promote cell proliferation as well as apoptosis (Hori, Sen et al. 2013). Therefore, the decrease in FRC numbers observed with Notch1/2 and RBP-Jκ deletions (**Table2**) could also be due to a dampening of FRC proliferation and/or reduced cell survival if the canonical Notch signaling is lacking. Furthermore, this slight decrease observed in adult Notch1/2$^{ccl19cre+}$ mice was not observed in single floxed mice, which may reflect a synergistic action of Notch1 and Notch2. As this FRC decrease was only present in adult mice but not 3 weeks old mice (**Table3**), we propose that this signal is not critical for FRC expansion early in development but that it has a potential homeostatic role. However, this FRC decrease was stronger with RBP-Jκ deletion than Notch1/2, which could suggest a role for another Notch receptor such as Notch3, highly expressed in FRC at RNA level, through a canonical signaling.

An increased expression of the pdpn surface marker combined with increased size and granularity in pLN FRC was also observed in adult Notch1/2$^{ccl19cre+}$ mice (**Table1**). These different parameters have already been described to be upregulated in FRC during activation (Acton, Farrugia et al. 2014) (Yang, Vogt et al. 2014). FRC are mainly defined by their expression of pdpn, and this transmembrane glycoprotein was identified as an important regulator of contractile force of FRC during homeostasis, which maintains LN microarchitecture by regulating actomyosin-dependent contractility. More precisely, extra-cellular and transmembrane domains of pdpn play an important role in this regulation, the former one by interacting with CD44 and galectin-8 that regulate FRC migration and adhesion *in vitro*, and the latter one by being required for pdpn association with lipid rafts which are responsible in many tissues for epithelial-mesenchymal transition and cell migration (Astarita, Cremasco et al. 2015) (Fernandez-Munoz, Yurrita et al. 2011). Study of pdpn-/- FRC showed that they have thin but extended membrane protrusions and covered a smaller area in 3D compared to WT FRC. Consequently, pdpn was proposed to control FRC stretching versus contractility (Astarita, Cremasco et al. 2015). During homeostasis, pdpn maintains FRC highly contracted. But during LN activation, interactions between FRC and DC, which express the pdpn receptor CLEC-2, lead to pdpn inhibition. This blocking inhibits the cell contractility, regulates proliferation to allows expansion of the FRC network and eventually LN enlargement (Astarita, Cremasco et al. 2015). High pdpn epression as observed in naive LN FRC upon Notch1/2 deletion may explain the increase in FRC size due to reduced cellular contraction, if the pdpn is engaged by ligands.

As previously described for activated pLN (Yang, Vogt et al. 2014), the seemingly increased activation state of Notch1/2 deleted FRC could lead to modifications in their 3D network organization.

Notch signaling activation in LEC, have been linked with pdpn down-regulation *in vitro,* through reduced transcription of the target genes Hey1 and Hey2 (Kang, Yoo et al. 2010). In our study, deletion of Notch1/2 and downstream signaling in FRC could explain the upregulation of pdpn expression through dampening of Hey1 and Hey2 transcription.

In summary, deletion of Notch1/2 in FRC affects their pdpn expression, size and network organization. The fact that we observed an increase in pdpn expression and FRC size also upon RBPj or Notch2 deletion suggests a link between these two parameters that depend on canonical Notch2 signaling. I propose that the increased pdpn expression affects FRC contraction which leads to larger FRC size and a modified network organization. In order to determine the molecular mechanism of Notch signaling, expression of molecules known to interact with pdpn and to regulate contractility, such as CD44 and galectin-8, could be verified.

The implication of the Hippo signaling pathway dependent on the YAP/TAZ molecules should also be considered for FRC. Recent studies have reported an aberrant activation of this pathway in case of fibrosis such as in the lung (Liu, Lagares et al. 2015), kidney (Seo, Kim et al. 2016) and skin (Piersma, de Rond et al. 2015). In fibroblasts, the two highly related cofactors YAP and TAZ act as sensors of the rigidity of the ECM, cell polarity, cell density and cytoskeletal organization (Panciera, Azzolin et al. 2017). In response to mechanical stress, YAP/TAZ are activated and are described as a forward loop that accelerates the fibrotic process through stimulation of cell contraction, ECM production and expression of profibrotic factors (Noguchi, Saito et al. 2018). Despite the well-known role of this pathway in fibroblasts outside SLO, only one very recent study described the YAP/TAZ molecules as regulators of FRC maintenance in pLN (Choi, Baet et al. 2019).

Several lines of evidence suggest a possible connection between YAP/TAZ and Notch signaling within cells. One the one hand, a crosstalk between YAP/TAZ and Notch signaling has been observed in different tissues such as epidermis and liver where activation of YAP/TAZ can induce the transcription of Notch receptors and/or ligands (Totaro, Castellan et al. 2018). On the other hand, in vascular smooth muscle NICD and YAP were shown to physically interact in order to promote gene transcription (Totaro, Castellan et al. 2018). Whether these two pathways interact in FRC remains to be investigated. Analysis of the different factors involved in YAP/TAZ and pdpn signaling could be done in Notch1/2^{CCL19cre} mice, in order to gain a better mechanistic insight.

In a second step, the LN phenotype of YAP^{CCL19cre} mice could be investigated and compared with Notch1/2^{CCL19cre} mice. Functionally, both pathways may collaborate in maintaining the 3D network of fibroblasts and their ECM, thereby contributing to LN stability and stiffness.

Compression tests can be performed on LN of Notch1/2^{CCL19cre} mice and YAP^{CCL19cre} mice to assess this property (Astarita, Cremasco et al. 2015).

In conclusion, the mechanism of how Notch signaling in pLN FRC regulates their activation, 3D organization and function still needs to be studied further.

2. Non-canonical Notch signaling regulates MAdCAM expression?

Notch signaling in immune cells is well known to regulate cell differentiation or cell fate decisions (Radtke, Fasnacht et al. 2010) (Lewis, Caton et al. 2011). In several fibroblast studies, Notch signaling has been described to play a role in their differentiation into myofibroblasts, as defined by high α-SMA and ECM expression (Dees, Tomcik et al. 2011) (Hu and Phan 2016). Therefore, FRC subsets were studied after Notch deletion to understand if Notch could play a role in FRC differentiation into subsets.

My study of FRC subsets in Notch1/2^{CCL19cre} mice revealed a normal differentiation into TRC and MedRC that make up more than 90% of FRC suggesting the majority of FRC can develop in absence of Notch1/2 signaling, at least based on cell numbers in pLN isolated from 3 weeks old and adult mice. In contrast, we noted a strong decrease in MRC numbers upon pLN digestion and flow cytometry analysis, most strikingly upon deletion of Notch1/2 with a trend visible also upon Notch2 deletion (**Table2**). Histological analysis with the use of the MRC markers RANK-L and pdpn did not confirm this observation with the MRC layer still being present between the SCS and the B-cell follicle. Identification of MRC by flow cytometry with only one subset-specific marker, which is the adhesion molecule MAdCAM, may hide a simple downregulation of MAdCAM expression due to missing Notch signaling. Due to the fact that MRC are surrounded by a layer of lymphatics which express high levels of MAdCAM, our histological analysis did not allow to establish whether MAdCAM+ MRC are present. This MRC decrease observed by flow cytometry was only seen in adult mice but not in 3 weeks old mice (**Table3**). It is possible that MAdCAM expression on FRC is downregulated in adult mice if Notch signaling is not maintained. MAdCAM has not been identified as a direct Notch target gene in the literature, but induction of its expression was described to be mediated by tumor necrosis factor-α (TNF) and LTα (Takeuchi and Baichwal 1995) (Cuff, Schwartz et al. 1998).

During wound response in the skin, Notch1, expressed by epithelial cells, is upregulated and drives expansion of TNF-α in order to recruit ILC3 (Ki, Hodgkinson et al. 2016).

During murine embryogenesis, LTo cells interact with a subset of ILC3 through LTβR and TNFR signaling, leading to the expression of MAdCAM in Lto cells (Hoorweg, Narang et al. 2015).

It was postulated that MRC represent direct descendants of LTo. Therefore, Notch signaling could lead to upregulation of TNF-α that leads to ILC3 stimulation that could feed back onto MRC to maintain MAdCAM expression. As the decrease of MRC numbers by flow cytometry is not observed upon deletion of RBPj, MAdCAM may be regulated by non-canonical Notch signaling. Therefore, we can also hypothesize that NICD interacts with transcription factors other than RBP-Jκ. NICD has already been reported to influence NFκB signaling, but we still lack a precise understanding (Osipo, Golde et al. 2008). As an example, N1-ICD was described to form a complex with NFκB and thereby to enhance transcriptional activities by NFκB, for example by positively regulating the IFN-γ promoter in peripheral T cells (Shin, Minter et al. 2006). Study of the MAdCAM promoter revealed the presence of two NFκB binding sites, which were essentials for inducing MAdCAM expression (Takeuchi and Baichwal 1995). Therefore, inhibition of Notch signaling may downregulate MAdCAM expression through a non-canonical Notch signaling that could use NFκB proteins or through indirect signaling via ILC3. These different possibilities need to be further investigated, both by histology and flow cytometry. Currently, I cannot exclude the alternative possibility that MRC isolated from pLN of Notch1/2$^{ccl19cre+}$ mice are more fragile and are lost upon enzymatic digestion and/or exclusion of cells staining with dead cell markers.

3. ECM genes: direct Notch-target genes in FRC?

In addition to these effects on FRC size, phenotype and structure, secretory functions such as ECM deposition and/or remodelling are also affected by Notch1/2 deletion in FRC. A strong decrease of several ECM proteins present within the basement membrane (laminin, collagen IV, fibronectin) and microfibrillar zone (ERTR7) of the conduit network was observed with Notch1/2, Notch2 and RBPj deletion suggesting a role for the canonical Notch2 signaling pathway in ECM production/remodelling by pLN FRC (**Table 2**). Several studies have shown that ECM proteins, most prominently collagen I, can be considered as direct Notch target genes in fibroblasts outside of SLO (Hu, Ou-Yang et al. 2014) (Hu, Wu et al. 2015) (Dees, Tomcik et al. 2011). Procopio and colleagues studied RBPj-binding sites by chromatin immunoprecipitation and identified in human dermal fibroblasts several promoters of ECM genes as RBPj-targets, including the ones of collagen1α2, collagen3α1, different laminin chains and fibrillin-1 (Procopio, Laszlo et al. 2015) (**Fig.6**).

Therefore, these data suggest a direct transcriptional regulation of ECM genes by Notch signaling in fibroblasts that may lead to a defect in protein expression if Notch signaling is defective.

We can therefore propose that laminin, fibronectin and collagen IV are likely to be direct target genes in FRC, which need ongoing Notch signaling during development and homeostasis to ensure normal ECM production and proper conduit development. Compared to previous studies on fibroblasts that show direct effect of Notch signaling in collagen I expression (Hu and Phan 2016), no decrease in collagen I protein staining or transcripts was observed in our study suggesting it may not be a Notch1/2 target in pLN FRC.

However, a different organization of these collagen I fibers was also noted. The decrease of the protein of the microfibrillar zone identified by the ERTR-7 antibody may indicate that other microfibrillar proteins could also be affected by Notch1/2 deletion in FRC such as fibrillin-1 whose promoter has a RBP-J binding site (Procopio, Laszlo et al. 2015) (**Fig.6**). Proteins of the microfibrillar zone, such as fibrillin-1, were described as key factors in collagen core stability. In fact, in a fibrillin-1 deletion mouse model (mgR mice), multi-oriented and disorganized collagen fiber bundles were observed in the periodontal ligaments (Ganburged, Suda et al. 2010). Consequently, a decrease of microfibrillar proteins such as those labelled by the ERTR-7 antibody could affect the structure and stability of collagen I fibers in pLN conduits of Notch1/2^{ccl19cre} mice.

An increased degradation of the basement membrane and microfibrillar zone proteins could also be responsible for the altered ECM in Notch1/2^{ccl19cre} mice. Degradation of ECM proteins is a very important process in development, tissue remodelling and repair. This process involves many proteinases with the major group of enzymes belonging to matrix metalloproteinases (MMPs) (Visse and Nagase 2003). Currently 24 MMPs have been identified in vertebrates, and classified in different categories according to their biological effects (Jablonska-Trypuc, Matejczyk et al. 2016). According to our gene array data, FRC express several MMPs at high level, including MMP 2, 3, 9 and. 14 (unpublished observations) (Malhotra, Fletcher et al. 2012). In the study of Procopio et al. several promoters of MMP, including MMP2 and MMP9, have been identified as having RBP-J binding sites (Procopio, Laszlo et al. 2015). These MMPs have been described to degrade substrates such as collagen IV and fibronectin. Therefore, increased degradation of ECM by MMPs due to missing Notch2 signaling in FRC may also explain the findings. In conclusion, by abrogation of Notch2 or RBPj in FRC, ECM target genes of the basement membrane and microfibrillar zone may not be transcribed at normal levels, or later degraded resulting in the altered conduit network phenotype visible already in pLN of 3 weeks old mice (**Table 3**) with the defect persisting into adulthood.

In order to test this hypothesis, transcriptional analysis of ECM and MMPs genes, by qRT-PCR or RNA-sequencing can be performed on FRC from wt versus Notch2^{ccl19cre} mice.

Alternatively, *ex-vivo* FRC from wt versus Notch1/2^{ccl19cre} mice could be put in culture and tested for their production level of ECM proteins, in presence or absence of Tissue Inhibitors of MMPs (TIMPs) or other MMP inhibitors to test the involvement of MMPs.

As previously described in the introduction, the conduit network system allows the fast delivery of low molecular weight substances, such as lymph-born cytokines and antigens, into lymphoid B and T zones. Conduit-associated DC are capable of taking-up and processing soluble antigens from the conduit network systems (Sixt, Kanazawa et al. 2005). In order to assess this conduit functionality in our mice showing reduced ECM levels, subcutaneous injection of fluorescent tracers with different molecular weights are currently being tested in Notch1/2 ^{CCL19Cre} mice. Analysis of conduit-associated DC and their capacity to acquire lymph-borne antigen, such as quenched ova which becomes fluorescent upon endocytosis (Sixt, Kanazawa et al. 2005). A recent study highlights a new function of this conduit network system, the fast delivery of secreted IgM, upon immunization, out of LN. Therefore, in order to assess if the conduit network system is still functional, the IgM response to infection or immunization should be investigated in Notch1/2 ^{CCL19Cre} mice, with IgM detection on LN sections and in serum.

4. CCL19: a non-canonical Notch-target gene?

In the present study, we observed a 50% decrease of *ccl19* transcript levels in stromal cell fractions of Notch1/2$^{CCL19Cre+}$ pLN and spleen. Given the fact that CCL19 is produced mainly by FRC, and that other cytokine transcripts typical for FRC, such as *ccl21* or *il-7*, are not downregulated, along with the not much altered TRC numbers, we can conclude that Notch1/2 signaling is a specific regulator of *ccl19* transcription in FRC. This decrease was always correlated with the CCL19 protein levels measured by flow cytometry using indirect read-outs of CCR7 surface expression and ligand accessibility on T cells demonstrating that T cells in Notch1/2$^{CCL19Cre+}$ pLN see less CCL19 protein in their environment. The decrease of *ccl19* transcripts along with increased CCR7 staining was also observed in Notch2$^{CCL19Cre+}$ pLN. Nevertheless, RBP-Jκ deletion did not lead to altered *ccl19* levels with the flow cytometric analysis of CCR7 staining showing much weaker effects than in the Notch1/2 and Notch2 deletion models (**Table 2**). Therefore, Notch 2 receptor signaling via an RBP-Jκ independent pathway regulates *ccl19* expression, either directly or indirectly.

So far, no study has reported a possible interaction between Notch signaling and CCL19 expression, as expected for a direct regulation.

However, there is evidence for Notch signaling regulating CCR7 expression in mammary cancer stem-like cells (Boyle, Gieniec et al. 2017). Analysis of the human *ccl19* promoter

sequence presented in the study of Pietilä et al. identified two NFκB binding sites in the proximal promoter parts (Pietila, Veckman et al. 2007). We have previously described that one of the non-canonical Notch pathways is characterized by the interaction of NICD with other transcription factors than RBPj, such as NFκB. Currently, no study has reported yet a N2-ICD interaction with members of the NFκB transcription factor family. But the possibility that in LN FRC N2-ICD associates with NFκB transcription factors, as described for N1-ICD, and thereby regulates *ccl19* promoter activity needs to be considered, especially as RBPj binds to several chemokine promoters in human skin fibroblasts (Procopio, Laszlo et al. 2015) (**Fig.31**).

We also have to consider that CCL19 may be indirectly regulated, and dependent on other defects observed upon Notch1/2 deletion in FRC. In the RBP-j deletion model we did not observe much of a difference in *ccl19* expression (**Table 2**), while we observed ECM loss, aberrant LEC localization and altered B cell follicles, similar to Notch1/2$^{CCL19cre+}$ pLN. Based on these findings we believe that the *ccl19* decrease is not linked to these other phenotypes.

Despite being described as a homeostatic chemokine, CCL19 can also be induced in certain inflammatory circumstances (Comerford, Harata-Lee et al. 2013). CCL19 production has been reported to be only partially LTαβ-dependent, in contrast to the lymphoid tissue CCL21 form which was shown to be strongly LTαβ-dependent (Ngo, Korner et al. 1999) (Lo, Chin et al. 2003). Therefore, it remains to be established whether the Notch signaling acts in parallel to the lymphotoxin pathway, or whether it acts upstream of it.

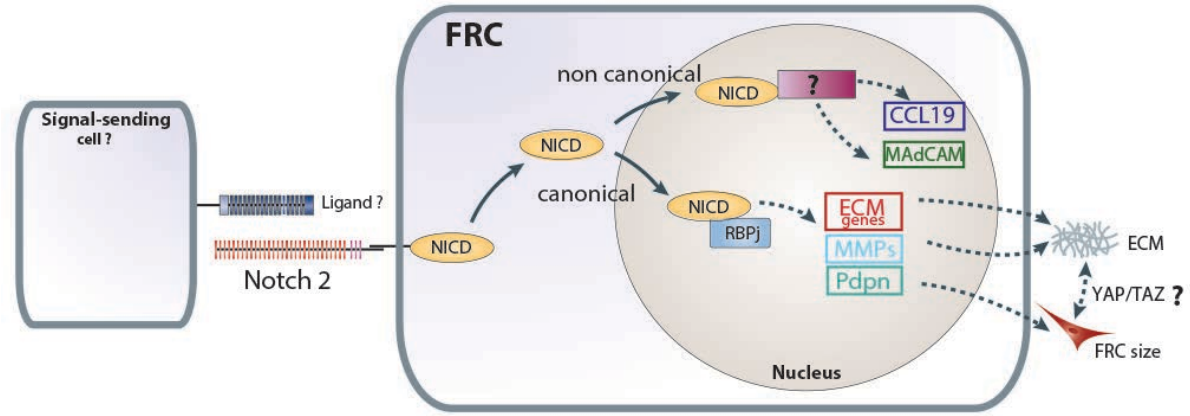

Figure 31: Summary of direct (FRC-intrinsic) Notch signaling effects in pLN FRC. We describe in this thesis that canonical Notch2 signaling in FRC seems to regulate pdpn expression. Pdpn regulation has been described to regulate FRC morphology through contraction and elongation (Astarita, Cremasco et al. 2015) which could lead to modification of FRC 3D network. By deleting Notch2, ECM was affected. Canonical Notch2 signaling may regulate ECM production and/or MMPs, expressed by FRC, responsible of ECM degradation. Modification of ECM network has also been described to regulate YAP/TAZ signaling responsible of cell-contraction. Non-canonical signaling, in an RBPj-independent way, was described to possibly regulate CCL19 and MAdCAM expression in FRC. According to the literature, NFκB could be a potential binding partner of NICD to regulate CCL19 and MAdCAM expression.

In summary, Notch signaling seems to play different roles in FRC (**Fig.31**). A canonical Notch signaling pathway seems to regulate various aspects of FRC biology, including their number, size, pdpn expression and 3D organization (**Fig.31**).
Notch 2 rather than Notch 1 seems to be the important receptor for the phenotypes observed in the Notch1/2-deficient mice. But Notch2 signaling also regulates FRC functions such as CCL19 and ECM production through RBPj-dependent and independent signaling pathways, respectively (**Fig.31)**.

III. Indirect effects

CCL19, mainly produced by T-zone FRC, was proposed to be important for the recruitment of T cells and DC within the T-zone of pLN (Ngo, Korner et al. 1999). Once within the T-zone, T cells and DC crawl along the FRC network wrapped around the ECM-based conduits (Bajenoff, Egen et al. 2006). This network forms a migration “road” for these cells to facilitate their interaction. Therefore, the regulation of ECM and CCL19 production by Notch signaling in FRC is likely to affect neighbouring cells that directly depend on and interact with FRC, including immune and non-immune cells localizing next to FRC. These “indirect” effects were observed for T and B lymphocytes but also for LEC and BEC (**Table 4**).

1. Decreased T cell numbers within pLN: due to low CCL19 levels?

CD4+ and CD8+ T cell populations were similarly decreased by 32% in naive pLN of Notch1/2^{CCL19cre} mice. As pLN of Notch2^{CCL19cre} but not RBPj^{CCL19cre} mice show a comparable reduction in the naive T cell pool we conclude that in pLN FRC Notch2 signaling via a non-canonical pathway regulates the development of T zone niches or peripheral T cell homeostasis.
In Notch1/2^{ccl19cre} mice, no difference in transcripts for the T cell survival factor IL-7 was observed in pLN, similar to the situation in Notch2^{ccl19cre} mice. Only the spleen of Notch1/2^{ccl19cre} mice showed reduced *il-7* levels that could explain the lower splenic T cell numbers (**Table 1**). Altogether, however, we did not observe a strong correlation of the T cell decrease with changes in *il-7* transcripts suggesting the defect is not IL-7 related, although we cannot exclude differences at the level of IL-7 protein availability to naive T cells, as IL-7 can be bound to extracellular matrix (Ortiz Franyuti, Mitsi et al. 2018) which is affected in these Notch1/2$^{CCL19cre+}$ mice.

Based on the study of RBPj mice, that have no T cell number decrease but a 37% decrease of FRC number as well as an increased TRC activation state, we propose that the T-cell phenotype observed in Notch1/2$^{CCL19cre+}$ and Notch2$^{CCL19cre+}$ mice is not tightly linked to FRC numbers or activation state. Similarly, the presence of aberrant lymphatics within the T-zone of RBPj$^{ccl19cre+}$ mice also suggest that these lymphatics are not directly linked to the T-cell decrease.

Naive T cell migration within LN has been shown to be regulated by chemokines, including CCL19 and CCL21, and integrin adhesiveness (Woolf, Grigorova et al. 2007). ECM, surrounded by FRC, form this migrating road for lymphocytes while the chemokines promote the random motility. Therefore, modification of the ECM structure in Notch1/2 and Notch2 deletion may affect naive T cell motility or retention within T zones. Arguing against this hypothesis, the ECM phenotype present in pLN of RBPj$^{CCL19cre+}$ mice was not associated with a T cell decrease.

A T cell decrease could have been explained by a defect in thymic T cell maturation or T cell homing to pLN. However, the thymic T cell development appeared normal and short-term lymphocyte transfers into Notch1/2^{CCL19+} mice did not reveal any obvious pLN homing defect.

But we noted that the T cell population defect was always observed in mice which also had decreased CCL19 expression, such as in mice deficient for Notch1/2 and Notch2, but not in those deficient for Notch1 or RBPj suggesting there may be a causal relationship (**Table 2**). The changes in *ccl19* transcripts were always mirrored in the CCR7 staining on lymphocytes suggesting that indeed T and B lymphocytes encounter less CCL19 protein. However, it has been described that adult CCL19-/- mice have a reduction in total T cells found in spleen and blood but not in pLN (Link, Vogt et al. 2007). CCL19 was described to be critical for proper formation of splenic T-zones after birth thereby regulating the number of T zone niches that develop (Schaeuble, Britschgi et al. 2017). Despite a stronger initial accumulation of transferred WT T cells in pLN of CCL19-/- mice compared to spleen and mesenteric LN, a gradual decrease of these transferred WT T cells was observed in pLN over the three weeks of observation. In addition, CCL19 promoted T cell survival in vitro suggesting a problem of T cell survival in absence of CCL19 *in vivo* (Link, Vogt et al. 2007). Therefore, the Notch2-dependant decrease of CCL19 could induce a reduced T cell survival within pLN (**Fig.32**). The absence of a T cell decrease in 3 weeks old mice despite a slightly reduced *ccl19* transcript level may indicate that T-cell survival issues become only detectable and accentuated after several weeks in a CCL19^{low} environment.

In order to verify this hypothesis, the study of lymphocyte populations should be investigated in heterozygote CCL19 KO mice, which most likely mimics the 50% decrease of *ccl19* transcript levels observed in the Notch1/2 deletion model. Lower CCL19 levels could also affect the random motility of T cells despite the presence of CCL21, with possible alterations in the interaction with DC. As previously described in *plt/plt* mice (lacking both CCL19 and CCL21) (Mori, Nakano et al. 2001) (Link, Vogt et al. 2007) and more recently in CCL21-deficient mice (Kozai, Kubo et al. 2017), the presence of CCL21 is primordial for T cell homing into LN T-zones. The hypothesis of the effect of lower CCL19 levels in random T cell motility could be tested by intravital 2-photon microscopy of marked T cells transferred into mice having differently marked DC, such as CD11c-eyfp, to monitor simultaneously their efficiency in scanning antigen presenting cells (Lindquist, Shakhar et al. 2004).

2. Reduced B cell-follicle demarcation: Role for misplaced lymphatic vessels?

T cells were not the only cell-type affected by absent Notch1/2 signaling in FRC. Despite a good T/B segregation within pLN, the shape of B-cell follicles appeared modified upon deletion of Notch1/2, or of RBPj when adult mice were investigated, with the outline of B-cell follicles appearing less well demarcated (**Table 2**). This modified architecture was already visible in 3 weeks old mice lacking Notch1/2 or Notch2 in FRC (**Table 3**). Therefore, this phenotype is Notch2 dependent, and as observed in adult mice, also linked to the canonical Notch signaling, and already present during LN development before appearance of the T cell phenotype.

Modification of the B-cell follicle organization could be linked with signals triggered by follicular cells themselves or modifications of T-zone factors that affect these follicles indirectly. First, the chemokine CXCL13 mainly produced by FDC has been described to play a crucial role for B-cell follicle organization through the attraction of CXCR5-expressing B cells and promotion of their motility (Gunn, Ngo et al. 1998) (Stachowiak, Wang et al. 2006). Altered B-cell follicle structures have been previously described in mice deficient for CXCL13 or its receptor CXCR5 (Ansel, Ngo et al. 2000). However, no decrease of *cxcl13* transcript levels were observed in our qRT-PCR analysis of the different mouse strains. Preliminary histological evidence suggests that CXCL13 protein is distributed normally within the follicles of Notch1/2-deficient mice.

Given that activated FDC also express CCL19Cre (Fasnacht, Huang et al. 2014), the study of FDC populations in Notch1/2^{CCL19Cre} mice could be interesting to understand if these cells

show Notch1/2 deletion and get modified in absence of Notch1/2 signaling potentially resulting in altered B-cell follicles. Other mechanisms could be implicated in B cell follicle generation or maintenance and need to be investigated in future, such as for example migratory signals delivered by EBI2, expressed on B cells but not crucial for embryonic SLO development (Pereira, Kelly et al. 2009), which was shown to control B-cell organization within the SLO (Gatto, Wood et al. 2011) (Pereira, Kelly et al. 2009).

Alternatively, signals outside of the B-cell follicle may be responsible for the structural modifications observed. It has been suggested that functional afferent lymphatic vessels are required for proper lymph-node organization via regulation of cell adhesion molecules in HEV (Mebius, Streeter et al. 1991) A study of Thomas et al. on K14-VEGFR-3-Ig mice with lymphatic growth defects restricted to the skin, showed that skin draining LN were disorganized as consequence, and B cells were less concentrated in follicles (Thomas, Rutkowski et al. 2012). In parallel, in this study no difference for CCL21 and CXCL13 levels were observed but a different distribution of these chemokines (Thomas, Rutkowski et al. 2012). Therefore, that study shows that lymphatic drainage is implicated in proper B-cell follicle organization and FRC/FDC function, but the mechanism remains to be defined.

Thus, the presence of bona fide lymphatic vessels within the T-cell zone, in pLN of Notch1/2, Notch2 and RBPj deleted mice (**Table 2**) could be involved in the disorganization of B cell follicles.

In summary, many hypotheses could explain how Notch signaling in FRC or FDC could regulate the B-cell follicle structure (**Fig.32**). In order to gain a better understanding of this phenotype, several aspects will need to be analyzed in more depth, including the lymphatics, FDC, CXCL13 and EBI2.

3. Notch signaling regulates pLN vasculature

In our study, an aberrant localization of lyve1+ lymphatic vessel structures was observed within T-zones, rather than being limited to the SCS and medulla, of naive adult pLN, of mice lacking either Notch1/2, Notch2 or RBPj in FRC (**Table 2**). Therefore, this phenotype appears in absence of canonical Notch2 signaling. However, it has been reported that between 5% to 20% of LEC express the CCL19cre transgene (Chai, Onder et al. 2013) (Fasnacht, Huang et al. 2014), so it will be important to investigate whether those LEC developing within the T-zone have ablated Notch signaling. Furthermore, inhibition of Notch signaling in LEC through the study of inducible Prox1-Cre mice crossed with Notch1$^{fl/fl}$ mice, has already been reported to result in excessive numbers of Prox-1+ progenitor cells during embryonic development (Murtomaki, Uh et al. 2013).

In order to exclude the possibility that non-specific inhibition of Notch signaling in some lymphatics, via CCL19cre expression, could upregulate Prox1+ cells in our deletion model, we are currently generating Notch2^{CCL19cre} mice carrying also an allele of a fluorescent cre reporter (ROSA26-EYFP), to understand if these aberrant lymphatic vessels within the T cell zone are preferentially expressing CCL19-driven Cre.

Preliminary data based on 3D histology of adult pLN with Notch1/2 deletion in FRC point to an increased presence of blood vessels within the central T cell zone, rather than being enriched within the outer T zone. The mechanism responsible for this positioning in specific areas is not known but may involve pericytes that are also targeted by the CCL19cre transgene. By flow cytometry I observed decreased BEC numbers in pLN of adult mice lacking either Notch1/2 or Notch2 in FRC. We cannot exclude that the modification of the ECM network which maintains LN architecture could also change the efficiency of the digestion protocol in Cre+ mice, as suggested above for MRC. The use of additional BEC markers, such as PNAd to identify HEV, could allow a better identification of BEC subset populations by flow cytometry in order to better orient future studies.

According to histology data, Notch deletion in FRC seems to regulate vascularization of pLN. FRC surrounding HEVs (presumably including pericytes) have been described to support endothelial cells through VEGF-A production (Chyou, Ekland et al. 2008) (Tan, Yeo et al. 2012 JI). Stromal cells are a much stronger constitutive source of VEGF-A and VEGF-C in naive pLN than immune cells, with FRC showing very high expression (Malhotra, Fletcher et al. 2012). VEGF-A, a very potent chemoattractive signal for endothelial cells and a ligand responsible for activation of VEGFR signaling, has clearly emerged as the VEGF family member responsible of blood vascular angiogenesis, via the binding to VEGFR2 and VEGFR1 on endothelial cells (Simons, Gordon et al. 2016). In contrast, VEGF-C has been described to mediate lymphangiogenesis via VEGFR3.

Notch signaling in endothelial cells themselves has been extensively studied. It mediates a broad spectrum of functions in the regulation of vascularization through modulation of VEGFR expression (Thomas, Baker et al. 2013) (Hellstrom, Phng et al. 2007). On the contrary, only few studies have indicated a regulation of VEGF ligand expression by the Notch signaling pathway. Procopio et al. identified by ChIP analysis of human dermal fibroblasts, that RBPj binds to the promoters of VEGF-B and -C (Procopio, Laszlo et al. 2015). Another study which examined VEGF-C expression levels after Notch activation in embryonic endothelium, showed that VEGF-C expression was not affected by Notch signaling (Gore, Swift et al. 2011). Therefore, deregulation of VEGF-A and VEGF-C expression in FRC by missing Notch signaling may be the cause of the vascular

modifications observed for both lymphatic and blood vessels. qRT-PCR analysis or RNA sequencing on *ex-vivo* FRC of Notch1/2^{CCL19Cre} mice or on FRC with Notch stimulation *in vitro* could be performed to address whether VEGF is regulated by this pathway, and identify other target genes relevant for vessel development.

RBPj binding sites were also identified on the promoter of semaphorin3E in human dermal fibroblasts (Procopio, Laszlo et al. 2015). Class III semaphorins typically play a role in neuronal axon guidance but also in regulation of angiogenesis (Sakurai, Doci et al. 2012). A very recent study highlights that members of the semaphorin-plexin family are expressed in FRC, with RNA expression of these semaphorin molecules being downregulated upon CLEC-2-Fc binding to podoplanin on FRC *in vitro* (Martinez, Pankova et al. 2019). Therefore, the negative regulation of pdpn expression by canonical Notch signaling *in vitro*, as previously described for LEC (Kang, Yoo et al. 2010), could also affect class III semaphorin expression and regulate angiogenesis within pLN. The factor downstream of canonical Notch2 signaling in FRC that may regulate angiogenesis or vessel positioning is an interesting lead for future research (**Fig.32**). The expression of VEGF-A and VEGF-C, as well as class III semaphorins by FRC indicate that FRC probably play a role in vascular development or homeostasis within pLN through direct communication with endothelial cells. Therefore, expression level of these different molecules could be assessed in future by qRT-PCR analysis or with a broad-spectrum approach, such as gene array or RNA sequencing analysis on pLN FRC purified from Notch1/2^{CCL19Cre} versus wt mice.

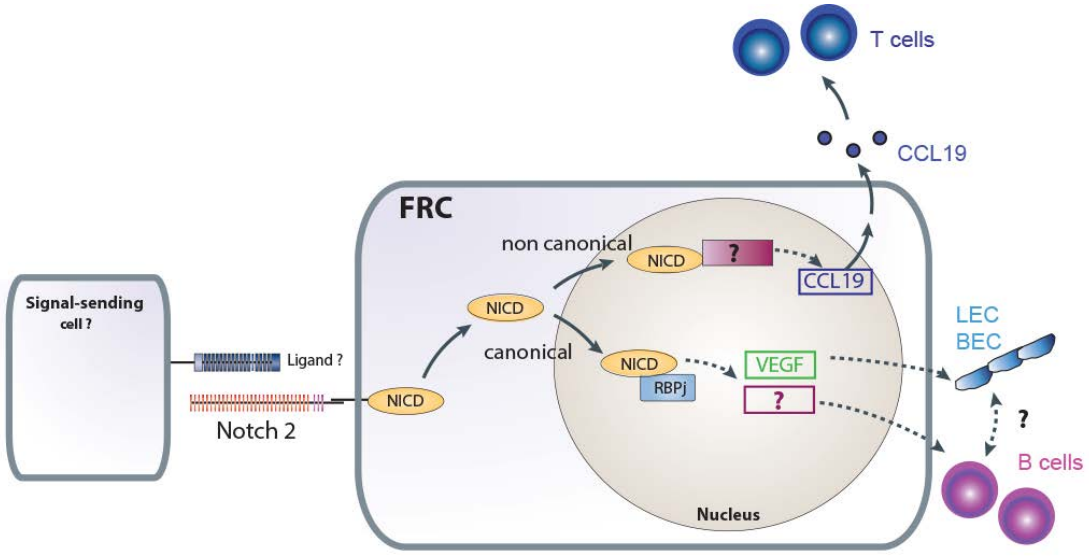

Figure 32: Summary of the « indirect » (FRC-extrinsic) effects of Notch signaling in FRC. Several direct effects of Notch signaling in FRC, previously described, may regulate neighbouring immune and stromal cells. Regulation of CCL19 expression on FRC by Notch2 signaling could then regulate T-cell survival or retention within pLN. Modifications of B-cell follicle structure as well as vascularisation of pLN were identified to be regulated by canonical Notch2 signaling. The expression of VEGF in FRC may be regulated by Notch signaling and potentially affecting pLN vascularisation. Altered vessel development in pLN may also lead to changes in the B-cell follicle structure

In summary, loss-of-function approaches revealed that despite relatively weak surface Notch2 expression in FRC, this pathway is responsible for triggering changes in neighboring cells such as observed for T-cell accumulation or survival, B-cell follicle organization and lymphatic vessel localization (**Fig.32**).

Notch signaling in FRC appears to induce CCL19 which controls T-cell population size presumably by promoting T cell survival. Notch signaling in FRC may also trigger VEGF and/or semaphorin expression which then may regulate the growth and placement of neighboring endothelial cells. The possibility that CCL19cre directly affects Notch signaling in FDC thereby changing B cell follicle shape needs to be further investigated along with a possible role of T zone lymphatic vessels in this process.

IV. General conclusions and perspectives

In this study, we have highlighted the multiple functions of Notch signaling in FRC from the regulation of FRC themselves through their size, phenotype and 3D organization, to their function as source of ECM and cytokines such as CCL19. FRC have been described to regulate LN homeostasis through interactions with immune and stromal cells. Notch signaling in FRC appears to be another way for FRC to regulate neighbouring immune and stromal cells. Several aspects and questions need to be investigated to gain a better mechanistic understanding: When are these signals given? By which ligand-expressing cell? What are the direct consequences upon Notch signaling? What are the delayed or more long-term effects?

Several hypotheses are discussed below for one of these burning questions: Which cell and ligand triggers the activation of Notch signaling in FRC? Analysis of mice deficient in DLL1/4 ligands in FRC have highlighted the critical importance of FRC as Notch ligand source in development of Tfh cells, ESAM+ DC and marginal zone B cells (Fasnacht, Huang et al. 2014). The same mice were used to demonstrate that graft versus host disease is also dependent on FRC providing these ligands to trigger pathogenic T cell responses (Chung, Ebens et al. 2017). As I show now in my thesis that FRC express also the two receptors Notch1 and Notch2, this raises the possibility of cis or trans signaling between FRC forming cell contacts. Usually the presence of ligand and receptor on the same cell, referred as cis-interaction, inhibits Notch signaling via downregulation of the Notch receptor (Andersson, Sandberg et al. 2011). Therefore, it is possible that FRC could signal in trans to neighbouring FRC.

Preliminary histological analysis, performed on pLN with specific deletion of DLL1 and DLL4 in FRC (DLL1/4^{CCL19Cre}), did not reproduce phenotypes observed upon Notch1/2 deletion in FRC such as ECM downregulation, modified B-cell follicle structure and lymphatics present in T zones (data not shown). Therefore, DLL1/DLL4 expression by FRC does not seem to be the critical ligand source or the critical ligands.

Gene array data on murine LN FRC published by the Immunological Genome Project identified Jagged-1 as another ligand expressed by FRC (Malhotra, Fletcher et al. 2012). Jagged-1 has been described to physically interact with Notch2, as well as with Notch1 and Notch3 (Shimizu, Chiba et al. 1999). Jagged1-Notch2 interactions have been reported in different contexts such as erythropoiesis and kidney fibrosis (Zeuner, Francescangeli et al. 2011) (Huang, Park et al. 2018). Therefore Jagged-1 expressing FRC could potentially trigger Notch2 signaling in FRC in a paracrine fashion. In order to identify which ligands can potentially activate Notch2 signaling in FRC, *in vitro* tests are currently being performed on FRC cell line with or without ligand stimulation.

What other cells could then provide Notch ligands? Preliminary histological analysis on pLN from TCR$\beta\delta^{-/-}$ mice showed no difference in term of ECM production and lymphatic vessel presence in paracortical regions (data not-shown). Therefore T cells are probably not providing ligands to FRC leading to these two downstream effects. Other stromal cells could possibly trigger Notch signaling in FRC by providing ligands, such as LEC and BEC, that share the FRC environment, and express high levels of DLL1, DLL4 and Jagged-1 (Malhotra, Fletcher et al. 2012) (Fasnacht, Huang et al. 2014). However, only a minority of FRC have direct cell-cell contact with endothelial cells. Future studies should also investigate roles of other immune cells, such as ILC3 and myeloid cells which have a high RNA expression level of DLL1 and Jagged-1 respectively (Malhotra, Fletcher et al. 2012).

FRC are an important ligand source for Notch-driven immune cell development (Fasnacht, Huang et al. 2014). Our study now shows that Notch signaling seems to play an important role in regulation of FRC themselves and their functions in SLO during development and homeostasis, with some observations being reminiscent of Notch signaling in fibroblasts of inflammatory sites. In future, additional approaches need to be taken to understand how the different phenotypes observed are linked and formed. But the importance of this signaling pathway during homeostasis could suggest that this pathway is also important during LN swelling and immune response. While preliminary evidence did not reveal a striking defect in the T cell response to vaccination in pLN lacking Notch signaling in FRC, infections with pathogens need to be investigated, and the humoral arm of adaptive immunity needs to be carefully studied.

Contributions by others

Seyran Mutlu perfomed histological and some of the flow cytometry analysis on three weeks old mice on spleen and pLN of the different mouse strains. She also set up the quantification method for ECM and Lyve1+ proteins on histological sections of pLN. She also performed RNA extraction and qRT-PCR analysis on pLN of three weeks old mice.

Stéphanie Favre perfomed dissection, stainings and confocal analysis on pLN of Notch1/2 deletion mouse model. She also performed all the genotyping experiments of the different mouse strains used in this thesis work.

Leonardo Scarpellino performed RNA extraction and qRT-PCR analysis on pLN for some mouse strains used in this thesis work.

Contributions to other projects

I. A new FRC subset involved in plasma cell homeostasis

Identification of a new subset of lymph node stromal cells involved in regulating plasma cell homeostasis

HY. Huang, A. Rivas-Caicedo, F. Renevey, H. Cannelle, E. Peranzoni, L. Scarpellino, DL. Hardie, A. Pommier, K. Schaeuble, S. Favre, TK. Vogt, F. Arenzana-Seisdedos, P. Schneider, CD. Buckley, E. Donnadieu and SA. Luther

Published in *Proc Natl Acad Sci USA* Jul 17;115(29):E6826-E6835. doi: 10.1073/pnas.1712628115.

Abstract:

Antibody-secreting plasma cells (PC) arise rapidly during adaptive immunity to control infections. The early PC are retained within the reactive lymphoid organ where their localization and homeostasis relies on extrinsic factors, presumably produced by local niche cells. While myeloid cells have been proposed to form those niches, the contribution by co-localizing stromal cells has remained unclear. Here, we characterized a subset of fibroblastic reticular cells (FRC) that forms a dense meshwork throughout medullary cords of lymph nodes (LN) where PC reside. This medullary FRC type is shown to be anatomically, phenotypically and functionally distinct from T zone FRC, both in mice and humans. By using static and dynamic imaging approaches, we provide evidence that medullary FRC are the main cell type in contact with PC guiding them in their migration. Medullary FRC also represent a major local source of the PC survival factors IL-6, BAFF and CXCL12, besides producing also APRIL. *In vitro*, medullary FRC alone or in combination with macrophages promote PC survival while other LN cell types do not have this property. Thus, we propose that this new FRC subset, together with medullary macrophages, forms PC survival niches within the LN medulla, and thereby helps promoting the rapid development of humoral immunity which is critical in limiting early pathogen spread.

I contributed to this project driven by a previous post-doc in the lab, Hsin-Ying Huang, to do the experiments needed for the revision of the manuscript. I performed flow cytometry experiments, with digested lymph nodes from immunized mice of different mouse strains.

II. FRC attenuate chronic antiviral T cell responses

Attenuation of chronic antiviral T cell responses through constitutive COX-2 dependent prostanoid synthesis by lymph node fibroblasts

K. Schaeuble, H. Cannelle, S. Favre, H.Y. Huang, S.G. Oberle, D. Zehn and SA. Luther

Accepted in *Plos Biology - In press (June 2019)*

Abstract:

Fibroblastic reticular cells (FRC) of lymphoid T zones actively promote T cell trafficking, homeostasis and expansion, but can also attenuate excessive T cell responses via inducible nitric oxide and constitutive prostanoid release. It has remained unclear under which conditions these FRC-derived mediators can dampen T cell responses and whether this occurs *in vivo*. Here we confirm that murine lymph node FRC produce prostaglandin E_2 (PGE_2) in a cyclooxygenase-2 (COX2)-dependent and inflammation-independent fashion. We show that this COX2/PGE_2 pathway is active during both strong and weak T cell responses, in contrast to nitric oxide which only comes into play during strong T cell responses. In chronic infections *in vivo,* PGE_2-receptor signaling in virus-specific CD8 T cells was shown by others to suppress T cell survival and function. Using CCL19cre x $COX2^{flox/flox}$ mice we now identify $CCL19cre^{+}$ FRC as the critical source of this COX2-dependent suppressive factor, suggesting PGE_2-expressing FRC within lymphoid tissues are an interesting therapeutic target to improve T cell mediated pathogen control during chronic infection.

I contributed to this project driven by a previous post-doc in the lab, Karin Schaeuble, to do the experiments needed for the initial submission and revision of the manuscript. I performed several flow cytometry experiments for her: 1) on CCL19Cre x $Cox2^{flox/flox}$ mice for different time-points after activation to characterize the role of Cox2 in LN FRC; 2) on CCL19Cre x $Cox2^{flox/flox}$ mice crossed with ROSA26-EYFP mice in order to investigate the Cre activity in naïve and infected mice; 3) to compare the memory response to immunization by WT versus iNOS KO mice.

III. FRC also promote T-cell responses through IL-33 release

IL-33 produced by fibroblastic reticular cells boosts antiviral CD8$^+$ T cell responses in reactive lymph nodes

P. Aparicio-Domingo, H. Cannelle, MB. Buechler, S. Nguyen, SM. Kallert, S. Favre, N. Papazian, B. Ludewig, T. Cupedo, DD. Pinschewer, SJ. Turley, SA. Luther

Submitted for publication to the *Proc Natl Acad Sci USA*

Abstract:

Upon viral infection, stressed or damaged cells can release alarmins like interleukin-33 (IL-33) that act as endogenous danger signals alerting innate and adaptive immune cells. IL-33 coming from a non-hematopoietic source has been identified as an important factor driving expansion of anti-viral CD8$^+$ T cells. However, the nature of IL-33-producing cells and the signals leading to its release are still poorly understood. Whether nuclear IL-33 has a role in regulating gene expression within these stromal cells has also remained unclear. Tracking IL-33 production in a murine reporter model, we identify fibroblastic reticular cells (FRCs) and lymphatic endothelial cells (LECs) as the main IL-33 sources in lymph nodes (LN) of naïve and virus-infected mice. During infection with lymphocytic choriomeningitis virus (LCMV) clone 13, stromal cells release IL-33 into the extracellular compartment due to active secretion or necrosis, thereby augmenting the anti-viral T cell response. Using mice lacking IL-33 selectively in FRCs versus LECs we identified T zone FRCs as the key IL-33 source driving anti-viral CD8$^+$ T cell responses. Despite its nuclear localization, FRC-derived IL-33 was dispensable as a transcriptional regulator of FRC gene expression and homeostasis, but functioned solely as a secreted cytokine. Collectively, these findings show that LN FRCs not only regulate the homeostasis and priming of T cells but also their expansion several days into the anti-viral immune response.

I was involved during one year in the first steps of this collaborative Sinergia project by characterizing and using a conditional IL-33 allele plasmid generated by an international public consortium (mousephenotype.org). The resulting floxed mice were planned to be crossed to either CCL19 Cre (FRC specific), Prox-1CreERT2 (LEC specific) or PDGFb-CreERT2 (BEC specific) recombinase transgenic mouse lines.

My main task was to check the plasmid construction by enzymatic digests and sequencing, to prepare the plasmid for embryonic stem cell targeting and to identify embryonic stem cells clones with correctly targeted IL-33 alleles using PCR and southern blotting.

Once we heard about two existing floxed IL33 mouse lines present in the US, and one lab willing to share them with us, we stopped the generation of our own IL-33$^{fl/fl}$ mice. At this point in time I had obtained interesting results with my Notch1/2-conditional mutant mice and therefore left the IL-33 project to Patricia Aparicio-Domingo

Material and Methods

Mice. C57BL/6 mice were obtained from Harlan Olac (Netherlands) and OT-I and OT-II mice from the Jackson Laboratory (bred to CD45.1+ B6 mice). Other mice used in this thesis include Notch1^{CCL19Cre}, Notch2^{CCL19Cre}, Notch1/2^{CCL19Cre}, and RBPj^{CCL19Cre} mice. They were generated by intercrossing CCL19Cre (Chai, Onder et al. 2013) with Notch1 flox/flox (Radtke, Wilson et al. 1999), Notch2 flox/flox (Besseyrias, Fiorini et al. 2007) and/or RBPj flox/flox (Han, Tanigaki et al. 2002) mice. Cre- littermate mice were used as controls. Mice were used between 8 and 16 weeks of age for adult experiments, and between 2 and 3 weeks of age for postnatal experiments. All mouse experiments were authorized by the Swiss Federal Veterinary Office.

Adoptive cell transfer and immunization. For adoptive T cell transfers 1 x 10^4 OTI and 1 x 10^4 OTII lymphocytes isolated from spleen and pLN of OT-I and OT-II mice (both CD45.1+), after red blood cell lysis, were transferred i.v. into recipient Notch1/2^{CCL19Cre} mice (CD45.2+). The next day (D0), mice were immunized by subcutaneous injections into 6 sites in the flank with each site receiving 50 µg Ovalbumin (OVA; sigma) diluted in Montanide ISA 25 (25% in PBS; Seppic, France). Final injection volume per site is 50 µL, injected with insulin syringe (Micro-fine; BD). Mice were sacrificed at day 4.5 (D4.5) and/or day 8.5 (D8.5) after immunization.

Stromal cell and DC isolation of lymph-nodes. To isolate lymph node stromal cells and DC, pLN (axillary, brachial and inguinal) were collected. Then they were enzymatically digested for 30 min at 37°C under continuous stirring in complete DMEM medium (Gibco) containing 2% FCS, 3mg/mL of Collagenase IV (Worthington), 2mM of CaCl2 and 40µg/mL of DNAseI (Roche). Every 15 minutes, the cell suspension was gently pipetted to break up remaining aggregates, and then spinned down for 7 min at 1200 rpm (4°C) and resuspended in complete DMEM medium (DMEM containing 2% FCS) or FACS buffer (PBS, 2% FCS, 0,02% NaN_3 and 2mM EDTA). Viable cells were counted by Trypan blue staining before antibody labelling.

Cell isolation of splenocytes and thymocytes. To isolate lymphocytes and thymocytes from spleen and thymus, respectively, both organs were collected. Then they were meshed through a 40-µm filter using a plunger and complete DMEM medium (Gibco) containing 2% FCS.

Gene arrays. Female C57BL/6 mice of 9-10 weeks of age, either naïve on day 8.5 after immunization with OVA/Montanide were sacrificed and draining pLN isolated. Each fibroblast sample (n=3) was derived by pooling cells from pLN of three (immunized) to four (naïve) mice. After pLN digestion and staining, three FRC subsets were sorted among CD45- CD35- CD31- PDGFRa+ gp38+ cells: MedRC (MadCAM- BP3-), TRC (MadCAM-, BP3+) and MRC (MadCAM+, BP3+). MRC were sorted only for immunized samples due to low cell numbers in naive pLN. For each sample, 15,000-55,000 cells were sorted directly into lysis buffer (RNeasy micro kit, Qiagen). RNA isolation and hybridization to Affymetrix gene ST 1.0 arrays were done at the Genomic Technologies facility (UNIL).

Lymphocytes migration assay in vivo using short-term cell transfers. In order to assess the capacity of lymphocytes to home into LN and spleen of N1/N2^{CCL19Cre} mice, WT splenocytes were isolated in complete DMEM medium (Gibco) containing 2% FCS. Cells were resuspended at 50 million cells /ml in PBS. Cells were then incubated 10 minutes at 37°C with 5µM of the dye eFluor 670 (eBioscience). After 10 min, FCS was added to stop the reaction and cells were spun down and resuspended in PBS. Cells were injected into mice by retro-orbital intravenous injection (100µL of cells/ mouse). Mice were sacrificed 2 days or 5 hours after cell transfer.

Flow Cytometry. Cells were blocked with anti-CD16/32 antibody for 20 min on ice, and then stained with antibodies listed in Table 2 for 30 min at 4°C in FACS buffer. Biotin-conjugated primary antibodies were detected with streptavidin coupled to fluorochromes. Dead cells were excluded with 7AAD (Invitrogen) or Zombie Aqua kit (BioLegend). If needed cells were fixed and permeabilized with BD Cytofix/Cytoperm kit (BD Bioscience) for intracellular staining. Samples were acquired on a LSR-Fortessa Flow Cytometer (BD Bioscience) and analysed with FlowJo software. Notch1, Notch2 and Notch 3 antibodies are PE-conjugated. In order to obtain a better signal, an amplification of the PE signal was used (according to the instructions of the manufacturer FASER kit – PE – Miltenyi Biotec). CCL19-Fc staining was performed as described previously (Britschgi, Link et al. 2008). Flow cytometry antibodies used are listed in **Table 5.**

Immunofluorescence staining and imaging of thin tissue sections. 8µm-cryostat sections of tissue-Tek OCT (Sakura Finetek)-embedded pLN and spleen were collected on Superforst/Plus glass slides (Fischer Scientific). Then slides were air dried few hours, fixed for 10 min using ice-cold 100% acetone and then rehydrated in PBS. Slides were quenched using 0,15% H_2O_2, blocked with 0,1% BSA and 1% animal serum in PBS. Primary antibody staining was performed overnight at 4°C using antibodies listed in **Table 6**. If needed, a further staining step was performed using secondary antibodies coupled to fluorochromes for 1h at RT. For the intracellular staining of the transcription factor Prox1, 0.1% of triton-X-100 (AppliChem) was used for the antibody mix. Images were acquired on Leica microscope and treated with Photoshop (Adobe) or Fiji software (ImageJ).

Quantification of 2D histological images of thin tissue sections. Histological quantifications were performed using Fiji Software.

In order to measure the mean fluorescent intensity (MFI) for ECM conduit networks within the LN T cell-zone, 20X images with a zvi format (16-bits) were opened in Fiji. Three small regions (150 x 150 pixels) per picture were chosen focussing on the T zone conduit network while excluding vessels to allow the quantification of ECM within conduits. For each region and staining (laminin, ERTR7 and Collagen I), the MFI was measured and compared between Cre- and Cre+ mice using Fiji and Graph Pad prism software.

In order to measure the % area of the T-cell zone covered by lyve1+ pixels, stitched images of whole LN with a zvi format (16 bits) were opened in Fiji. Both channel images (Lyve1 and CD3 stainings) were converted into binary images. First to delimit the T-cell zone, a threshold was manually applied on CD3 stainings to obtain the area covered by T cells. Then this region was applied to the lyve1 staining. A threshold was also set for positive lyve-1 staining before calculating the % area covered by lyve1+ pixels.

Immunofluorescence staining and confocal imaging of thick tissue sections. LN were collected and fixed for 24h in 1% PFA before being embedded in 4% low melting agarose. 50µm and 100µm-vibratome sections of agarose-embedded LN were collected in a 48 well-plate with PBS - 0.1M Glycine to block free PFA. Sections were blocked with 0.2% Triton-X-100, 0.5% BSA and 1% animal serum in PBS overnight at 4°C on a shaker. Primary antibody staining was performed during two days at 4°C with antibodies listed in Table 3. After an overnight wash step, secondary stainings were performed overnight at 4°C.

After DAPI staining, a clearing step was performed with Rapiclear 1.47 (Sunjin Lab) and sections were mounted on glass slides with spacers (Sunjin Lab). Images were acquired on Zeiss LMS80 confocal and treated with Imaris (BitPlan) software.

Quantitative Realtime PCR. To investigate the transcriptional profile of the stromal cell enriched tissue fraction of lymphoid tissues from adult mice, spleen or pLN were meshed through a 40µm filter. The non-soluble fraction (stroma cell enriched fraction) remaining in the filter was harvested in TRIzol (Ambion, Life technologies). For 2-3 weeks old mice, whole LN were directly harvested in TRIzol, homogenized by bead beating followed by RNA extraction. Reverse transcription was performed using the SuperScript II (ThermoFischer) enzyme. The cDNA was purified with the Nucleospin extract II kit (Macherey-Nagel) according to the instructions by the manufacturer. PCR were performed on a LightCycler 1.5 (Roche diagnostics). Efficiency-corrected RNA expression was normalized to the expression of the two housekeeping genes *hprt* and *tbp*. Sequences of primers used are shown in **Table7**.

Statistical Analysis. Statistical significance was assessed using Prism software (GraphPad). Unpaired two-tailed Student's t-test was used to compare two data groups. P values are indicated as * for $p < 0.05$, ** for $p< 0.01$, *** for $p<0.001$, **** for $p<0.0001$.

Table 5: Antibody list for flow cytometry analysis

Target	Species	Clone	Conjugate	Vendor
CCL19-Fc	Human		None	homemade
CCR7	Rat	4B12	None	
CCL21	Rabbit	Exodus-2	None	Peprotech
CD4	Rat	GK1.5	PE	Biolegend
CD8a	Rat	53-6.7	PE-Cy7	Biolegend
CD11b	Rat	M1/70	Alexa 700	ebioscience
CD11c	Arm. Hamster	N418	PE-Cy5.5	ebioscience
CD19	Rat	ID3	BV605	BD
CD31	Rat	390	Pacific Blue	Biolegend
CD35	Rat	7E9	PE-Cy7	Biolegend
CD44	Rat	IM7	FITC	Home-made

CD45.1	Mouse	A20.1	FITC	Biolegend
CD62L	Rat	MEL-14	Al700	eBioscience
CD45pan	Rat	30F11	APC-Cy7	Biolegend
CD157	Mouse	BP-3.4	Al647	Home-made
CD157	Mouse	BP-3	PE	BD Pharmingen
F4/80	Rat	F4/80	FITC	Home-made
Gr-1	Rat	RB6-8c5	APCe780	eBioscience
HFN-14Fc	Human		None	Schneider Lab (DB-UNIL)
IgG (Rabbit)	Donkey		Al647	Molecular Probes
IgG (Rat)	Donkey		PE	Jackson Immunoresearch
IgG (Human)	Goat		biotin	Jackson Immunoresearch
IgG2a	Rat		None	BioXCell
Podoplanin	Syr. Hamster	8.1.1	PE	Biolegend
Podoplanin	Syr. Hamster	8.1.1	Al647	Home-made
MAdCAM	Rat	MECA-367	biotin	ebioscience
MHCII	Rat	M5/114.1.5.2	Al647	Biolegend
Notch1	Rat	22E5	PE	ebioscience
Notch2	Rat	16F11	PE	ebioscience
Notch3	Arm. Hamster	HMN3-133	PE	Biolegend
Streptavidin			Alexa 488	Molecular Probes
Streptavidin			PE	ebioscience
TCRb	Arm. Hamster	H57-597	APCe780	ebioscience

Table6 : Antibody list for histology

Target	Species	Clone	Conjugate	Vendor
CD3	Arm. Hamster	145-2c11	None	ebioscience
CD31	Rat	GC-51	None	Home-made
CD34	Rat	RAM34	None	ebioscience
CD45R/B220	Rat	RA3-6B2	None	Home-made
CD169	Rat	3D6.112	None	Bio Rad
Collagen I	Goat	Polyclonal	None	Southern Biotech
Collagen IV	Goat	Polyclonal	None	Southern Biotech
Desmin	Rabbit	Polyclonal	None	Invitrogen
ERTR7	Rat	ERTR7	None	BioXCell
Fibronectin	Rabbit	Polyclonal	None	Sigma
IgG (Arm. Hamster)	Goat		biotin	Jackson Immunoresearch
IgG (goat)	Donkey		Cy3	Jackson Immunoresearch
IgG (rabbit)	Donkey		Al488	Molecular Probes
IgG (rabbit)	Donkey		Al647	Molecular Probes
IgG (rat)	Donkey		biotin	Jackson Immunoresearch
IgG (rat)	Donkey		Cy3	Jackson Immunoresearch
IgG (Syr. Hamster)	Goat		Cy3	Jackson Immunoresearch
Laminin	Rabbit	Polyclonal	None	Sigma
Lyve1	Rabbit	Polyclonal	None	RELIA Tech
MAdCAM	Rat	MECA-367	None	BioXCell
Podoplanin	Syr. Hamster	8.1.1	None	Home-made
Prox1	Rabbit		None	ReliaTech
Streptavidin			Al488	Molecular Probes
Streptavidin			Cy3	Jackson Immunoresearch
RANK-L	Rabbit	Polyclonal	None	Peprotech

Table 7: Primers used for quantitative Realtime-PCR

Target gene	Forward	Reverse
ccl19	CTGCCTCAGATTATCTGCCAT	GTCTTCCGCATCATTAGCAC
ccl21	TGAGCCTCCTTAGCCTGGTC	GTACTTAAGGCAGCAGTCCTGA
collagen 1a1	GCTCCTCTTAGGGGCCACT	CCACGTCTCACCATTGGGG
collagen 1a2	GTAACTTCGTGCCTAGCAACA	CCTTTGTCAGAATACTGAGCAGC
cxcl13	GACGCTCAGCACAGCAAC	TTGAAATCACTCCAGAACACCTAC
hprt	GTTGGATATGCCCTTGAC	AGGACTAGAACACCTGCT
il-7	GTGCCACATTAAAGACAAAGAAG	GTGCCACATTAAAGACAAAGAAG
il-6	ATGGATGCTACCAAACTGGAT	TGAAGGACTCTGGCTTTGTCT
il-33	TCCAACTCCAAGATTTCCCCG	CATGCAGTAGACATGGCAGAA
tbp	CCTTCACCAATGACTCCTATGACC	AGTTTACAGCCAAGATTCACGG

References

Acton, S. E., A. J. Farrugia, J. L. Astarita, D. Mourao-Sa, R. P. Jenkins, E. Nye, S. Hooper, J. van Blijswijk, N. C. Rogers, K. J. Snelgrove, I. Rosewell, L. F. Moita, G. Stamp, S. J. Turley, E. Sahai and C. Reis e Sousa (2014). "Dendritic cells control fibroblastic reticular network tension and lymph node expansion." Nature **514**(7523): 498-502.

Ager, A. and M. J. May (2015). "Understanding high endothelial venules: Lessons for cancer immunology." Oncoimmunology **4**(6): e1008791.

Aguzzi, A., J. Kranich and N. J. Krautler (2014). "Follicular dendritic cells: origin, phenotype, and function in health and disease." Trends Immunol **35**(3): 105-113.

Andersen, P., H. Uosaki, L. T. Shenje and C. Kwon (2012). "Non-canonical Notch signaling: emerging role and mechanism." Trends Cell Biol **22**(5): 257-265.

Andersson, E. R. and U. Lendahl (2014). "Therapeutic modulation of Notch signalling--are we there yet?" Nat Rev Drug Discov **13**(5): 357-378.

Andersson, E. R., R. Sandberg and U. Lendahl (2011). "Notch signaling: simplicity in design, versatility in function." Development **138**(17): 3593-3612.

Angeli, V., F. Ginhoux, J. Llodra, L. Quemeneur, P. S. Frenette, M. Skobe, R. Jessberger, M. Merad and G. J. Randolph (2006). "B cell-driven lymphangiogenesis in inflamed lymph nodes enhances dendritic cell mobilization." Immunity **24**(2): 203-215.

Ansel, K. M., V. N. Ngo, P. L. Hyman, S. A. Luther, R. Forster, J. D. Sedgwick, J. L. Browning, M. Lipp and J. G. Cyster (2000). "A chemokine-driven positive feedback loop organizes lymphoid follicles." Nature **406**(6793): 309-314.

Aoyagi-Ikeda, K., T. Maeno, H. Matsui, M. Ueno, K. Hara, Y. Aoki, F. Aoki, T. Shimizu, H. Doi, K. Kawai-Kowase, T. Iso, T. Suga, M. Arai and M. Kurabayashi (2011). "Notch induces myofibroblast differentiation of alveolar epithelial cells via transforming growth factor-{beta}-Smad3 pathway." Am J Respir Cell Mol Biol **45**(1): 136-144.

Asperti-Boursin, F., E. Real, G. Bismuth, A. Trautmann and E. Donnadieu (2007). "CCR7 ligands control basal T cell motility within lymph node slices in a phosphoinositide 3-kinase-independent manner." J Exp Med **204**(5): 1167-1179.

Astarita, J. L., V. Cremasco, J. Fu, M. C. Darnell, J. R. Peck, J. M. Nieves-Bonilla, K. Song, Y. Kondo, M. C. Woodruff, A. Gogineni, L. Onder, B. Ludewig, R. M. Weimer, M. C. Carroll, D. J. Mooney, L. Xia and S. J. Turley (2015). "The CLEC-2-podoplanin axis controls the contractility of fibroblastic reticular cells and lymph node microarchitecture." Nat Immunol **16**(1): 75-84.

Auderset, F., S. Schuster, N. Fasnacht, M. Coutaz, M. Charmoy, U. Koch, S. Favre, A. Wilson, F. Trottein, J. Alexander, S. A. Luther, H. R. MacDonald, F. Radtke and F. Tacchini-Cottier (2013). "Notch signaling regulates follicular helper T cell differentiation." J Immunol **191**(5): 2344-2350.

Bajenoff, M., J. G. Egen, L. Y. Koo, J. P. Laugier, F. Brau, N. Glaichenhaus and R. N. Germain (2006). "Stromal cell networks regulate lymphocyte entry, migration, and territoriality in lymph nodes." Immunity **25**(6): 989-1001.

Bajenoff, M. and R. N. Germain (2009). "B-cell follicle development remodels the conduit system and allows soluble antigen delivery to follicular dendritic cells." Blood **114**(24): 4989-4997.

Bajenoff, M., N. Glaichenhaus and R. N. Germain (2008). "Fibroblastic reticular cells guide T lymphocyte entry into and migration within the splenic T cell zone." J Immunol **181**(6): 3947-3954.

Balogh, P., Y. Aydar, J. G. Tew and A. K. Szakal (2002). "Appearance and phenotype of murine follicular dendritic cells expressing VCAM-1." Anat Rec **268**(2): 160-168.

Bannard, O., R. M. Horton, C. D. Allen, J. An, T. Nagasawa and J. G. Cyster (2013). "Germinal center centroblasts transition to a centrocyte phenotype according to a timed program and depend on the dark zone for effective selection." Immunity **39**(5): 912-924.

Belandia, B., S. M. Powell, J. M. Garcia-Pedrero, M. M. Walker, C. L. Bevan and M. G. Parker (2005). "Hey1, a mediator of notch signaling, is an androgen receptor corepressor." Mol Cell Biol **25**(4): 1425-1436.

Besseyrias, V., E. Fiorini, L. J. Strobl, U. Zimber-Strobl, A. Dumortier, U. Koch, M. L. Arcangeli, S. Ezine, H. R. Macdonald and F. Radtke (2007). "Hierarchy of Notch-Delta interactions promoting T cell lineage commitment and maturation." J Exp Med **204**(2): 331-343.

Bigas, A., D. I. Martin and L. A. Milner (1998). "Notch1 and Notch2 inhibit myeloid differentiation in response to different cytokines." Mol Cell Biol **18**(4): 2324-2333.

Borggrefe, T. and F. Oswald (2009). "The Notch signaling pathway: transcriptional regulation at Notch target genes." Cell Mol Life Sci **66**(10): 1631-1646.

Boyle, S. T., K. A. Gieniec, C. E. Gregor, J. W. Faulkner, S. R. McColl and M. Kochetkova (2017). "Interplay between CCR7 and Notch1 axes promotes stemness in MMTV-PyMT mammary cancer cells." Mol Cancer **16**(1): 19.

Bray, S. J. (2006). "Notch signalling: a simple pathway becomes complex." Nat Rev Mol Cell Biol **7**(9): 678-689.

Britschgi, M. R., A. Link, T. K. Lissandrin and S. A. Luther (2008). "Dynamic modulation of CCR7 expression and function on naive T lymphocytes in vivo." J Immunol **181**(11): 7681-7688.

Castagnaro, L., E. Lenti, S. Maruzzelli, L. Spinardi, E. Migliori, D. Farinello, G. Sitia, Z. Harrelson, S. M. Evans, L. G. Guidotti, R. P. Harvey and A. Brendolan (2013). "Nkx2-5(+)islet1(+) mesenchymal precursors generate distinct spleen stromal cell subsets and participate in restoring stromal network integrity." Immunity **38**(4): 782-791.

Chai, Q., L. Onder, E. Scandella, C. Gil-Cruz, C. Perez-Shibayama, J. Cupovic, R. Danuser, T. Sparwasser, S. A. Luther, V. Thiel, T. Rulicke, J. V. Stein, T. Hehlgans and B. Ludewig (2013). "Maturation of lymph node fibroblastic reticular cells from myofibroblastic precursors is critical for antiviral immunity." Immunity **38**(5): 1013-1024.

Chang, J. E. and S. J. Turley (2015). "Stromal infrastructure of the lymph node and coordination of immunity." Trends Immunol **36**(1): 30-39.

Chigurupati, S., T. V. Arumugam, T. G. Son, J. D. Lathia, S. Jameel, M. R. Mughal, S. C. Tang, D. G. Jo, S. Camandola, M. Giunta, I. Rakova, N. McDonnell, L. Miele, M. P. Mattson and S. Poosala (2007). "Involvement of notch signaling in wound healing." PLoS One **2**(11): e1167.

Chillakuri, C. R., D. Sheppard, S. M. Lea and P. A. Handford (2012). "Notch receptor-ligand binding and activation: insights from molecular studies." Semin Cell Dev Biol **23**(4): 421-428.

Chung, J., C. L. Ebens, E. Perkey, V. Radojcic, U. Koch, L. Scarpellino, A. Tong, F. Allen, S. Wood, J. Feng, A. Friedman, D. Granadier, I. T. Tran, Q. Chai, L. Onder, M. Yan, P. Reddy, B. R. Blazar, A. Y. Huang, T. V. Brennan, D. K. Bishop, B. Ludewig, C. W. Siebel, F. Radtke, S. A. Luther and I. Maillard (2017). "Fibroblastic niches prime T cell alloimmunity through Delta-like Notch ligands." J Clin Invest **127**(4): 1574-1588.

Chyou, S., F. Benahmed, J. Chen, V. Kumar, S. Tian, M. Lipp and T. T. Lu (2011). "Coordinated regulation of lymph node vascular-stromal growth first by CD11c+ cells and then by T and B cells." J Immunol **187**(11): 5558-5567.

Chyou, S., E. H. Ekland, A. C. Carpenter, T. C. Tzeng, S. Tian, M. Michaud, J. A. Madri and T. T. Lu (2008). "Fibroblast-type reticular stromal cells regulate the lymph node vasculature." J Immunol **181**(6): 3887-3896.

Coles, M., D. Kioussis and H. Veiga-Fernandes (2010). "Cellular and molecular requirements in lymph node and Peyer's patch development." Prog Mol Biol Transl Sci **92**: 177-205.

Collu, G. M., A. Hidalgo-Sastre and K. Brennan (2014). "Wnt-Notch signalling crosstalk in development and disease." Cell Mol Life Sci **71**(18): 3553-3567.

Comerford, I., Y. Harata-Lee, M. D. Bunting, C. Gregor, E. E. Kara and S. R. McColl (2013). "A myriad of functions and complex regulation of the CCR7/CCL19/CCL21 chemokine axis in the adaptive immune system." Cytokine Growth Factor Rev **24**(3): 269-283.

Cordle, J., C. Redfieldz, M. Stacey, P. A. van der Merwe, A. C. Willis, B. R. Champion, S. Hambleton and P. A. Handford (2008). "Localization of the delta-like-1-binding site in human Notch-1 and its modulation by calcium affinity." J Biol Chem **283**(17): 11785-11793.

Cornejo, M. G., V. Mabialah, S. M. Sykes, T. Khandan, C. Lo Celso, C. K. Lopez, P. Rivera-Munoz, P. Rameau, Z. Tothova, J. C. Aster, R. A. DePinho, D. T. Scadden, D. G. Gilliland and T. Mercher (2011). "Crosstalk between NOTCH and AKT signaling during murine megakaryocyte lineage specification." Blood **118**(5): 1264-1273.

Cuff, C. A., J. Schwartz, C. M. Bergman, K. S. Russell, J. R. Bender and N. H. Ruddle (1998). "Lymphotoxin alpha3 induces chemokines and adhesion molecules: insight into the role of LT alpha in inflammation and lymphoid organ development." J Immunol **161**(12): 6853-6860.

Cupedo, T., M. F. Vondenhoff, E. J. Heeregrave, A. E. De Weerd, W. Jansen, D. G. Jackson, G. Kraal and R. E. Mebius (2004). "Presumptive lymph node organizers are differentially represented in developing mesenteric and peripheral nodes." J Immunol **173**(5): 2968-2975.

Das, A., B. A. Heesters, A. Bialas, J. O'Flynn, I. R. Rifkin, J. Ochando, N. Mittereder, G. Carlesso, R. Herbst and M. C. Carroll (2017). "Follicular Dendritic Cell Activation by TLR Ligands Promotes Autoreactive B Cell Responses." Immunity **46**(1): 106-119.

Dees, C., M. Tomcik, P. Zerr, A. Akhmetshina, A. Horn, K. Palumbo, C. Beyer, J. Zwerina, O. Distler, G. Schett and J. H. Distler (2011). "Notch signalling regulates fibroblast activation and collagen release in systemic sclerosis." Ann Rheum Dis **70**(7): 1304-1310.

Dougall, W. C., M. Glaccum, K. Charrier, K. Rohrbach, K. Brasel, T. De Smedt, E. Daro, J. Smith, M. E. Tometsko, C. R. Maliszewski, A. Armstrong, V. Shen, S. Bain, D. Cosman, D. Anderson, P. J. Morrissey, J. J. Peschon and J. Schuh (1999). "RANK is essential for osteoclast and lymph node development." Genes Dev **13**(18): 2412-2424.

El Shikh, M. E. and C. Pitzalis (2012). "Follicular dendritic cells in health and disease." Front Immunol **3**: 292.

Fasnacht, N., H. Y. Huang, U. Koch, S. Favre, F. Auderset, Q. Chai, L. Onder, S. Kallert, D. D. Pinschewer, H. R. MacDonald, F. Tacchini-Cottier, B. Ludewig, S. A. Luther and F. Radtke (2014). "Specific fibroblastic niches in secondary lymphoid organs orchestrate distinct Notch-regulated immune responses." J Exp Med **211**(11): 2265-2279.

Fernandez-Munoz, B., M. M. Yurrita, E. Martin-Villar, P. Carrasco-Ramirez, D. Megias, J. Renart and M. Quintanilla (2011). "The transmembrane domain of podoplanin is required for its association with lipid rafts and the induction of epithelial-mesenchymal transition." Int J Biochem Cell Biol **43**(6): 886-896.

Fletcher, A. L., S. E. Acton and K. Knoblich (2015). "Lymph node fibroblastic reticular cells in health and disease." Nat Rev Immunol **15**(6): 350-361.

Fooksman, D. R., T. A. Schwickert, G. D. Victora, M. L. Dustin, M. C. Nussenzweig and D. Skokos (2010). "Development and migration of plasma cells in the mouse lymph node." Immunity **33**(1): 118-127.

Ganburged, G., N. Suda, M. Saito, Y. Yamazaki, K. Isokawa and K. Moriyama (2010). "Dilated capillaries, disorganized collagen fibers and differential gene expression in periodontal ligaments of hypomorphic fibrillin-1 mice." Cell Tissue Res **341**(3): 381-395.

Gatto, D., K. Wood and R. Brink (2011). "EBI2 operates independently of but in cooperation with CXCR5 and CCR7 to direct B cell migration and organization in follicles and the germinal center." J Immunol **187**(9): 4621-4628.

Gore, A. V., M. R. Swift, Y. R. Cha, B. Lo, M. C. McKinney, W. Li, D. Castranova, A. Davis, Y. S. Mukouyama and B. M. Weinstein (2011). "Rspo1/Wnt signaling promotes angiogenesis via Vegfc/Vegfr3." Development **138**(22): 4875-4886.

Grabowska, J., M. A. Lopez-Venegas, A. J. Affandi and J. M. M. den Haan (2018). "CD169(+) Macrophages Capture and Dendritic Cells Instruct: The Interplay of the Gatekeeper and the General of the Immune System." Front Immunol **9**: 2472.

Gretz, J. E., C. C. Norbury, A. O. Anderson, A. E. Proudfoot and S. Shaw (2000). "Lymph-borne chemokines and other low molecular weight molecules reach high endothelial venules via specialized conduits while a functional barrier limits access to the lymphocyte microenvironments in lymph node cortex." J Exp Med **192**(10): 1425-1440.

Grosveld, G. C. (2009). "Gamma-secretase inhibitors: Notch so bad." Nat Med **15**(1): 20-21.

Gunn, M. D., V. N. Ngo, K. M. Ansel, E. H. Ekland, J. G. Cyster and L. T. Williams (1998). "A B-cell-homing chemokine made in lymphoid follicles activates Burkitt's lymphoma receptor-1." Nature **391**(6669): 799-803.

Gunn, M. D., K. Tangemann, C. Tam, J. G. Cyster, S. D. Rosen and L. T. Williams (1998). "A chemokine expressed in lymphoid high endothelial venules promotes the adhesion and chemotaxis of naive T lymphocytes." Proc Natl Acad Sci U S A **95**(1): 258-263.

Haines, N. and K. D. Irvine (2003). "Glycosylation regulates Notch signalling." Nat Rev Mol Cell Biol **4**(10): 786-797.

Hamada, Y., Y. Kadokawa, M. Okabe, M. Ikawa, J. R. Coleman and Y. Tsujimoto (1999). "Mutation in ankyrin repeats of the mouse Notch2 gene induces early embryonic lethality." Development **126**(15): 3415-3424.

Han, H., K. Tanigaki, N. Yamamoto, K. Kuroda, M. Yoshimoto, T. Nakahata, K. Ikuta and T. Honjo (2002). "Inducible gene knockout of transcription factor recombination signal binding protein-J reveals its essential role in T versus B lineage decision." Int Immunol **14**(6): 637-645.

Hara, T., S. Shitara, K. Imai, H. Miyachi, S. Kitano, H. Yao, S. Tani-ichi and K. Ikuta (2012). "Identification of IL-7-producing cells in primary and secondary lymphoid organs using IL-7-GFP knock-in mice." J Immunol **189**(4): 1577-1584.

Heesters, B. A., R. C. Myers and M. C. Carroll (2014). "Follicular dendritic cells: dynamic antigen libraries." Nat Rev Immunol **14**(7): 495-504.

Hellstrom, M., L. K. Phng and H. Gerhardt (2007). "VEGF and Notch signaling: the yin and yang of angiogenic sprouting." Cell Adh Migr **1**(3): 133-136.

Henkel, T., P. D. Ling, S. D. Hayward and M. G. Peterson (1994). "Mediation of Epstein-Barr virus EBNA2 transactivation by recombination signal-binding protein J kappa." Science **265**(5168): 92-95.

Hori, K., A. Sen and S. Artavanis-Tsakonas (2013). "Notch signaling at a glance." J Cell Sci **126**(Pt 10): 2135-2140.

Hozumi, K., N. Negishi, D. Suzuki, N. Abe, Y. Sotomaru, N. Tamaoki, C. Mailhos, D. Ish-Horowicz, S. Habu and M. J. Owen (2004). "Delta-like 1 is necessary for the generation of marginal zone B cells but not T cells in vivo." Nat Immunol **5**(6): 638-644.

Hu, B. and S. H. Phan (2016). "Notch in fibrosis and as a target of anti-fibrotic therapy." Pharmacol Res **108**: 57-64.

Hu, B., Z. Wu, D. Bai, T. Liu, M. R. Ullenbruch and S. H. Phan (2015). "Mesenchymal deficiency of Notch1 attenuates bleomycin-induced pulmonary fibrosis." Am J Pathol **185**(11): 3066-3075.

Hu, M., H. F. Ou-Yang, C. G. Wu, S. Y. Qu, X. T. Xu and P. Wang (2014). "Notch signaling regulates col1alpha1 and col1alpha2 expression in airway fibroblasts." Exp Biol Med (Maywood) **239**(12): 1589-1596.

Huang, H. Y., A. Rivas-Caicedo, F. Renevey, H. Cannelle, E. Peranzoni, L. Scarpellino, D. L. Hardie, A. Pommier, K. Schaeuble, S. Favre, T. K. Vogt, F. Arenzana-Seisdedos, P. Schneider, C. D. Buckley, E. Donnadieu and S. A. Luther (2018). "Identification of a new subset of lymph node stromal cells involved in regulating plasma cell homeostasis." Proc Natl Acad Sci U S A **115**(29): E6826-E6835.

Huang, S., J. Park, C. Qiu, K. W. Chung, S. Y. Li, Y. Sirin, S. H. Han, V. Taylor, U. Zimber-Strobl and K. Susztak (2018). "Jagged1/Notch2 controls kidney fibrosis via Tfam-mediated metabolic reprogramming." PLoS Biol **16**(9): e2005233.

Huppert, S. S., A. Le, E. H. Schroeter, J. S. Mumm, M. T. Saxena, L. A. Milner and R. Kopan (2000). "Embryonic lethality in mice homozygous for a processing-deficient allele of Notch1." Nature **405**(6789): 966-970.

Iso, T., L. Kedes and Y. Hamamori (2003). "HES and HERP families: multiple effectors of the Notch signaling pathway." J Cell Physiol **194**(3): 237-255.

Izon, D. J., J. C. Aster, Y. He, A. Weng, F. G. Karnell, V. Patriub, L. Xu, S. Bakkour, C. Rodriguez, D. Allman and W. S. Pear (2002). "Deltex1 redirects lymphoid progenitors to the B cell lineage by antagonizing Notch1." Immunity **16**(2): 231-243.

Jablonska-Trypuc, A., M. Matejczyk and S. Rosochacki (2016). "Matrix metalloproteinases (MMPs), the main extracellular matrix (ECM) enzymes in collagen degradation, as a target for anticancer drugs." J Enzyme Inhib Med Chem **31**(sup1): 177-183.

Jarjour, M., A. Jorquera, I. Mondor, S. Wienert, P. Narang, M. C. Coles, F. Klauschen and M. Bajenoff (2014). "Fate mapping reveals origin and dynamics of lymph node follicular dendritic cells." J Exp Med **211**(6): 1109-1122.

Jarriault, S., C. Brou, F. Logeat, E. H. Schroeter, R. Kopan and A. Israel (1995). "Signalling downstream of activated mammalian Notch." Nature **377**(6547): 355-358.

Jiao, Z., W. Wang, J. Ma, S. Wang, Z. Su and H. Xu (2012). "Notch signaling mediates TNF-alpha-induced IL-6 production in cultured fibroblast-like synoviocytes from rheumatoid arthritis." Clin Dev Immunol **2012**: 350209.

Jin, S., A. P. Mutvei, I. V. Chivukula, E. R. Andersson, D. Ramskold, R. Sandberg, K. L. Lee, P. Kronqvist, V. Mamaeva, P. Ostling, J. P. Mpindi, O. Kallioniemi, I. Screpanti, L. Poellinger, C. Sahlgren and U. Lendahl (2013). "Non-canonical Notch signaling activates IL-6/JAK/STAT signaling in breast tumor cells and is controlled by p53 and IKKalpha/IKKbeta." Oncogene **32**(41): 4892-4902.

Junt, T., E. A. Moseman, M. Iannacone, S. Massberg, P. A. Lang, M. Boes, K. Fink, S. E. Henrickson, D. M. Shayakhmetov, N. C. Di Paolo, N. van Rooijen, T. R. Mempel, S. P. Whelan and U. H. von Andrian (2007). "Subcapsular sinus macrophages in lymph nodes clear lymph-borne viruses and present them to antiviral B cells." Nature **450**(7166): 110-114.

Kaiser, A., E. Donnadieu, J. P. Abastado, A. Trautmann and A. Nardin (2005). "CC chemokine ligand 19 secreted by mature dendritic cells increases naive T cell scanning behavior and their response to rare cognate antigen." J Immunol **175**(4): 2349-2356.

Kang, J., J. Yoo, S. Lee, W. Tang, B. Aguilar, S. Ramu, I. Choi, H. H. Otu, J. W. Shin, G. P. Dotto, C. J. Koh, M. Detmar and Y. K. Hong (2010). "An exquisite cross-control mechanism among endothelial cell fate regulators directs the plasticity and heterogeneity of lymphatic endothelial cells." Blood **116**(1): 140-150.

Katakai, T. (2012). "Marginal reticular cells: a stromal subset directly descended from the lymphoid tissue organizer." Front Immunol **3**: 200.

Katakai, T., T. Hara, M. Sugai, H. Gonda and A. Shimizu (2004). "Lymph node fibroblastic reticular cells construct the stromal reticulum via contact with lymphocytes." J Exp Med **200**(6): 783-795.

Katakai, T., H. Suto, M. Sugai, H. Gonda, A. Togawa, S. Suematsu, Y. Ebisuno, K. Katagiri, T. Kinashi and A. Shimizu (2008). "Organizer-like reticular stromal cell layer common to adult secondary lymphoid organs." J Immunol **181**(9): 6189-6200.

Kedl, R. M. and B. A. Tamburini (2015). "Antigen archiving by lymph node stroma: A novel function for the lymphatic endothelium." Eur J Immunol **45**(10): 2721-2729.

Kelch, I. D., G. Bogle, G. B. Sands, A. R. Phillips, I. J. LeGrice and P. R. Dunbar (2015). "Organ-wide 3D-imaging and topological analysis of the continuous microvascular network in a murine lymph node." Sci Rep **5**: 16534.

Kendall, R. T. and C. A. Feghali-Bostwick (2014). "Fibroblasts in fibrosis: novel roles and mediators." Front Pharmacol **5**: 123.

Kidd, S., M. R. Kelley and M. W. Young (1986). "Sequence of the notch locus of Drosophila melanogaster: relationship of the encoded protein to mammalian clotting and growth factors." Mol Cell Biol **6**(9): 3094-3108.

Kim, J. E., J. H. Lee, K. H. Jeong, G. M. Kim and H. Kang (2014). "Notch intracellular domain expression in various skin fibroproliferative diseases." Ann Dermatol **26**(3): 332-337.

Kofler, N. M., C. J. Shawber, T. Kangsamaksin, H. O. Reed, J. Galatioto and J. Kitajewski (2011). "Notch signaling in developmental and tumor angiogenesis." Genes Cancer **2**(12): 1106-1116.

Kong, Y. Y., H. Yoshida, I. Sarosi, H. L. Tan, E. Timms, C. Capparelli, S. Morony, A. J. Oliveira-dos-Santos, G. Van, A. Itie, W. Khoo, A. Wakeham, C. R. Dunstan, D. L. Lacey, T. W. Mak, W. J. Boyle and J. M. Penninger (1999). "OPGL is a key regulator of osteoclastogenesis, lymphocyte development and lymph-node organogenesis." Nature **397**(6717): 315-323.

Kopan, R. and M. X. Ilagan (2009). "The canonical Notch signaling pathway: unfolding the activation mechanism." Cell **137**(2): 216-233.

Kozai, M., Y. Kubo, T. Katakai, H. Kondo, H. Kiyonari, K. Schaeuble, S. A. Luther, N. Ishimaru, I. Ohigashi and Y. Takahama (2017). "Essential role of CCL21 in establishment of central self-tolerance in T cells." J Exp Med **214**(7): 1925-1935.

Kraal, G. (1992). "Cells in the marginal zone of the spleen." Int Rev Cytol **132**: 31-74.

Kranich, J., N. J. Krautler, E. Heinen, M. Polymenidou, C. Bridel, A. Schildknecht, C. Huber, M. H. Kosco-Vilbois, R. Zinkernagel, G. Miele and A. Aguzzi (2008). "Follicular dendritic cells control engulfment of apoptotic bodies by secreting Mfge8." J Exp Med **205**(6): 1293-1302.

Krebs, L. T., Y. Xue, C. R. Norton, J. R. Shutter, M. Maguire, J. P. Sundberg, D. Gallahan, V. Closson, J. Kitajewski, R. Callahan, G. H. Smith, K. L. Stark and T. Gridley (2000). "Notch signaling is essential for vascular morphogenesis in mice." Genes Dev **14**(11): 1343-1352.

Ladi, E., J. T. Nichols, W. Ge, A. Miyamoto, C. Yao, L. T. Yang, J. Boulter, Y. E. Sun, C. Kintner and G. Weinmaster (2005). "The divergent DSL ligand Dll3 does not activate Notch signaling but cell autonomously attenuates signaling induced by other DSL ligands." J Cell Biol **170**(6): 983-992.

Lewis, K. L., M. L. Caton, M. Bogunovic, M. Greter, L. T. Grajkowska, D. Ng, A. Klinakis, I. F. Charo, S. Jung, J. L. Gommerman, Ivanov, II, K. Liu, M. Merad and B. Reizis (2011). "Notch2 receptor signaling controls functional differentiation of dendritic cells in the spleen and intestine." Immunity **35**(5): 780-791.

Link, A., T. K. Vogt, S. Favre, M. R. Britschgi, H. Acha-Orbea, B. Hinz, J. G. Cyster and S. A. Luther (2007). "Fibroblastic reticular cells in lymph nodes regulate the homeostasis of naive T cells." Nat Immunol **8**(11): 1255-1265.

Liu, F., D. Lagares, K. M. Choi, L. Stopfer, A. Marinkovic, V. Vrbanac, C. K. Probst, S. E. Hiemer, T. H. Sisson, J. C. Horowitz, I. O. Rosas, L. E. Fredenburgh, C. Feghali-Bostwick, X. Varelas, A. M. Tager and D. J. Tschumperlin (2015). "Mechanosignaling through YAP and TAZ drives fibroblast activation and fibrosis." Am J Physiol Lung Cell Mol Physiol **308**(4): L344-357.

Liu, Z. J., T. Shirakawa, Y. Li, A. Soma, M. Oka, G. P. Dotto, R. M. Fairman, O. C. Velazquez and M. Herlyn (2003). "Regulation of Notch1 and Dll4 by vascular endothelial growth factor in arterial endothelial cells: implications for modulating arteriogenesis and angiogenesis." Mol Cell Biol **23**(1): 14-25.

Lo, J. C., R. K. Chin, Y. Lee, H. S. Kang, Y. Wang, J. V. Weinstock, T. Banks, C. F. Ware, G. Franzoso and Y. X. Fu (2003). "Differential regulation of CCL21 in lymphoid/nonlymphoid tissues for effectively attracting T cells to peripheral tissues." J Clin Invest **112**(10): 1495-1505.

Lobry, C., P. Oh, M. R. Mansour, A. T. Look and I. Aifantis (2014). "Notch signaling: switching an oncogene to a tumor suppressor." Blood **123**(16): 2451-2459.

Luther, S. A., H. L. Tang, P. L. Hyman, A. G. Farr and J. G. Cyster (2000). "Coexpression of the chemokines ELC and SLC by T zone stromal cells and deletion of the ELC gene in the plt/plt mouse." Proc Natl Acad Sci U S A **97**(23): 12694-12699.

Luther, S. A., T. K. Vogt and S. Siegert (2011). "Guiding blind T cells and dendritic cells: A closer look at fibroblastic reticular cells found within lymph node T zones." Immunol Lett **138**(1): 9-11.

Malhotra, D., A. L. Fletcher, J. Astarita, V. Lukacs-Kornek, P. Tayalia, S. F. Gonzalez, K. G. Elpek, S. K. Chang, K. Knoblich, M. E. Hemler, M. B. Brenner, M. C. Carroll, D. J. Mooney, S. J. Turley and C. Immunological Genome Project (2012). "Transcriptional profiling of stroma from inflamed and resting lymph nodes defines immunological hallmarks." Nat Immunol **13**(5): 499-510.

Mebius, R. E. (2003). "Organogenesis of lymphoid tissues." Nat Rev Immunol **3**(4): 292-303.

Mebius, R. E. and G. Kraal (2005). "Structure and function of the spleen." Nat Rev Immunol **5**(8): 606-616.

Mebius, R. E., P. R. Streeter, J. Breve, A. M. Duijvestijn and G. Kraal (1991). "The influence of afferent lymphatic vessel interruption on vascular addressin expression." J Cell Biol **115**(1): 85-95.

Meurette, O. and P. Mehlen (2018). "Notch Signaling in the Tumor Microenvironment." Cancer Cell **34**(4): 536-548.

Milano, J., J. McKay, C. Dagenais, L. Foster-Brown, F. Pognan, R. Gadient, R. T. Jacobs, A. Zacco, B. Greenberg and P. J. Ciaccio (2004). "Modulation of notch processing by gamma-secretase inhibitors causes intestinal goblet cell metaplasia and induction of genes known to specify gut secretory lineage differentiation." Toxicol Sci **82**(1): 341-358.

Mionnet, C., S. L. Sanos, I. Mondor, A. Jorquera, J. P. Laugier, R. N. Germain and M. Bajenoff (2011). "High endothelial venules as traffic control points maintaining lymphocyte population homeostasis in lymph nodes." Blood **118**(23): 6115-6122.

Mishima, K., T. Watabe, A. Saito, Y. Yoshimatsu, N. Imaizumi, S. Masui, M. Hirashima, T. Morisada, Y. Oike, M. Araie, H. Niwa, H. Kubo, T. Suda and K. Miyazono (2007). "Prox1 induces lymphatic endothelial differentiation via integrin alpha9 and other signaling cascades." Mol Biol Cell **18**(4): 1421-1429.

Miyamoto, A., R. Lau, P. W. Hein, J. M. Shipley and G. Weinmaster (2006). "Microfibrillar proteins MAGP-1 and MAGP-2 induce Notch1 extracellular domain dissociation and receptor activation." J Biol Chem **281**(15): 10089-10097.

Miyasaka, M. and T. Tanaka (2004). "Lymphocyte trafficking across high endothelial venules: dogmas and enigmas." Nat Rev Immunol **4**(5): 360-370.

Mori, S., H. Nakano, K. Aritomi, C. R. Wang, M. D. Gunn and T. Kakiuchi (2001). "Mice lacking expression of the chemokines CCL21-ser and CCL19 (plt mice) demonstrate delayed but enhanced T cell immune responses." J Exp Med **193**(2): 207-218.

Mueller, S. N. and R. N. Germain (2009). "Stromal cell contributions to the homeostasis and functionality of the immune system." Nat Rev Immunol **9**(9): 618-629.

Murtomaki, A., M. K. Uh, Y. K. Choi, C. Kitajewski, V. Borisenko, J. Kitajewski and C. J. Shawber (2013). "Notch1 functions as a negative regulator of lymphatic endothelial cell differentiation in the venous endothelium." Development **140**(11): 2365-2376.

Nakano, H. and M. D. Gunn (2001). "Gene duplications at the chemokine locus on mouse chromosome 4: multiple strain-specific haplotypes and the deletion of secondary lymphoid-organ chemokine and EBI-1 ligand chemokine genes in the plt mutation." J Immunol **166**(1): 361-369.

Nandagopal, S., D. Wu and F. Lin (2011). "Combinatorial guidance by CCR7 ligands for T lymphocytes migration in co-existing chemokine fields." PLoS One **6**(3): e18183.

Neves, A., K. English and J. R. Priess (2007). "Notch-GATA synergy promotes endoderm-specific expression of ref-1 in C. elegans." Development **134**(24): 4459-4468.

Ngo, V. N., H. Korner, M. D. Gunn, K. N. Schmidt, D. S. Riminton, M. D. Cooper, J. L. Browning, J. D. Sedgwick and J. G. Cyster (1999). "Lymphotoxin alpha/beta and tumor necrosis factor are required for stromal cell expression of homing chemokines in B and T cell areas of the spleen." J Exp Med **189**(2): 403-412.

Niessen, K., G. Zhang, J. B. Ridgway, H. Chen, G. Kolumam, C. W. Siebel and M. Yan (2011). "The Notch1-Dll4 signaling pathway regulates mouse postnatal lymphatic development." Blood **118**(7): 1989-1997.

Noguchi, S., A. Saito and T. Nagase (2018). "YAP/TAZ Signaling as a Molecular Link between Fibrosis and Cancer." Int J Mol Sci **19**(11).

Nolte, M. A., J. A. Belien, I. Schadee-Eestermans, W. Jansen, W. W. Unger, N. van Rooijen, G. Kraal and R. E. Mebius (2003). "A conduit system distributes chemokines and small blood-borne molecules through the splenic white pulp." J Exp Med **198**(3): 505-512.

Oka, C., T. Nakano, A. Wakeham, J. L. de la Pompa, C. Mori, T. Sakai, S. Okazaki, M. Kawaichi, K. Shiota, T. W. Mak and T. Honjo (1995). "Disruption of the mouse RBP-J kappa gene results in early embryonic death." Development **121**(10): 3291-3301.

Onder, L., P. Narang, E. Scandella, Q. Chai, M. Iolyeva, K. Hoorweg, C. Halin, E. Richie, P. Kaye, J. Westermann, T. Cupedo, M. Coles and B. Ludewig (2012). "IL-7-producing stromal cells are critical for lymph node remodeling." Blood **120**(24): 4675-4683.

Onder, L., E. Scandella, Q. Chai, S. Firner, C. T. Mayer, T. Sparwasser, V. Thiel, T. Rulicke and B. Ludewig (2011). "A novel bacterial artificial chromosome-transgenic podoplanin-cre mouse targets lymphoid organ stromal cells in vivo." Front Immunol **2**: 50.

Ong, C. T., H. T. Cheng, L. W. Chang, T. Ohtsuka, R. Kageyama, G. D. Stormo and R. Kopan (2006). "Target selectivity of vertebrate notch proteins. Collaboration between discrete domains and CSL-binding site architecture determines activation probability." J Biol Chem **281**(8): 5106-5119.

Ortiz Franyuti, D., M. Mitsi and V. Vogel (2018). "Mechanical Stretching of Fibronectin Fibers Upregulates Binding of Interleukin-7." Nano Lett **18**(1): 15-25.

Osipo, C., T. E. Golde, B. A. Osborne and L. A. Miele (2008). "Off the beaten pathway: the complex cross talk between Notch and NF-kappaB." Lab Invest **88**(1): 11-17.

Oswald, F., M. Winkler, Y. Cao, K. Astrahantseff, S. Bourteele, W. Knochel and T. Borggrefe (2005). "RBP-Jkappa/SHARP recruits CtIP/CtBP corepressors to silence Notch target genes." Mol Cell Biol **25**(23): 10379-10390.

Palframan, R. T., S. Jung, G. Cheng, W. Weninger, Y. Luo, M. Dorf, D. R. Littman, B. J. Rollins, H. Zweerink, A. Rot and U. H. von Andrian (2001). "Inflammatory chemokine transport and presentation in HEV: a remote control mechanism for monocyte recruitment to lymph nodes in inflamed tissues." J Exp Med **194**(9): 1361-1373.

Panciera, T., L. Azzolin, M. Cordenonsi and S. Piccolo (2017). "Mechanobiology of YAP and TAZ in physiology and disease." Nat Rev Mol Cell Biol **18**(12): 758-770.

Pereira, J. P., L. M. Kelly, Y. Xu and J. G. Cyster (2009). "EBI2 mediates B cell segregation between the outer and centre follicle." Nature **460**(7259): 1122-1126.

Pham, T. H., P. Baluk, Y. Xu, I. Grigorova, A. J. Bankovich, R. Pappu, S. R. Coughlin, D. M. McDonald, S. R. Schwab and J. G. Cyster (2010). "Lymphatic endothelial cell sphingosine kinase activity is required for lymphocyte egress and lymphatic patterning." J Exp Med **207**(1): 17-27.

Phan, T. G., J. A. Green, E. E. Gray, Y. Xu and J. G. Cyster (2009). "Immune complex relay by subcapsular sinus macrophages and noncognate B cells drives antibody affinity maturation." Nat Immunol **10**(7): 786-793.

Piersma, B., S. de Rond, P. M. Werker, S. Boo, B. Hinz, M. M. van Beuge and R. A. Bank (2015). "YAP1 Is a Driver of Myofibroblast Differentiation in Normal and Diseased Fibroblasts." Am J Pathol **185**(12): 3326-3337.

Pietila, T. E., V. Veckman, A. Lehtonen, R. Lin, J. Hiscott and I. Julkunen (2007). "Multiple NF-kappaB and IFN regulatory factor family transcription factors regulate CCL19 gene expression in human monocyte-derived dendritic cells." J Immunol **178**(1): 253-261.

Procopio, M. G., C. Laszlo, D. Al Labban, D. E. Kim, P. Bordignon, S. H. Jo, S. Goruppi, E. Menietti, P. Ostano, U. Ala, P. Provero, W. Hoetzenecker, V. Neel, W. W. Kilarski, M. A. Swartz, C. Brisken, K. Lefort and G. P. Dotto (2015). "Combined CSL and p53 downregulation promotes cancer-associated fibroblast activation." Nat Cell Biol **17**(9): 1193-1204.

Py, B. F., S. F. Gonzalez, K. Long, M. S. Kim, Y. A. Kim, H. Zhu, J. Yao, N. Degauque, R. Villet, P. Ymele-Leki, M. Gadjeva, G. B. Pier, M. C. Carroll and J. Yuan (2013). "Cochlin produced by follicular dendritic cells promotes antibacterial innate immunity." Immunity **38**(5): 1063-1072.

Radtke, F., N. Fasnacht and H. R. Macdonald (2010). "Notch signaling in the immune system." Immunity **32**(1): 14-27.

Radtke, F., H. R. MacDonald and F. Tacchini-Cottier (2013). "Regulation of innate and adaptive immunity by Notch." Nat Rev Immunol **13**(6): 427-437.

Radtke, F., A. Wilson, G. Stark, M. Bauer, J. van Meerwijk, H. R. MacDonald and M. Aguet (1999). "Deficient T cell fate specification in mice with an induced inactivation of Notch1." Immunity **10**(5): 547-558.

Ran, Y., F. Hossain, A. Pannuti, C. B. Lessard, G. Z. Ladd, J. I. Jung, L. M. Minter, B. A. Osborne, L. Miele and T. E. Golde (2017). "gamma-Secretase inhibitors in cancer clinical trials are pharmacologically and functionally distinct." EMBO Mol Med **9**(7): 950-966.

Randall, T. D., D. M. Carragher and J. Rangel-Moreno (2008). "Development of secondary lymphoid organs." Annu Rev Immunol **26**: 627-650.

Randolph, G. J., V. Angeli and M. A. Swartz (2005). "Dendritic-cell trafficking to lymph nodes through lymphatic vessels." Nat Rev Immunol **5**(8): 617-628.

Rangarajan, A., C. Talora, R. Okuyama, M. Nicolas, C. Mammucari, H. Oh, J. C. Aster, S. Krishna, D. Metzger, P. Chambon, L. Miele, M. Aguet, F. Radtke and G. P. Dotto (2001). "Notch signaling is a direct determinant of keratinocyte growth arrest and entry into differentiation." EMBO J **20**(13): 3427-3436.

Rantakari, P., K. Auvinen, N. Jappinen, M. Kapraali, J. Valtonen, M. Karikoski, H. Gerke, E. K. I. Iftakhar, J. Keuschnigg, E. Umemoto, K. Tohya, M. Miyasaka, K. Elima, S. Jalkanen and M. Salmi (2015). "The endothelial protein PLVAP in lymphatics controls the entry of lymphocytes and antigens into lymph nodes." Nat Immunol **16**(4): 386-396.

Rauen, T., U. Raffetseder, B. C. Frye, S. Djudjaj, P. J. Muhlenberg, F. Eitner, U. Lendahl, J. Bernhagen, S. Dooley and P. R. Mertens (2009). "YB-1 acts as a ligand for Notch-3 receptors and modulates receptor activation." J Biol Chem **284**(39): 26928-26940.

Rodda, L. B., E. Lu, M. L. Bennett, C. L. Sokol, X. Wang, S. A. Luther, B. A. Barres, A. D. Luster, C. J. Ye and J. G. Cyster (2018). "Single-Cell RNA Sequencing of Lymph Node Stromal Cells Reveals Niche-Associated Heterogeneity." Immunity **48**(5): 1014-1028 e1016.

Roozendaal, R., R. E. Mebius and G. Kraal (2008). "The conduit system of the lymph node." Int Immunol **20**(12): 1483-1487.

Roozendaal, R., T. R. Mempel, L. A. Pitcher, S. F. Gonzalez, A. Verschoor, R. E. Mebius, U. H. von Andrian and M. C. Carroll (2009). "Conduits mediate transport of low-molecular-weight antigen to lymph node follicles." Immunity **30**(2): 264-276.

Rose, S., A. Misharin and H. Perlman (2012). "A novel Ly6C/Ly6G-based strategy to analyze the mouse splenic myeloid compartment." Cytometry A **81**(4): 343-350.

Saito, T., S. Chiba, M. Ichikawa, A. Kunisato, T. Asai, K. Shimizu, T. Yamaguchi, G. Yamamoto, S. Seo, K. Kumano, E. Nakagami-Yamaguchi, Y. Hamada, S. Aizawa and H. Hirai (2003). "Notch2 is preferentially expressed in mature B cells and indispensable for marginal zone B lineage development." Immunity **18**(5): 675-685.

Sakurai, A., C. L. Doci and J. S. Gutkind (2012). "Semaphorin signaling in angiogenesis, lymphangiogenesis and cancer." Cell Res **22**(1): 23-32.

Schaeuble, K., M. R. Britschgi, L. Scarpellino, S. Favre, Y. Xu, E. Koroleva, T. K. A. Lissandrin, A. Link, M. Matloubian, C. F. Ware, S. A. Nedospasov, A. V. Tumanov, J. G. Cyster and S. A. Luther (2017). "Perivascular Fibroblasts of the Developing Spleen Act as LTalpha1beta2-Dependent Precursors of Both T and B Zone Organizer Cells." Cell Rep **21**(9): 2500-2514.

Seo, E., W. Y. Kim, J. Hur, H. Kim, S. A. Nam, A. Choi, Y. M. Kim, S. H. Park, C. Chung, J. Kim, S. Min, S. J. Myung, D. S. Lim and Y. K. Kim (2016). "The Hippo-Salvador signaling pathway regulates renal tubulointerstitial fibrosis." Sci Rep **6**: 31931.

Seth, S., L. Oberdorfer, R. Hyde, K. Hoff, V. Thies, T. Worbs, S. Schmitz and R. Forster (2011). "CCR7 essentially contributes to the homing of plasmacytoid dendritic cells to lymph nodes under steady-state as well as inflammatory conditions." J Immunol **186**(6): 3364-3372.

Shimizu, K., S. Chiba, K. Kumano, N. Hosoya, T. Takahashi, Y. Kanda, Y. Hamada, Y. Yazaki and H. Hirai (1999). "Mouse jagged1 physically interacts with notch2 and other notch receptors. Assessment by quantitative methods." J Biol Chem **274**(46): 32961-32969.

Shin, H. M., L. M. Minter, O. H. Cho, S. Gottipati, A. H. Fauq, T. E. Golde, G. E. Sonenshein and B. A. Osborne (2006). "Notch1 augments NF-kappaB activity by facilitating its nuclear retention." EMBO J **25**(1): 129-138.

Siebel, C. and U. Lendahl (2017). "Notch Signaling in Development, Tissue Homeostasis, and Disease." Physiol Rev **97**(4): 1235-1294.

Simons, M., E. Gordon and L. Claesson-Welsh (2016). "Mechanisms and regulation of endothelial VEGF receptor signalling." Nat Rev Mol Cell Biol **17**(10): 611-625.

Sixt, M., N. Kanazawa, M. Selg, T. Samson, G. Roos, D. P. Reinhardt, R. Pabst, M. B. Lutz and L. Sorokin (2005). "The conduit system transports soluble antigens from the afferent lymph to resident dendritic cells in the T cell area of the lymph node." Immunity **22**(1): 19-29.

Stachowiak, A. N., Y. Wang, Y. C. Huang and D. J. Irvine (2006). "Homeostatic lymphoid chemokines synergize with adhesion ligands to trigger T and B lymphocyte chemokinesis." J Immunol **177**(4): 2340-2348.

Sundlisaeter, E., R. J. Edelmann, J. Hol, J. Sponheim, A. M. Kuchler, M. Weiss, I. A. Udalova, K. S. Midwood, M. Kasprzycka and G. Haraldsen (2012). "The alarmin IL-33 is a notch target in quiescent endothelial cells." Am J Pathol **181**(3): 1099-1111.

Surh, C. D. and J. Sprent (2008). "Homeostasis of naive and memory T cells." Immunity **29**(6): 848-862.

Takaba, H. and H. Takayanagi (2017). "The Mechanisms of T Cell Selection in the Thymus." Trends Immunol **38**(11): 805-816.

Takeuchi, M. and V. R. Baichwal (1995). "Induction of the gene encoding mucosal vascular addressin cell adhesion molecule 1 by tumor necrosis factor alpha is mediated by NF-kappa B proteins." Proc Natl Acad Sci U S A **92**(8): 3561-3565.

Thierry, G. R., M. Kuka, M. De Giovanni, I. Mondor, N. Brouilly, M. Iannacone and M. Bajenoff (2018). "The conduit system exports locally secreted IgM from lymph nodes." J Exp Med **215**(12): 2972-2983.

Thomas, J. L., K. Baker, J. Han, C. Calvo, H. Nurmi, A. C. Eichmann and K. Alitalo (2013). "Interactions between VEGFR and Notch signaling pathways in endothelial and neural cells." Cell Mol Life Sci **70**(10): 1779-1792.

Thomas, S. N., J. M. Rutkowski, M. Pasquier, E. L. Kuan, K. Alitalo, G. J. Randolph and M. A. Swartz (2012). "Impaired humoral immunity and tolerance in K14-VEGFR-3-Ig mice that lack dermal lymphatic drainage." J Immunol **189**(5): 2181-2190.

Tilley, A. E., B. G. Harvey, A. Heguy, N. R. Hackett, R. Wang, T. P. O'Connor and R. G. Crystal (2009). "Down-regulation of the notch pathway in human airway epithelium in association with smoking and chronic obstructive pulmonary disease." Am J Respir Crit Care Med **179**(6): 457-466.

Totaro, A., M. Castellan, D. Di Biagio and S. Piccolo (2018). "Crosstalk between YAP/TAZ and Notch Signaling." Trends Cell Biol **28**(7): 560-573.

Ueno, T., K. Hara, M. S. Willis, M. A. Malin, U. E. Hopken, D. H. Gray, K. Matsushima, M. Lipp, T. A. Springer, R. L. Boyd, O. Yoshie and Y. Takahama (2002). "Role for CCR7 ligands in the emigration of newly generated T lymphocytes from the neonatal thymus." Immunity **16**(2): 205-218.

Van Vliet, E., M. Melis, J. M. Foidart and W. Van Ewijk (1986). "Reticular fibroblasts in peripheral lymphoid organs identified by a monoclonal antibody." J Histochem Cytochem **34**(7): 883-890.

Visse, R. and H. Nagase (2003). "Matrix metalloproteinases and tissue inhibitors of metalloproteinases: structure, function, and biochemistry." Circ Res **92**(8): 827-839.

von Andrian, U. H. and T. R. Mempel (2003). "Homing and cellular traffic in lymph nodes." Nat Rev Immunol **3**(11): 867-878.

Webster, B., E. H. Ekland, L. M. Agle, S. Chyou, R. Ruggieri and T. T. Lu (2006). "Regulation of lymph node vascular growth by dendritic cells." J Exp Med **203**(8): 1903-1913.

Weng, A. P., A. A. Ferrando, W. Lee, J. P. t. Morris, L. B. Silverman, C. Sanchez-Irizarry, S. C. Blacklow, A. T. Look and J. C. Aster (2004). "Activating mutations of NOTCH1 in human T cell acute lymphoblastic leukemia." Science **306**(5694): 269-271.

Woolf, E., I. Grigorova, A. Sagiv, V. Grabovsky, S. W. Feigelson, Z. Shulman, T. Hartmann, M. Sixt, J. G. Cyster and R. Alon (2007). "Lymph node chemokines promote sustained T lymphocyte motility without triggering stable integrin adhesiveness in the absence of shear forces." Nat Immunol **8**(10): 1076-1085.

Yang, C. Y., T. K. Vogt, S. Favre, L. Scarpellino, H. Y. Huang, F. Tacchini-Cottier and S. A. Luther (2014). "Trapping of naive lymphocytes triggers rapid growth and remodeling of the fibroblast network in reactive murine lymph nodes." Proc Natl Acad Sci U S A **111**(1): E109-118.

Yang, J., F. Cornelissen, N. Papazian, R. M. Reijmers, M. Llorian, T. Cupedo, M. Coles and B. Seddon (2018). "IL-7-dependent maintenance of ILC3s is required for normal entry of lymphocytes into lymph nodes." J Exp Med **215**(4): 1069-1077.

Yuan, X., H. Wu, H. Xu, H. Xiong, Q. Chu, S. Yu, G. S. Wu and K. Wu (2015). "Notch signaling: an emerging therapeutic target for cancer treatment." Cancer Lett **369**(1): 20-27.

Zeuner, A., F. Francescangeli, M. Signore, M. A. Venneri, F. Pedini, N. Felli, A. Pagliuca, C. Conticello and R. De Maria (2011). "The Notch2-Jagged1 interaction mediates stem cell factor signaling in erythropoiesis." Cell Death Differ **18**(2): 371-380.

Zheng, W., T. Tammela, M. Yamamoto, A. Anisimov, T. Holopainen, S. Kaijalainen, T. Karpanen, K. Lehti, S. Yla-Herttuala and K. Alitalo (2011). "Notch restricts lymphatic vessel sprouting induced by vascular endothelial growth factor." Blood **118**(4): 1154-1162.

Zhu, M. and Y. X. Fu (2011). "The role of core TNF/LIGHT family members in lymph node homeostasis and remodeling." Immunol Rev **244**(1): 75-84.

Zimber-Strobl, U. and L. J. Strobl (2001). "EBNA2 and Notch signalling in Epstein-Barr virus mediated immortalization of B lymphocytes." Semin Cancer Biol **11**(6): 423-434.